THE EFFECT OF SURFACE VIBRATION ON NUCLEATE POOL BOILING AT LOW HEAT FLUXES

By

DONALD CRAIG PRICE

Bachelor of Science in Mechanical Engineering
Southern Methodist University
Dallas, Texas
May, 1961

Master of Science in Mechanical Engineering
Southern Methodist University
Dallas, Texas
January, 1963

Submitted to the Faculty of the Graduate School
of Oklahoma State University
in partial fulfillment of the requirements
for the degree of
DOCTOR OF PHILOSOPHY
July, 1966

THE EFFECT OF SURFACE VIBRATIONS

ON NUCLEATE POOL BOILING

AT LOW HEAT FLUXES

Thesis Approved:

Thesis Adviser

Dean of the Graduate School

ACKNOWLEDGMENTS

The author is grateful for the financial aid provided by the mechanical engineering department during the early period of his study at Oklahoma State University. Additional aid was received from the Ford Foundation in the form of a forgivable loan and from the National Aeronautics and Space Administration in the form of a research assistantship. Without this aid the work could not have continued. The funds for the construction of the experimental equipment were also provided by NASA and are gratefully appreciated.

The technical assistance provided by Mr. John McCandless and Mr. George Cooper was invaluable during the construction of the equipment. Mr. Jack Isham, an undergraduate student, was also of considerable help.

The discussions and bull sessions with my fellow graduate students helped to solve many of my experimental problems and served as an inspiration in times of greatest despair. This association was very important during my graduate study as it is to most students.

Several members of the faculty of the department are due special thanks. Professor J. D. Parker, my advisor during this period, was primarily responsible for the initiation of this investigation. His continued support, careful criticism, and helpful suggestions at crucial times enabled the author to complete the proposed research project. The author is grateful, most of all, for the confidence placed in him by Professor Parker and his delegation of responsibility in the fulfillment of the objectives of the research grant.

Other members of the faculty to whom the author is grateful are Professors J. A. Wiebelt, L. J. Fila, D. R. Haworth, and K. J. Bell who served as members of the advisory committee. Additional thanks are due Professor Fila for his very careful study of the final draft and his very helpful comments.

Professor F. C. McQuiston, laboratory supervisor, provided technical assistance and expert advice on several phases of the construction of the equipment and this is appreciated.

Professor R. L. Lowery deserves consideration for his assistance with the many and varied instrumentation and calibration problems.

Professor R. E. Little and Professor Lee Harrisberger offered many helpful suggestions concerning the design of the vibratory system for which the author is very grateful.

The author feels very fortunate to have attended a school where so many of the professors take an interest in the problems of research and extend a helping hand.

Above all others the author wishes to thank his wife, Barbara, and his three children who have continued to endure the hardships of graduate work. Without the encouragement and assistance of his family, the author could surely not have finished this work.

TABLE OF CONTENTS

LIST OF TABLES

LIST OF PLATES

LIST OF FIGURES

Figure		Page

CHAPTER I

INTRODUCTION

Nucleate boiling is that process whereby a liquid undergoes a change of phase at preferred nucleation sites on a hot surface resulting in the formation of vapor and an exchange of heat. It is distinguished from the other modes of surface ebullition, transition boiling and film boiling, by the manner of vapor generation and by the characteristics of heat transfer. Of the three types of boiling, nucleate boiling is the most common and the most technologically important.

The importance of nucleate boiling arises from its ability to remove enormous quantities of heat per unit time and area from a hot surface and to accomplish this heat transfer with a relatively low thermal potential. For this reason nucleate boiling is used in such applications as refrigeration, electrical power generation, and chemical processing. It is also used in nuclear reactors and other recently innovated devices which require extremely high heat fluxes in very small compact spaces such as rocket and jet-aircraft engines. Within the last few years engineers have succeeded in achieving heat fluxes equivalent to the energy flux from the sun at temperatures far below the 10,000^{o} F temperature of the surface of the sun.

In many of the aforementioned applications, accurate knowledge of the heat transfer characteristics and the heat transfer rates for given surface temperatures must be known. For standard nucleate boiling, adequate information is available in the literature; but whenever outside effects disturb the boiling process, this information does not always apply. Gravity changes, pressure variations, sound fields, and external agitation of the boiling fluid have been shown to have a pronounced effect on the rates of heat transfer experienced. A list of references in these areas is included in the appendices if further information is desired. The subject of this investigation is a problem which has not had prior study, but is considered to be one of the most important practical problems in the field of nucleate boiling. It is concerned with the effect of surface vibrations on the boiling process.

Since results of studies of the effect of surface vibrations on convective processes such as free convection, forced convection, and mass transfer indicated large increases in convective rates, there was a possibility that surface vibrations might also affect nucleate boiling, an essentially convective process. Based on these previous vibratory studies, a simple physical model consisting of a vibrating cylinder in a pool of saturated water was chosen. The experimental study consists of both a quantitative investigation to determine the effect of surface vibration on the numerical value of the heat transfer coefficient and a qualitative investigation to determine any visual changes in the nucleation process. In addition, a literature study of the nucleate boiling process formed the basis for a proposed physical mechanism of the interaction of surface vibrations and nucleate boiling. A comparison of the proposed mechanism and the recorded physical observations is then made.

The experimental equipment is described in detail including the construction and operation procedures. The experimental instrumentation is discussed and an analysis of the experimental uncertainties involved is presented.

In addition to the conclusions which resulted from this investigation, a number of new research ideas were developed and are discussed in some detail with recommendations for future research.

CHAPTER II

LITERATURE SURVEY

The present investigation was undertaken after an extensive study of the literature on boiling heat transfer. The four basic areas which were emphasized are:

a) Normal Nucleate Boiling

b) Effect of Gravity Fields

c) Effect of Miscellaneous Fluid Agitation

d) Effect of Surface Vibration

These areas are outlined in this chapter and references cited in case further information is desired.

Normal Nucleate Boiling

An abundance of literature is available in the area of nucleate boiling heat transfer. The important papers will not be discussed at this time but will form the basis for the proposed physical mechanism in a later chapter. In addition to these later references excellent summaries of nucleation, bubble growth, and the factors affecting growth are given by Ibele (1),* Irvine and Hartnett (2),

---

*Numbers in parenthesis refer to references in the bibliography.

Clark (3), and Kutalatadze (4).

Effect of Gravity Fields

The effect of force fields, either higher or lower than are normally encountered, on the heat flux levels in boiling heat transfer has become the subject of a number of investigations in the past few years. These papers naturally separate into two groups:

a) Low Gravity Effects

b) High Gravity Effects

A list of recent references pertaining to this effect are listed in Appendix A.

Effect of Miscellaneous Fluid Agitation

In the search of the literature several papers were found which dealt with effects of fluid agitation on the nucleate boiling process. These papers can be separated into six groups:

1) Vapor Agitation

2) Mechanical Agitation

3) Ultrasonic Agitation

4) Pressure Agitation

5) Electrostatic Agitation

6) Vortex Agitation

A list of references pertaining to these areas is presented in Appendix B.

Effect of Surface Vibrations

Convective processes such as free convection, forced convection, mass transfer, and nucleate boiling depend on the circulation of the warmer portions of the fluid throughout the cooler regions for the heat transfer mechanism. This transfer mechanism is enhanced by any form of agitation which serves to mix the fluid to a greater extent regardless of the nature of the agitation. In this section the discussion will be restricted to mechanical vibration of the heat transfer surface itself and the effects of this surface vibration on free convection, forced convection, nucleate boiling, and mass transfer will be discussed.

1. Free Convection

In 1938, Martinelli and Boelter (5) performed the initial investigation of the effect of vibration on free convection heat transfer. In their investigation the rate of heat transfer to ambient water from a 0.75 inch diameter horizontal cylinder was measured. This cylinder was vibrated sinusoidally in a vertical direction, with the amplitude of vibration varying from 0 to 0.10 inch and the frequency of vibration from 0 to 50 cycles per second. The temperature difference between the cylinder and the surrounding water was varied from 8 to 45^{o} F.

The experimental results were presented using the Nusselt, Grashof, Prandtl and Reynolds numbers in a dimensionless correlation. The velocity term used in the Reynolds number was the root square velocity of vibration of the cylinder.

In their correlation the Reynolds number had a critical value below which no effect on the rate of heat transfer on the cylinder was found. This critical value was approximately 1000. In this range free convection heat transfer was the controlling mode. As the Reynolds number was increased beyond this critical value, the rate of heat transfer increased with the increased velocity of vibration. At a sufficiently high value of Reynolds number the effect of free convection became negligible and the forced convection due to the vibration controlled the heat transfer.

In addition to the experimental investigation, an analytical solution of the problem of a vibrating body losing heat by free convection was presented for a similar system. Instead of a horizontal cylinder vibrating vertically, the analytical solution used an infinite vertical plate vibrated sinusoidally and vertically. The momentum equation, the equation of heat conduction, and the continuity equation were solved simultaneously with boundary conditions. The solution of this problem resulted in an expression strikingly similar to the experimental correlation. In view of the extensive assumptions made in the derivation of the equation, the agreement between the theoretical solution and the experimental solution was surprisingly good.

In 1955, Lemlich (6) studied the effects of vibration on heat transfer from three wires of different diameters, heated electrically in air. These wires were subjected to transverse vibrations with frequencies from 39 to 122 cycles per second and experienced increases in the heat transfer coefficients up to 400 per cent. The amplitude of vibration was also varied and increases in the coefficient were observed for increased in both the frequency and the amplitude. When the vibrations were changed from the horizontal direction to the vertical direction, no appreciable change in the effect of vibration on the coefficient was noted.

The experimental data was correlated by an equation as

$$\frac{h_v}{h} = 0.75 + 0.0031 \frac{Re_v^{2.05} (\beta \Delta T)^{0.33}}{(Gr\ Pr)^{0.41}} \tag{2-1}$$

The average deviation for the correlation was found to be $\pm$ 13 per cent. The value of the normal heat transfer coefficient, h, may be calculated from any suitable equation for free convection from a stationary cylinder. For a given value of h the average error in the vibratory coefficient, h_v, is approximately $\pm$ 8 per cent. In this equation the Reynolds number is based on the average velocity of the cylinder which is defined by

$$\bar{v} = 4af \tag{2-2}$$

where a = zero to peak amplitude, inches

f = vibrational frequency, cycles per second

Shine (7) investigated the effect of transverse vibrations on the heat transfer rate from a heated vertical plate in air. The temperature of the plate was varied from 131° F to 279° F. The frequency was varied from 11 to 315 cycles per second and the amplitude of vibration was varied from 0 to 0.061 inches. The experimental results were correlated with the intensity of vibration, defined as the product of the frequency and the amplitude of vibration. For intensities less than 1.0 no appreciable effect on the free convection from the plate was noticed. For intensities greater than 1.0, however, the heat transfer showed definite increases with intensity.

Teleki, Fand, and Kaye (8) studied the influence of vertical vibrations on the rate of heat transfer from a 7/8 inch diameter cylinder. The frequency of vibration was varied from 54 to 225 cycles per second and the amplitude was varied from 0 to 0.16 inches. With the temperature difference between the fluid and the surface varying from 15 to 150^{o} F, the heat transfer coefficient experienced increases up to 200 per cent. The increase was found to be a function of the intensity of vibration, which was varied from 0 to 1.1 ft/sec.

Dougall, Chiang, and Fand (9) made a study of the basic equations and the boundary conditions which govern the problem of coupled transverse vibrations and free convection from a heated horizontal cylinder. These equations and their solutions show that four parameters are needed to describe the flow. These are the Prandtl number, the Grashof number, and two vibration parameters. These vibration parameters are the amplitude of vibration to cylinder radius, a/R, and the product of the amplitude and the frequency of vibration, af.

Fand and Kaye (10) studied the effect of horizontal transverse sound fields on heat transfer from a horizontal cylinder. The experimental program yielded the following correlating equation for the heat transfer coefficient.

$$\frac{h_s}{h} = 2.95\ (D)^{1/4}\ (\Delta T)^{1/12}\ (af)^{2/3} \qquad (2\text{-}3)$$

This equation is shown to be a weak function of the temperature difference. Therefore for certain conditions ($D = 3/4$ inch, $\Delta T = 400^\circ$ F, and $af = 1.42$ ft/sec)

$$\frac{h_s}{h} = 3.05 \qquad (2\text{-}4)$$

In other words, the effect of sound is to triple the heat transfer rate.

More recently, Fand and Kaye (11) made an experimental investigation of the influence of vertical mechanical vibrations on heat transfer from a horizontal cylinder. The diameter of the cylinder was 7/8 inch and the ranges of the primary experimental variables were as follows:

1) temperature difference, 25 - 185° F
2) amplitude of vibration, 0 - 0.16 inch
3) frequency of vibration, 54 - 225 cycles per second
4) intensity of vibration, 0 - 1.22 ft/sec

For this case, too, the controlling vibrational variable was the intensity of vibration. For intensities of vibration less than 0.3 ft/sec, the influence of vibration upon heat transfer was found to be negligible. Above this critical intensity, surface vibration was found to increase the heat transfer coefficient. A flow visualization study indicated that the mechanism which caused the observed increase was vibrationally induced turbulence. This turbulent type of boundary layer flow is quite different from the thermo-acoustic streaming which develops near a cylinder in the presence of an acoustically induced horizontal sound field.

The results of their investigation showed that for temperature differences less than 100^{o} F, the heat transfer coefficient is independent of the temperature difference for high levels of vibrations. For temperature differences greater than 100^{o} F and for intensities of vibration greater than 0.9 ft/sec, the following equation applies

$$\frac{h_v}{h} = 3.32 \left\{ \frac{\Delta T}{D} \right\}^{-0.05} (af) \qquad (2\text{-}5)$$

For the conditions ($D = 7/8$ inch, $\Delta T = 100^{o}$ F, and $af = 1.0$ ft/sec) Equation 2-5 reveals that

$$\frac{h_v}{h} = 2.2 \qquad (2\text{-}6)$$

In other words the effect of the vibration of the surface is to more than double the heat transfer rate.

Fand and Peebles (12), (13), made a comparison between the influence of mechanical and acoustical vibrations on the heat transfer from a horizontal cylinder. This comparison led to the conclusion that the physical mechanism of interaction between free convection from a heated horizontal cylinder and horizontal transverse vibrations was essentially the same, whether the vibrations were acoustically or mechanically induced. In addition, the critical intensity, above which the rate of heat transfer increased significantly, was approximately 0.36 ft/sec. This critical intensity did not appear to be a function of the frequency of vibration.

For values of intensity greater than 0.7 ft/sec, Equation 2-3 may be used to compute the rate of heat transfer from a horizontal cylinder for either acoustically or mechanically induced horizontal transverse vibrations. The wide divergence between Equation 2-1 and Equation 2-3, both of which apply to horizontal cylinders subjected to horizontal transverse vibrations, was attributed to the large difference in the ratio of the amplitude of vibration to the diameter of the cylinder, a/D. Lemlich (6), using mechanical vibrations with $a/D = 4.0$, reported results as given by Equation 2-1. Fand and Kaye (10), using acoustical vibrations with $a/D = 0.016$, reported the results as given by Equation 2-3. Fand and Peebles (12), (13), however, used mechanically induced vibrations but with an a/D ratio of the same order of magnitude as Fand and Kaye. Their results were also given by Equation 2-3. It appears, therefore, that the nature of the vibration was not important as long as the a/D ratio was of approximately the same magnitude.

Russ (14), studied the effect of vibration on heat transfer from cylinders in free convection. The cylinders were in transverse vibration with frequencies from 0 to 130 cycles per second and amplitudes from 0 to 0.165 inches. The temperature of the surface varied from 125 to 167° F and the heat transfer coefficient was increased up to 300 per cent with vibration. Several different size cylinders were used including a 1/4 inch and 3/4 inch aluminum cylinder and a small 0.085 inch stainless steel cylinder. All of the cylinders were 10 inches long and were heated electrically. The vibrational intensities extended up to 8.5 inches per second. It was felt that this high value of intensity was mainly responsible for the 300 per cent increase in heat transfer coefficient.

Deaver, Penney, and Jefferson (15), investigated the effect of low frequency oscillations of large amplitudes on the rate of heat transfer from a small horizontal wire to water. Frequencies from 0 to 4.25 cycles per second and amplitudes up to 2.76 inches were employed. Temperature differences up to 140° F provided heat fluxes from 2000 to 300,000 BTU/hr ft^2. A Reynolds number was defined based on the mean velocity of the wire, and it was shown that the heat transfer rates could be predicted by either forced, free, or mixed convection correlations depending on the relative magnitudes of Reynolds and Grashof numbers.

In the free convection region, a good approximation for the

Nusselt number is given by

$$Nu = 1.15 [Gr\ Pr]^{0.15} \tag{2-7}$$

In the forced convection region, the Nusselt number may be estimated by the equation

$$Nu = [0.35 + 0.48\ Re_v^{0.52}]\ Pr^{0.3} \tag{2-8}$$

In the region of mixed convection a good approximation is given by

$$Nu = 0.44 [Gr\ Pr]^{0.5} \tag{2-9}$$

Equations 2-7, 2-8, and 2-9 represent heat transfer in the regions where free, forced, and mixed convection respectively control the rate of heat flow.

Blankenship and Clark (16) made a theoretical study of the effect of transverse oscillations on the free convection from a vertical plate. It was shown that oscillations decreased the steady heat transfer rate for laminar flow. This reduction was thought to be the result of an interaction between the viscous and inertia forces in the laminar boundary layer which caused a net decrease in the convective flow near the plate.

An additional study by Blankenship and Clark (17) reports the effect of transverse oscillations on free convection from a vertical plate. This investigation was of an experimental nature. The experimental heat transfer rate was found to decrease a small but definite amount as a result of the plate being oscillated normal to its own plane for small values of a vibrational Reynolds number. This confirmed the theoretical results of the previous paper.

As the Reynolds number increased, however, a sharp increase was noted in the heat transfer rate. Photographs taken of a smoke study of the flow indicated that a transition from laminar to turbulent flow in the free convection boundary layer was taking place when this increase occurred. This condition is indicated by a critical vibration Reynolds number dependent on the product of the Grashof and Prandtl numbers.

2. Forced Convection

Scanlan (18) studied the effects of vibrating a horizontal heating surface in a direction normal to the surface. For the experimental apparatus, a column of water 4-3/4 feet in height extending to a free surface in a constant head tank was vibrated at frequencies from 20 to 20,000 cycles per second by a variable frequency oscillator. Critical frequencies of 102, 72, and 51 cycles per second were predicted for heating surface total amplitues of 0.001, 0.002, and 0.004 inches respectively. The heat transfer coefficient increased with increasing frequency to a maximum value and then began to decrease again. As the amplitude increased for any given frequency, the heat transfer coefficient again increased. For the higher amplitudes as the frequency increased the heat transfer coefficient increased, dropped sharply, and then began to increase again with increasing frequency.

If the acceleration of the heating surface becomes sufficiently great in the direction away from the liquid, cavitation will occur. The resulting blanketing effect of the cavities would be expected to counteract the increase in the coefficient caused by mixing. Below a certain combination of frequency and amplitude, this blanketing will not occur. Above this point, the blanketing will increase with increased amplitude and frequency as that portion of the cycle during which the critical acceleration is exceeded becomes larger. Only during that half cycle, when the surface is moving away from the liquid, will the surface acceleration be directly effective in creating such a blanket. The dimensions of the flow system will affect the magnitude of the critical frequency at which the blanketing will begin. The physical properties will enter into the situation as will the contours, rigidity, and other properties of the containing walls.

Any dissolved gas in a liquid will encourage the breaking away of the liquid from the surface, lowering the critical frequency. Surface roughness or any other type of physical discontinuity also will encourage rupture of the liquid to surface interface. Surface tension will discourage the formation of voids. There is an upper limit above which the benefits due to vibration may decrease as the blanketing portion of each oscillatory cycle becomes larger.

Sreenivasan and Ramachandran (19) studied the effect of vibration on heat transfer from horizontal cylinders to an air stream flowing normal to it. The cylinder was made of copper and horizontally oriented. It was six inches long and was 0.344 inches in diameter. The cylinder was placed normal to an air stream and was sinusoidally vibrated in a direction perpendicular to the direction of the air stream. The flow velocity varied from approximately 19 feet per second to 92 feet per second and the double amplitude of vibration varied from approximately 0.3 to 1.2 inches and the frequency of vibration varied from approximately 3 to 47 cycles per second. When vibrational velocities as high as 20 per cent of the flow velocity were imposed, no appreciable change in the heat transfer coefficient was observed.

3. Boiling

Kovalenko (20) performed a preliminary experimental investigation to study the effect of vibrations on the boiling process. A copper tube was vibrated in the frequency range from 0.2 to 0.85 cycles per second, and the heat transfer rates to boiling water flowing in the tube were studied. For the most part the heat transfer coefficients were shown to decrease in the heat flux range from 4000 to 24,000 $kcal/m^2\,hr$. Slight increases in the heat transfer coefficients were noted in the heat flux range from 4000 to 6000 $k\,cal/m^2\,hr$ but were not considered promising enough to continue the study. Due to the unique nature of the geometry of this problem and the low frequencies involved, no significant comparisons can be made with the present investigation.

After a complete and thorough search of the literature, this was the only investigation of which the author has knowledge that deals with the interaction of surface vibration and nucleate boiling. The geometry and mode of vibration prevent any conclusions from being formed as to the effect of surface vibration with the geometry being used in the present investigation.

4. Mass Transfer

Lemlich and Levy (21) studied the effect of vibration on natural convective mass transfer. Small horizontal cylinders subliming to room air were vibrated in a vertical direction at 20 to 118 cycles per second. Increases of up to 660 per cent in the coefficient of mass transfer were observed. The coefficient of mass transfer increased with both the frequency and amplitude of vibration, but it was the amplitude of vibration which appeared to have the more pronounced effect in this case.

Jameson (22) studied the effect of vibrations on the mass transfer from cylinders composed of benzoic acid and a glycerol-water solution. The cylinders were approximately 0.43 inch in diameter and were vibrated at three amplitudes which resulted in three values of the ratio of the amplitude of vibration to the radius of the cylinder, a/r, equal to 0.102, 0.198, and 0.298. The frequency was varied over a range of values which gave vibratory Reynolds numbers up to 100. This experimental data was correlated by the mass transfer equation

$$Sh = 0.746\, Re_v^{1/2}\, Sc^{1/3} \left(\frac{a}{R}\right)^{1/6} \tag{2-10}$$

or by the analogous heat transfer equation

$$Nu = 0.746\, Re_v^{1/2}\, Pr^{1/3} \left(\frac{a}{R}\right)^{1/6} \tag{2-11}$$

This vibration yielded up to 28 times the free convection mass transfer rate.

CHAPTER III

EXPERIMENTAL PROGRAM

To study experimentally the effect of surface vibration on nucleate pool boiling, a convenient physical model was chosen. A horizontal cylinder with an internal electrical heater was immersed in a tank of water at saturation conditions. Power was supplied to the test section by a variable output transformer giving heat fluxes in the nucleate boiling range. The temperatures of the heat transfer surface and the water in the test tank were measured with thermocouples and recorded. The measurement of these quantities allowed the determination of the normal heat transfer coefficient.

A specially constructed vibration apparatus vibrated the cylinder in a vertical direction transverse to its axis. The frequency of the cylinder was controlled by varying the speed of the varidrive motor. The amplitude was controlled by a vibration head which changed the position of the output shaft. The variation of these two vibratory variables allowed a study of the effect of vibration on the heat transfer coefficient.

In the following sections the experimental equipment is described along with the instrumentation employed to take the required measurements. The procedure for operating the equipment is also described and wiring diagrams are included. Finally the sources of experimental uncertainty in the experimental program are discussed and analyzed.

Experimental Apparatus

The experimental apparatus used in this investigation was designed to study the effect of vibration on nucleate boiling heat transfer. The apparatus, therefore, consisted of a vibration device, an instrumented test section, a test tank, and the necessary control and measurement instrumentation. In the following sections the apparatus is described in greater detail.

1. Vibration Apparatus

The vibration apparatus was entirely mechanical in nature. The rotary motion produced by a U. S. Motors Varidrive high speed, variable speed motor was transmitted to the vibration head through a long shaft. The shaft ran through two SKF high speed, pillow block bearings mounted on a stand in front of the motor. The stand hung over the water test tank in such a way that the test section was located in the center of the tank. The vibration head was mounted to the end of the shaft by means of a threaded coupling brazed to the shaft. Plate I shows this apparatus clearly.

The vibration head consisted of an input shaft which was centered on the shaft of the motor. The output shaft could be varied to a position which was eccentric to the center line of the rotary motion. The

PLATE I
Vibration Apparatus

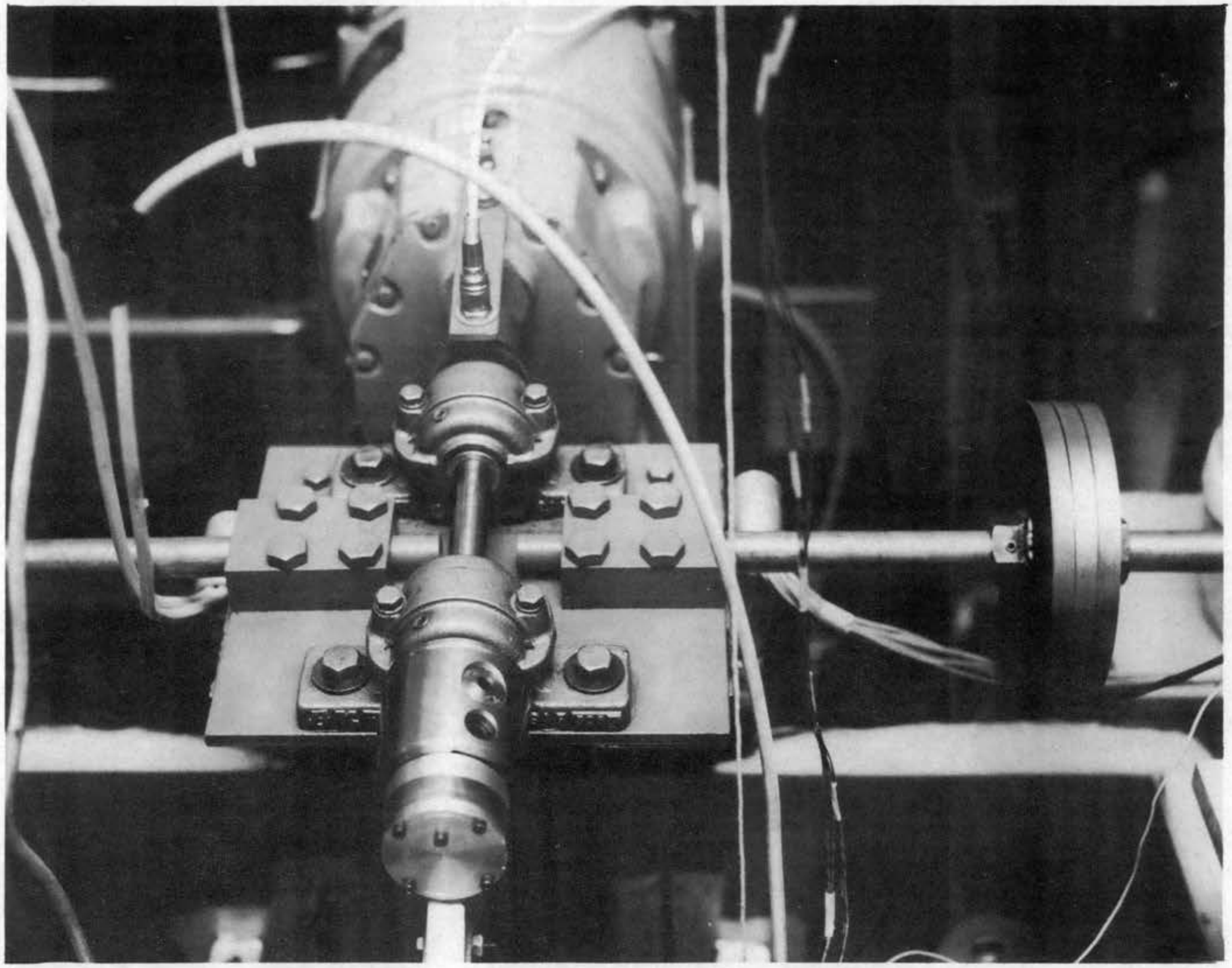

amount of eccentricity was controlled by a micrometer adjustment with the micrometer dial graduated in thousandths of an inch. The output shaft was connected to the yoke of the apparatus by an SKF high speed bearing pressed into a steel housing and enclosed by a solid aluminum plate on one side and an aluminum plate with a grease seal on the other. This specially constructed housing provided lubrication for the bearing while at the same time allowing the rotary motion to be changed to a vertical motion. This was accomplished by bolting the bearing housing to a flexible connecting arm which ran from the vibration head to the vibration yoke.

Before further construction, the entire system was aligned and balanced. The pillow block bearings and the coupling were adjusted so that the shaft ran true and system vibrations were at an absolute minimum. The vibration head was balanced on a highly sensitive balancing machine. This was necessary due to the non-symmetrical construction of the vibration head. Holes were drilled and tapped in the lighter side of the head and washer shaped weights were added at four separate points on the surface. Four points were necessary since rotary forces made necessary an angular balance and cantilever type torque forces necessitated a longitudinal balance.

The flexible connecting arm was constructed of three plates 1/8 inch thick and 4 inches wide, one spaced on each side of the bearing housing and one mounted in a slot milled in the center of the flange. The three plates were spaced approximately 1/8 inch apart.

The vibration yoke was very simply constructed. A 1/4 inch plate, approximately 18 inches long served as the base with two arms, one on each end, bolted to the plate on the bottom. Located at the top center of the plate were two mounting plates with angle braces to which the flexible connecting arm was bolted. These were welded to the plate. Plate II shows this construction in detail.

The two connecting arms were constructed of 5/8 inch hollow stainless steel tubing plugged at one end and with a flange welded to the other end for mounting to the main piece. The arms were hollow so that the power leads and thermocouple wire could be run to the test section. The arms were 15 inches long with a 5/8 inch hole drilled in the inside face of the tube 7 inches from the top to allow the wires to turn to the interior of the test section. On each arm two mounting brackets were welded, one 3 inches from the top and the other 2.5 inches from the bottom. These were used in the mounting procedure to insure vibration in a vertical direction. This orientation and the overall construction of the arm is seen in Figure 3-1.

Also shown in Figure 3-1 is the connecting flange by which the test section was properly positioned on the vibration yoke arms. This connecting flange consisted of two parts, each identical to the other except for the hole mated to the one in the side of the arm. These pieces were machined to fit the surface of the arm with bolt holes in each piece that matched the holes in the flange of the test section. The test section was thereby mounted firmly between the two arms of

PLATE II
Vibration Yoke and Test Section

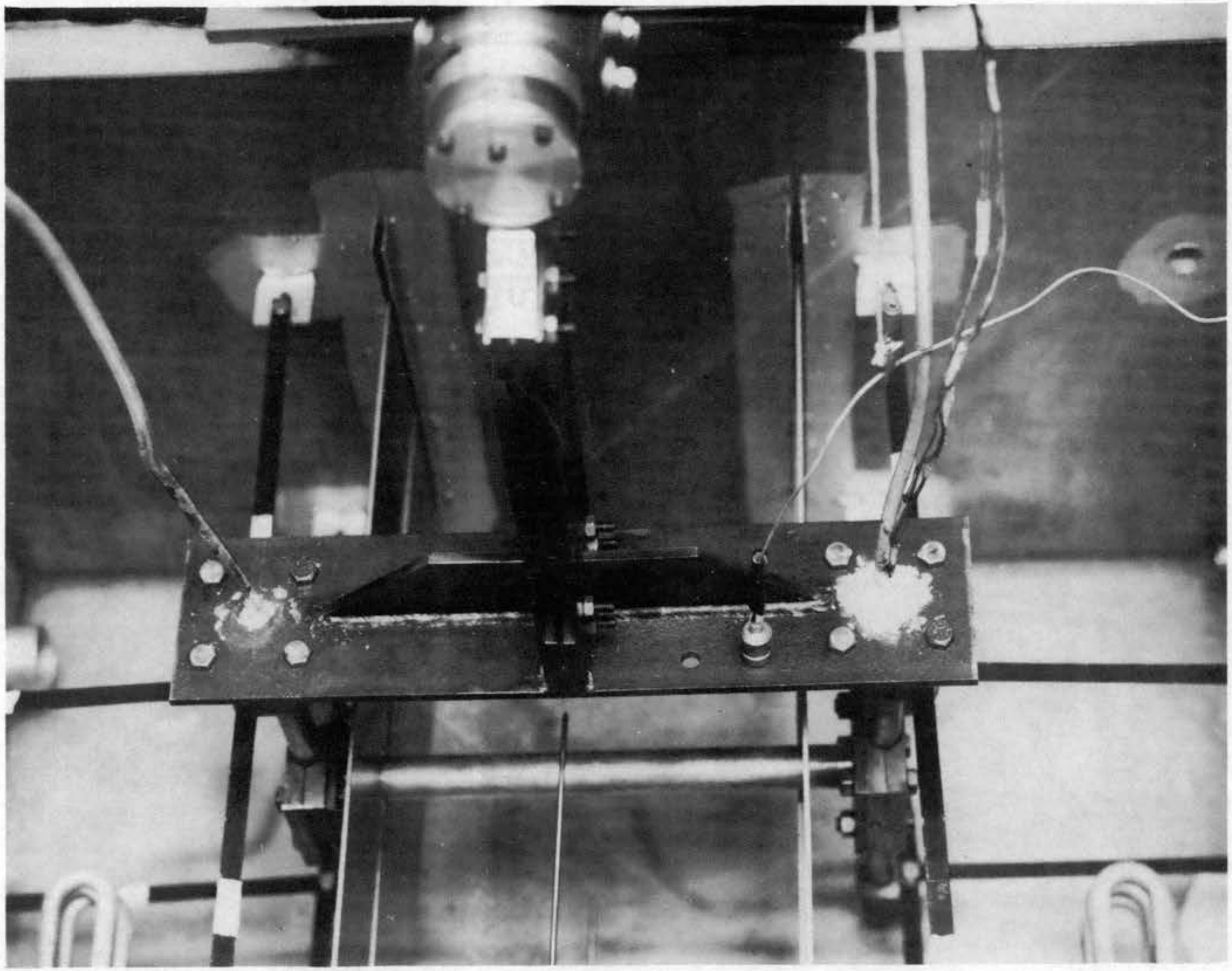

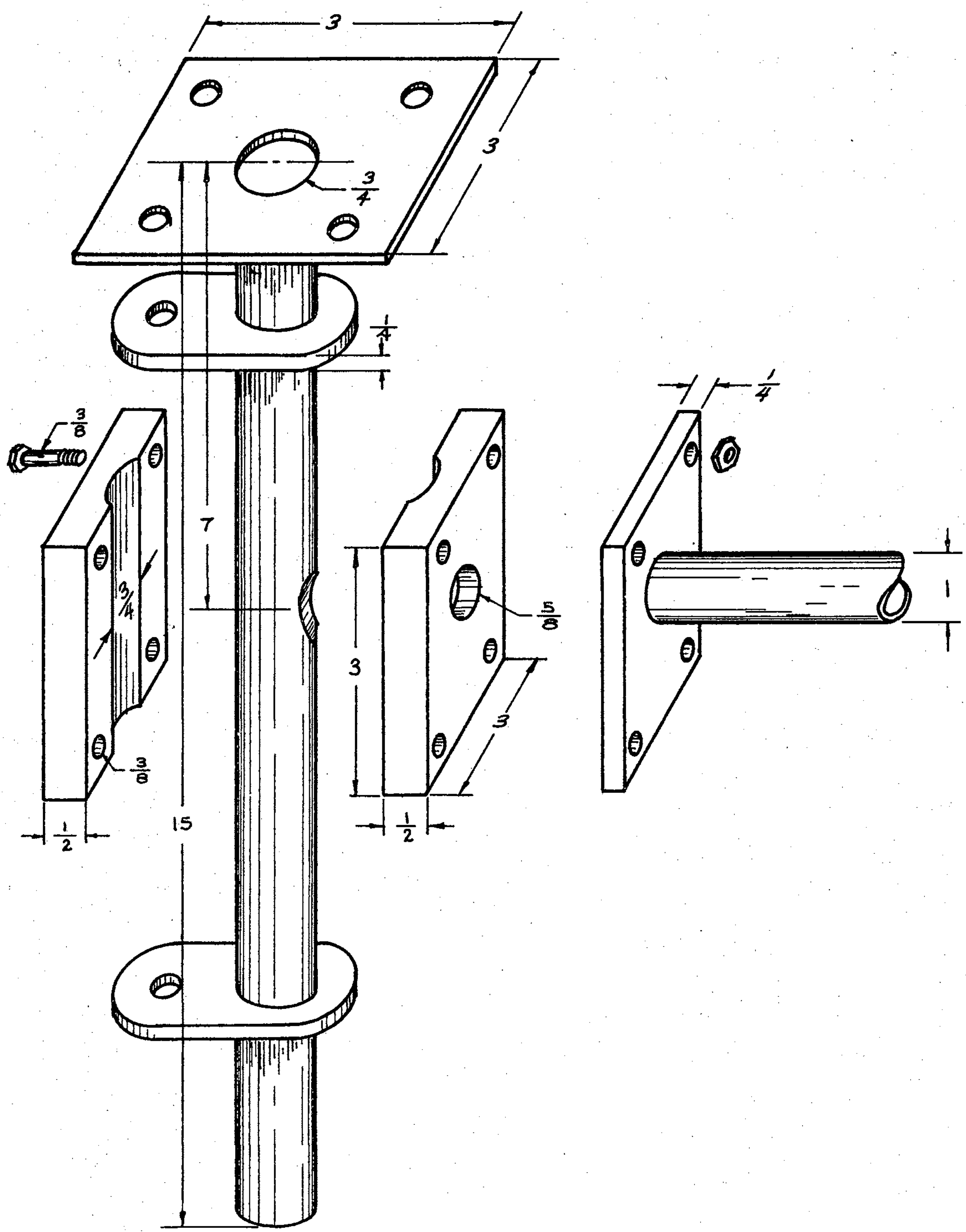

Figure 3-1. Assembly Drawing of Test Section and Yoke Arm Apparatus

the yoke. The entire assembly was sealed to prevent the entrance of water to the interior.

The entire yoke apparatus was held in place in the test tank by special connections at the top and bottom of the vertical arms. The connecting points can be seen in Figure 3-1. At each connection point the yoke was connected to the sides of the tank in three directions by a thin flexible connecting arm. This insured the vertical vibration of the test section. Were it not for these connections, the test section would not vibrate in a controlled manner.

In order to provide a sinusoidal vibration of the test section with as few other vibrations as possible, an analysis was made of the forces generated in the vibration system by the accelerations involved. It was found to be impractible to attempt operation under the force imbalance which was present. As solution to this problem, a vibration absorber was designed and constructed. It consisted of two cantilever arms with adjustable weights. One was mounted rigidly to each side of the same vibration stand on which the shaft and bearings were mounted. These weights could be adjusted as the frequency changed so that the vertical forces generated by the vibrating test section were at all times balanced and their effect nullified.

2. Heat Transfer Test Section

The test section consisted of a cylinder 12 inches in length with a flange silver soldered to each end. These flanges were mentioned earlier and may be seen in Figure 3-1 shown previously. The cylinder was made of copper and had an outside diameter of 1.0 inch and an inside diameter of 0.875 inch. Heat was generated internally by an electrical heater. The design of the internal electrical heater is discussed in Appendix C.

The heater was constructed of a ceramic base with heater wire wrapped tightly around it for a length of 7 inches. Power was supplied to the heater wire through power leads leading to copper plugs which are silver soldered to the heater wire at each end of the heater. The heater element was completely encased in Sauereisen electrical cement. This construction is shown in Figure 3-2.

The electrical cement prevented the electrical current from shorting through to the copper cylinder and yet allowed the heat to flow radially from the heater element to the water through the copper cylinder. At each step in the construction, the cement was allowed to cure in an oven at 120° F so that it would harden to a solid homogeneous mass through which heat might be conducted.

Figure 3-2 also shows the placement of the thermocouples used to measure the surface temperature of the cylinder. Four thermocouples, spaced at 90 degree intervals around the cylinder circumference, were silver soldered to the cylinder surface. The thermocouples were placed in a small hole drilled in the surface, and then silver soldered in place. These thermocouple readings were corrected for the conduction through the cylinder wall since the measurement is

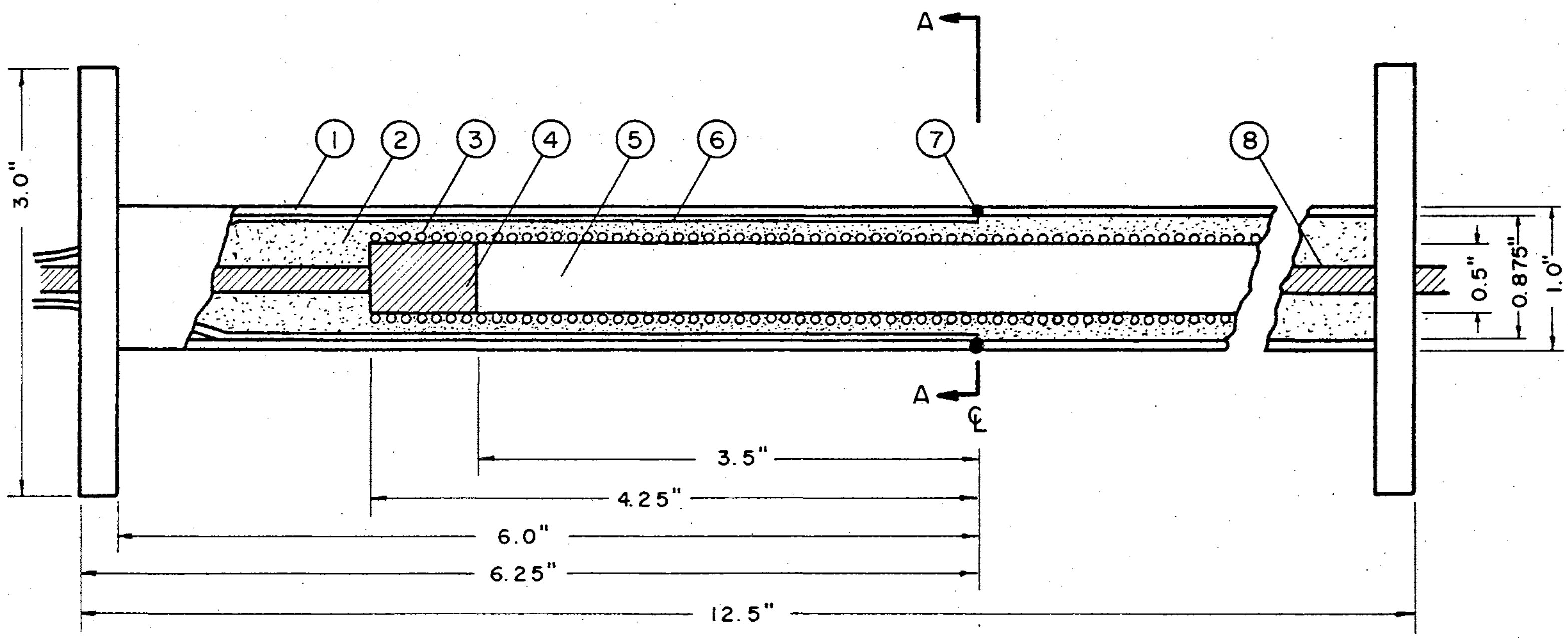

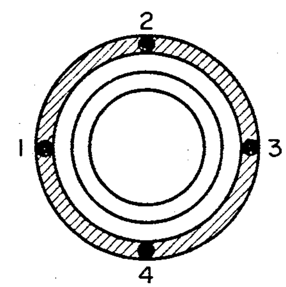

A-A
THERMOCOUPLE LOCATIONS

① COPPER CYLINDER
② SAVEREISEN CEMENT
③ NICHROME WIRE
④ COPPER PLUG
⑤ CERAMIC CORE
⑥ THERMOCOUPLE WIRE
⑦ THERMOCOUPLE JUNCTION
⑧ ELECTRICAL LEAD WIRE

Figure 3-2. Heat Transfer Test Section

actually that of the inside surface temperature. A discussion of the temperature distribution in the cylindrical test section and a calculation for the correction to the thermocouple readings is also presented in Appendix C.

3. Heat Transfer Test Tank

The test tank was made of stainless steel and was 24 inches wide and 36 inches long. The tank was 20 inches deep with two 4500 watt Chromolox immersion heaters mounted in the front. Also mounted in the front of the tank were two Minneapolis Honeywell Regulator Co. Megapak thermocouples which measured the temperature of the water in the tank.

Guide vanes were welded inside the tank and fluid baffles mounted in them to separate the test section from the currents generated within the tank. On the sides of the tank 12 flanges were welded which served as mounting brackets for the vertical guide arms which extended from the vibration yoke. These are shown in Plate II which shows the vibration yoke, the heat transfer test section and the inside of the test tank. Figure 3-3 shows a transparent view of the vibration yoke, test section, and their orientation within the tank. Plate III pictures the entire apparatus including the varidrive motor, test tank and the support base for this equipment. The entire apparatus was mounted on a heavy base comprised of four I-beams. The two largest I-beams were placed several feet apart and transverse to the shaft of the motor. These

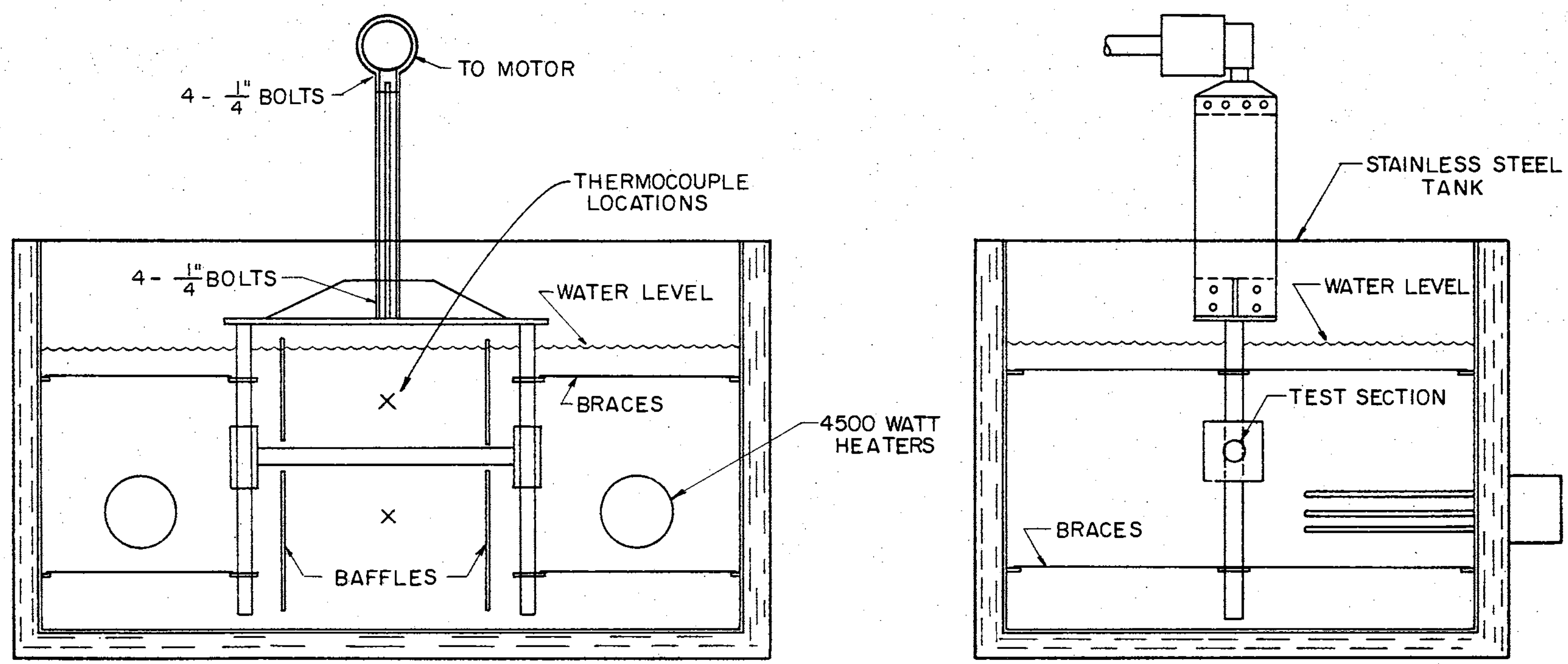

Figure 3-3. Test Tank and Test Section Orientation

PLATE III

Test Tank and Assorted Equipment

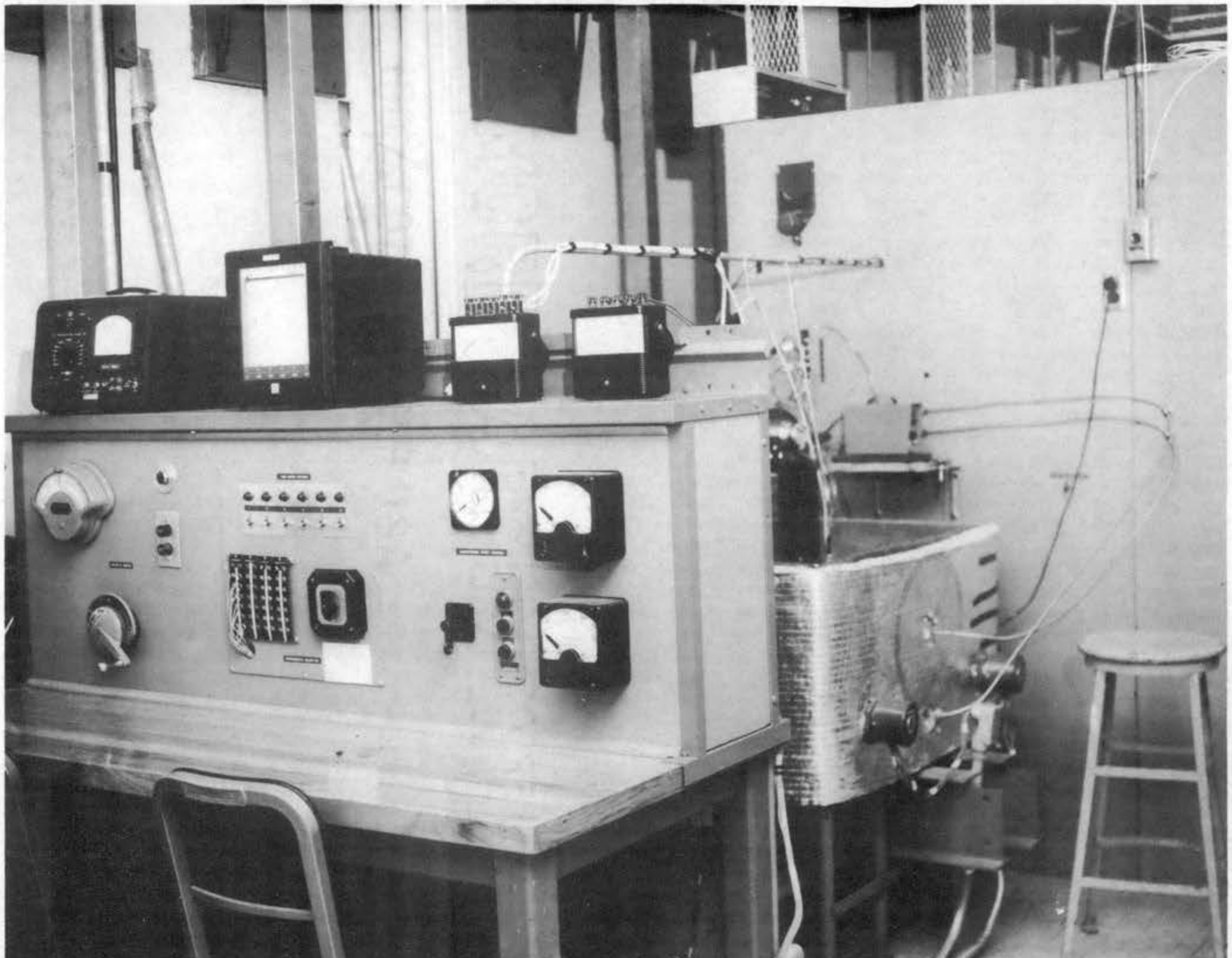

beams were isolated from the cement floor by a one inch thick felt pad. Two smaller I-beams were bolted to these beams and ran parallel to the shaft. Mounted to these smaller beams were the varidrive motor and the vibration stand. The test tank was mounted on a separate stand so that there was no contact between the tank and the I-beam base.

In order to prevent excessive moisture loss from the tank in the form of steam, it was necessary to install a cover on the tank. The cover was fabricated from 16 gauge copper flashing in such a way that it could be easily removed for cleaning the tank. It was also canted in such a way that condensing steam returned to the tank and very little makeup water was necessary.

During the heatup period the heating process was made more effective in providing uniformly heated water in short periods of time by the use of a propellor blade mounted on a shaft and attached to a motor which turned at approximately 1700 revolutions per minute. The temperature of the water in the tank was, therefore, uniform. This was substantiated by the measurements of the thermocouples installed in the tank. When measurements were to be taken, the motor was turned off and the currents allowed to subside. By this method a uniform temperature was achieved without disturbance to the test section.

4. Test Tank Viewing Chamber

In the course of the investigation, visual observations of the test section indicated a need for photographic data concerning the effect of vibration on boiling. In the front of the tank directly opposite the cylindrical test section, a window was installed for viewing the test section. Figure 3-4 is an assembly drawing of this viewing chamber. It consisted of a 6 inch I. D. aluminum tube approximately 10 inches in length with a flange welded to either end. Flange No. 1 was for mounting purposes only. Holes were drilled in the side of the tank to match the holes in the flange and a rubber gasket was used to seal the opening. Flange No. 2 was welded to the tube at the other end and had a groove machined to fit the 1/4 inch viewing glass. Flange No. 3 also had a machined groove on one side. Gasket material and a rubber sealing cement provided an effective sealant against the seepage of water from the tank. Plate IV shows a view of this from the outside of the tank.

The dimensions of this viewing chamber were such that a 5.5 inch diameter viewing window was available a distance of less than two inches from the surface of the cylinder. This arrangement provided an excellent view of the boiling process.

5. Photographic Equipment

A Wollensak Fastax High Speed Motion Picture Camera Model WF-4ST was used to take 16 mm pictures of the boiling process. The camera lens was located about 30 inches from the object. The camera was operated and controlled by a Wollensak WF 301 Fastax Control

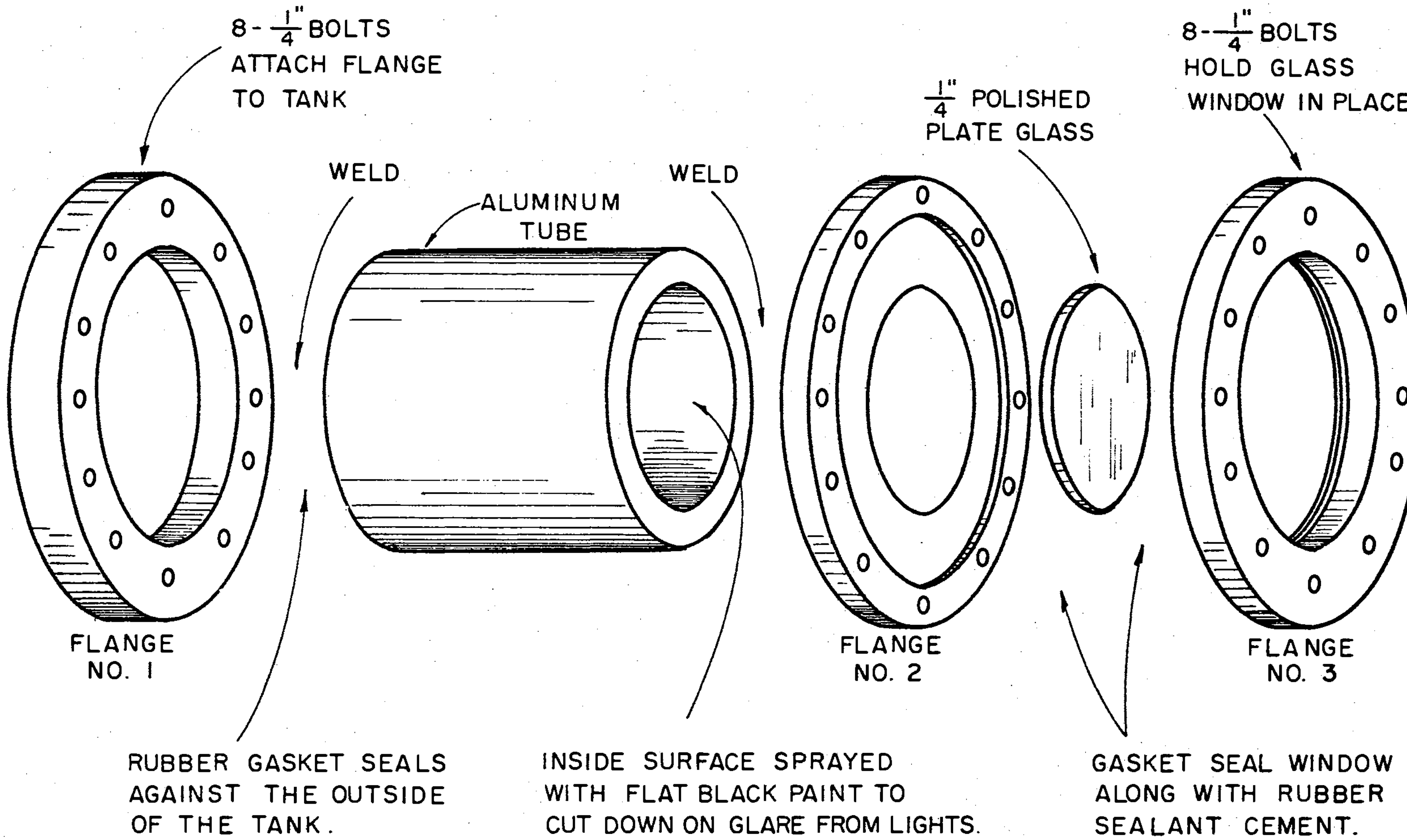

Figure 3-4. Assembly Drawing of Viewing Chamber

PLATE IV
View of Test Section Through Window

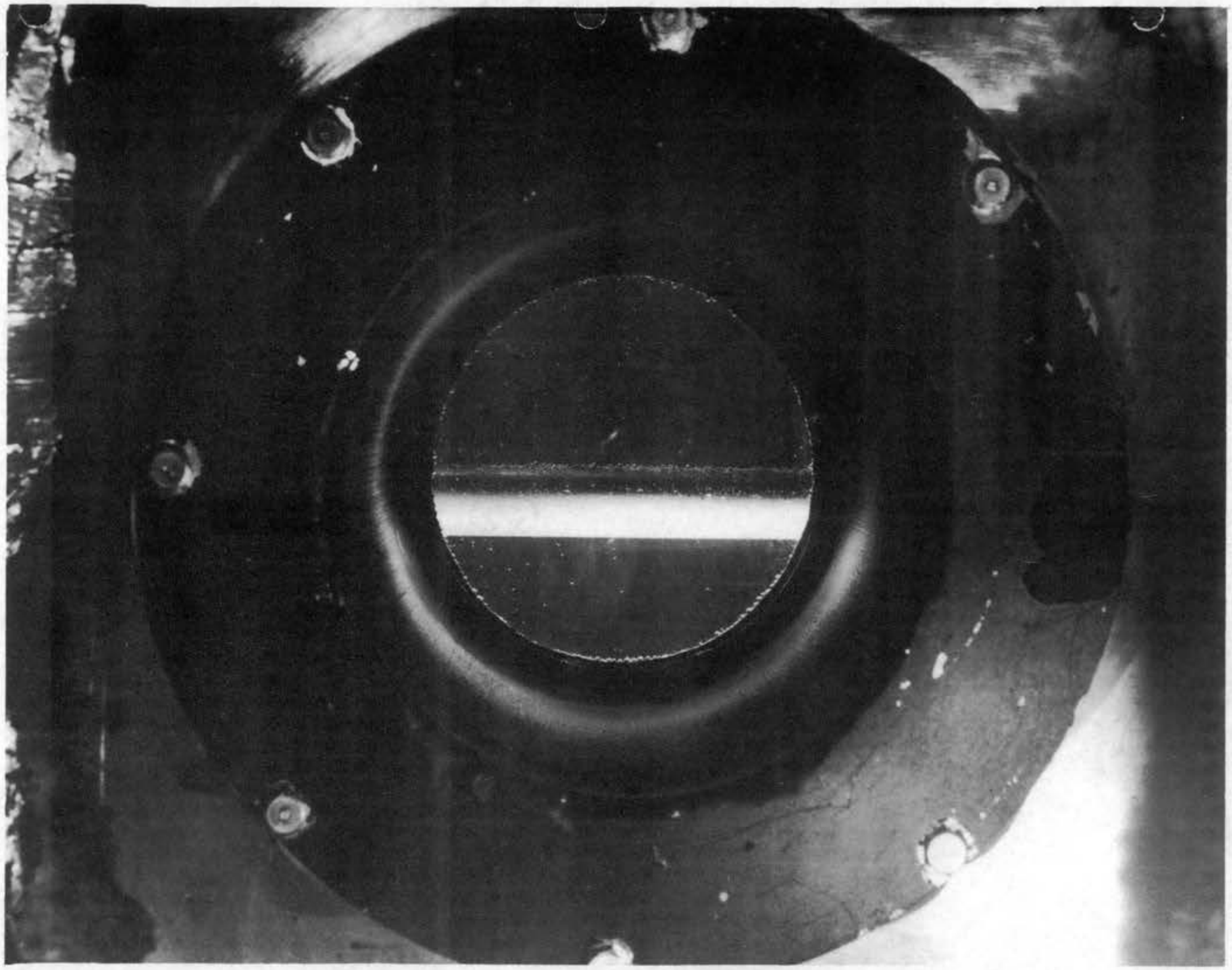

Unit. This unit was used, in this instance, only as a means of controlling the camera speed by varying the input voltage to the camera. It can, in some applications, be used to synchronize with the event to be photographed. Plate V shows the camera mounted in position before the tank. Beside the camera is the control unit used to control the speed of the camera.

The lighting for the photography was provided by two Sunset Zoom Gun 650 watt lamps positioned over the tank in such a way that they focused on the test section. The two beams overlapped to prevent shadows and provide even lighting. When the photos were taken, the bottom of the tank and the baffles at either end of the test section were covered with aluminum foil to take advantage of all available light. It was still difficult, however, to get enough light on the test section, especially the bottom, due to the covering of water between the lamps and the test section.

6. Power Supply

A Lincoln A. C. arc welder was used as the power supply for the test section. The power leads ran from the welder to a bus bar where one leg was connected to a current transformer which supplied the current for the control panel ammeter. The power leads then went through a magnetic switch box which was energized by a manual switch supply 220 volt power to the coil. In the off position, the switch prohibited power from reaching the test section. This was used solely

PLATE V
High Speed Camera Placed Before Viewing Window

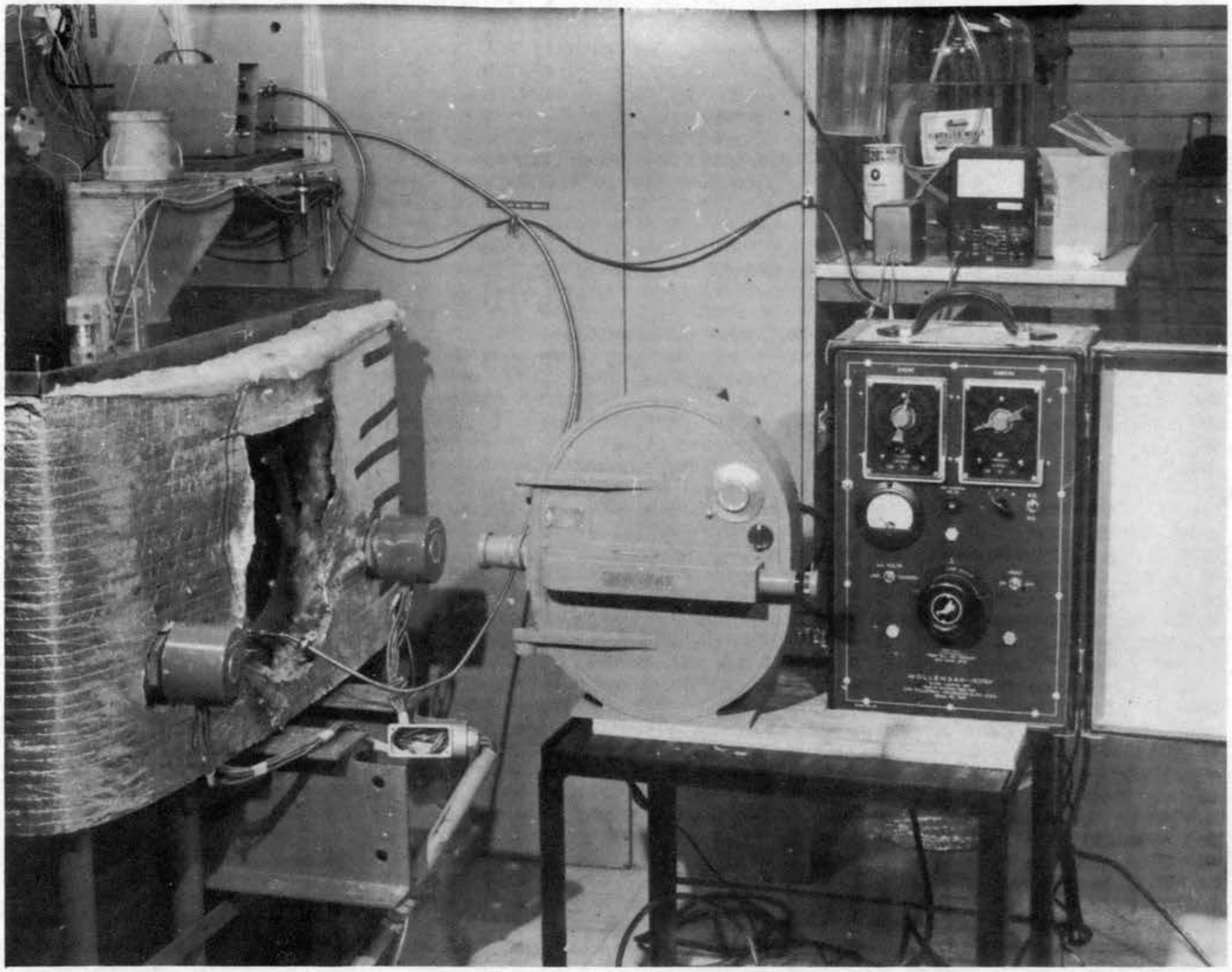

as a safety device. The power leads then went to a final bus bar where the voltage was measured before the leads went into the test section.

The power transformer was controlled from the remote panel with an on-off switch and a remote switching circuit. The minimum amperage from the transformer was approximately 44 amps. A single variable switch was used to increase the amperage from this value to the maximum value corresponding to resistance of the test section and the maximum closed circuit voltage of 40 volts. For currents lower than 44 amps a parallel switching circuit allowed two variable resistors to vary the current through the test section from zero to 44 amps. By this method a complete range of heat fluxes were available. A wiring diagram will be presented later and the operation of this parallel circuit will be discussed in detail.

An overall wiring diagram showing all power wiring except the control and measurement circuit for the test section is given in Figure 3-5. Shown are the fused switch box which supplied all electrical power, the circuitry for the varidrive motor, the wiring for the water tank heaters, and the control circuit for the AC power supply.

Instrumentation

The instrumentation in this investigation measured the variation in five basic variables. These are discussed in detail in the following sections.

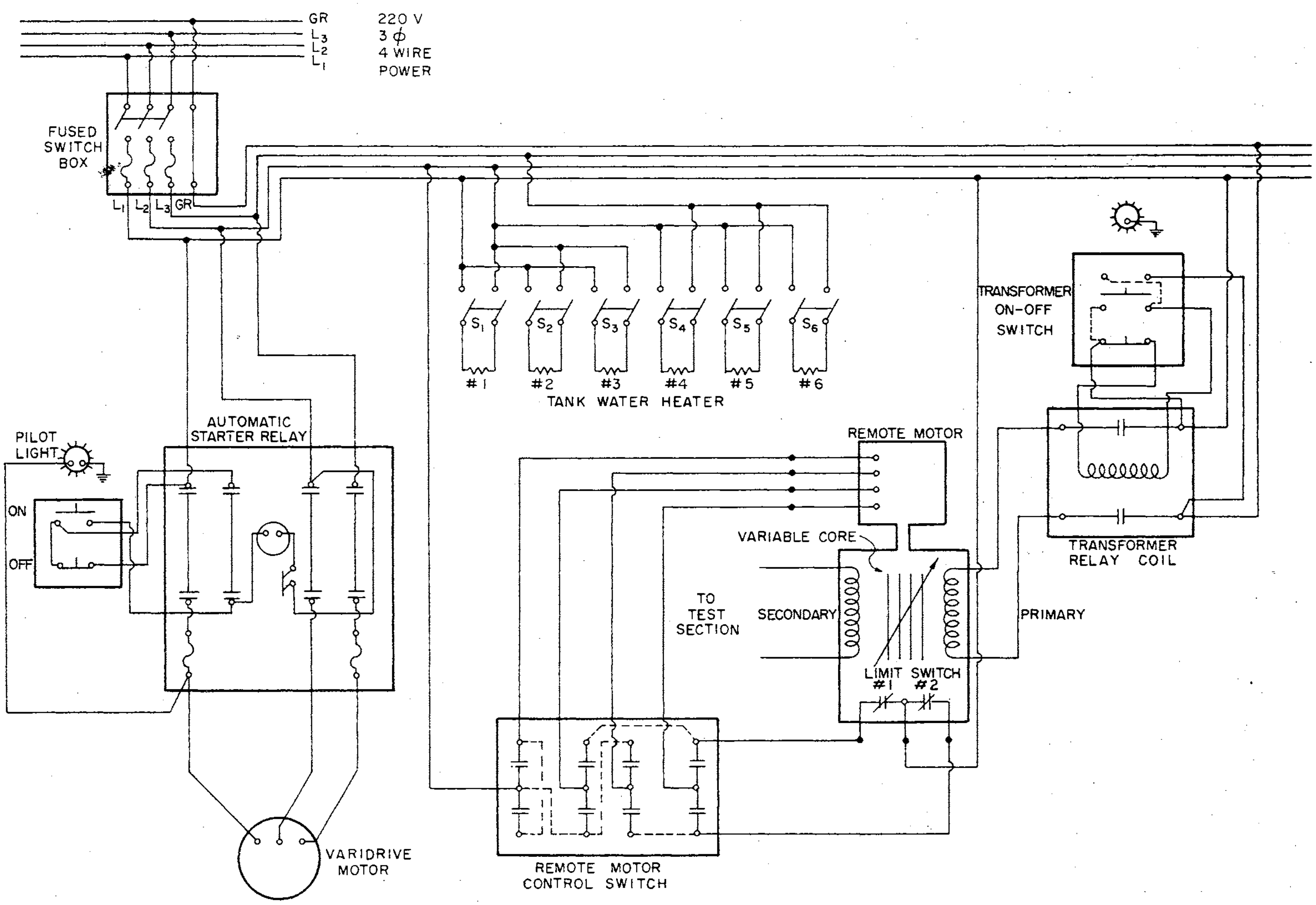

Figure 3-5. Electrical Wiring Diagram

1. Temperature

The surface temperature of the test section was measured using four thermocouples mounted in the surface of the cylinder. The temperature of the water was measured by two Megopak thermocouples mounted in the wall of the tank. The signal from these thermocouples was recorded by a Leeds and Northrup Speedomax H Azar recorder with the thermocouples selected by a thermocouple selection switch mounted on the control board. The calibration of the thermocouples is discussed in Appendix D, and the calibration of the recorder is given in Appendix E. The location of these thermocouples has been previously discussed.

2. Power

The power dissipated in the test section was calculated as the product of the current flow through the test section and the voltage drop across it. The current was measured by a Weston Model 904 AC Ammeter and the voltage was measured by a Weston Model 904 AC Voltmeter. The accuracy of these instruments was given by the manufacturer as 0.5 per cent of full scale. The power measurement circuit is shown in Figure 3-6.

3. Frequency

The frequency of vibration of the test section corresponded to the frequency of rotation of the shaft which transmitted power from the motor to the vibration head. A small gear was attached

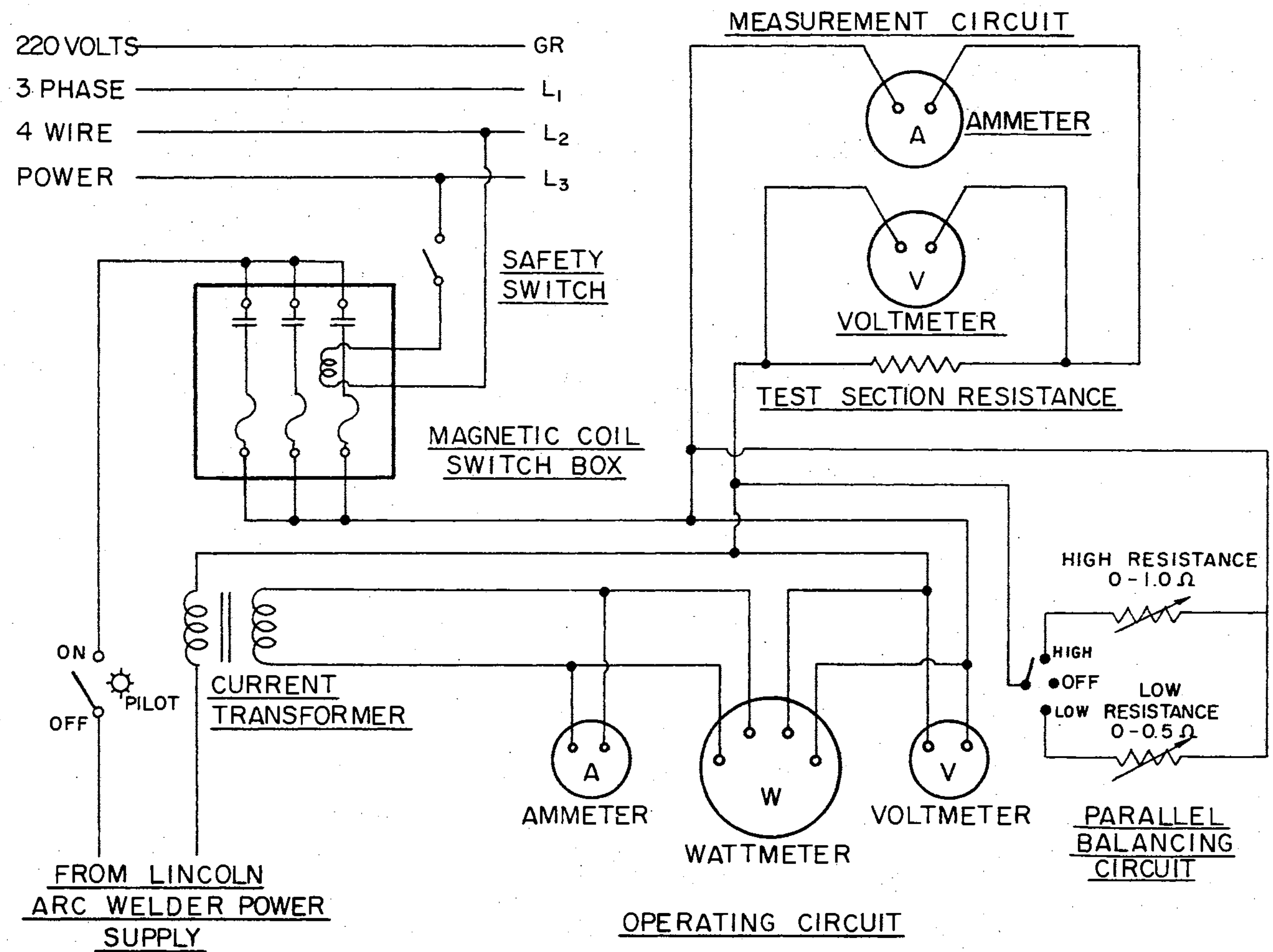

Figure 3-6. Test Section Power Circuitry and Instrumentation

to this shaft and an Electro 3030 magnetic pickup pulse generator was mounted close to the teeth of the gear. Each time the shaft made a complete revolution, the pickup device generated 80 pulses corresponding to the 80 teeth on the gear. These pulses were amplified by a Hewlett-Packard amplifier and counted by a Berkeley EPUT counter. This measurement circuit may be seen in Figure 3-7.

The counter was calibrated against WWV Radio for its frequency response and found to be within acceptable limits. The accuracy of the frequency measurement was increased even more by the fact that the reading from the counter was the number of cycles per second of the shaft multiplied by 80. The counter would have to have an error of 80 counts for an error of one cycle per second to be present in the actual frequency.

4. Amplitude

The amplitude of the test section was measured by a Schaevits linear variable differential transformer. The signal generated by the differential transformer was proportional to the displacement of a movable core and was indicated by a Ballantine Model 320 true root mean square electronic voltmeter. This same signal was displayed on a Textronik Type 502 dual beam oscilloscope.

The differential transformer consisted of two separate parts, the stem and the core. The movable stem was screwed into a

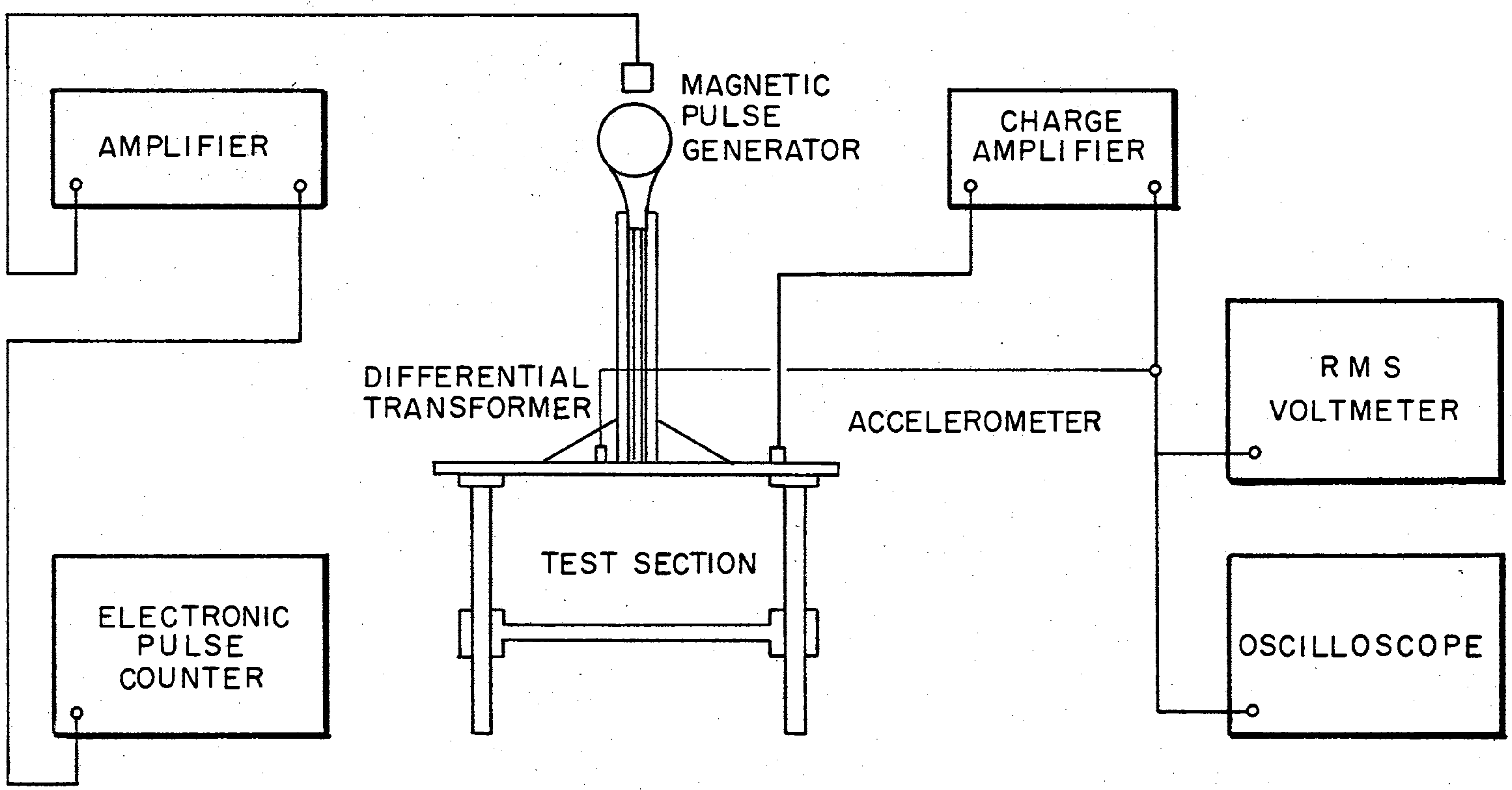

Figure 3-7. Frequency and Acceleration Measurement Circuitry

plexiglass mounting block which was bolted to the top of the vibration yoke at the center of the test section. This center position was the most accurate place to take the measurements. The fixed core was mounted to an aluminum frame by plexiglass, "split" blocks in order to hold it steady and keep it insulated from its surroundings and free from magnetic influences. Also mounted in this frame were female connections which were wired to the fixed core. The two input wires supplied a 6.8 volt A.C. signal from a regulated power supply. This input voltage was monitored by a Simpson volt-ohm meter. The two output wires extended to the Ballantine A.C. voltmeter and the monitoring oscilloscope. The entire fixed core apparatus was mounted on a plywood frame extending from the nearby wall. The frame was adequately braced and had a wire adjustment mechanism so that the position of the fixed core could be minutely adjusted to give the proper signal. If the core had not been adjusted properly, the signal would have been too large. Plate VI shows a view of the mounting of the differential transformer.

The calibration and operation of the differential transformer is discussed in detail in Appendix G. The method of using the differential transformer to measure amplitude in this specific application is discussed in the section concerning the operating procedure of the equipment. This measurement circuit may also be seen in Figure 3-7.

PLATE VI
Differential Transformer Mounted on the Vibration Yoke

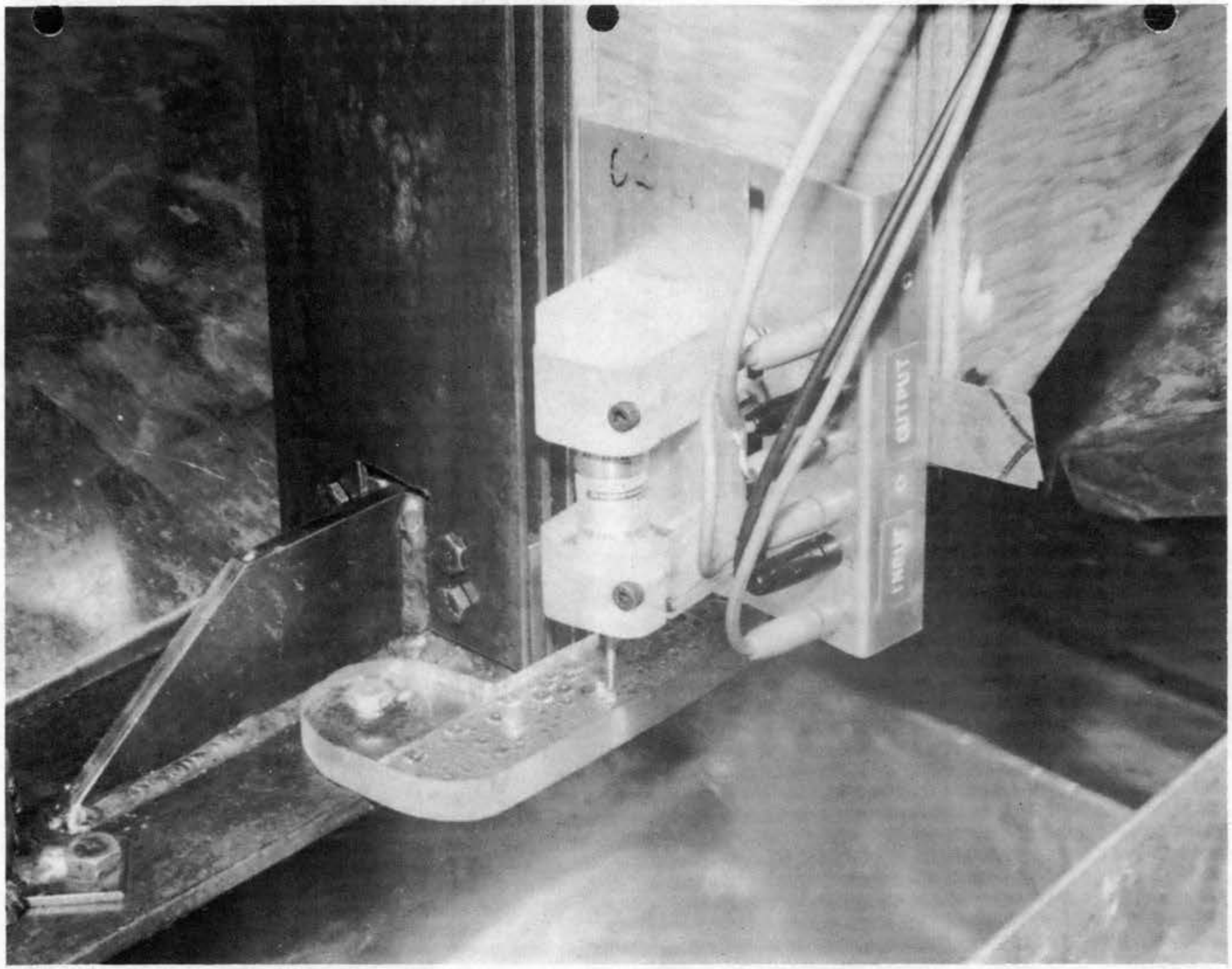

5. Acceleration

The measurement of the test section acceleration was accomplished with a Kistler Model 812 quartz accelerometer. The signal generated by the quartz accelerometer was an electrostatic charge proportional to the applied acceleration. A special Kistler Model 568 electrometer charge amplifier converted the charge signal to a voltage signal suitable for display on an oscilloscope and an indicating instrument. A Textronik Type 502 dual beam oscilloscope was used to view the wave pattern and the voltage was indicated by a Ballantine Model 320 true root mean square electronic voltmeter.

This measurement circuit may also be seen in Figure 3-7. The calibration of the accelerometer and other instrumentation associated with the acceleration measurement is discussed in detail in Appendix F.

Equipment Operating Procedure

In this section the procedure for starting and operating equipment is described in detail so that the equipment may be operated in the future with safety and accuracy. In addition, the method for recording data in an orderly and accurate manner is described.

1. Starting Procedure

The starting procedure was simple in content but a very long and tedious task. The steps were very methodical and are listed as follows:

a) turn on all recording equipment

b) clean out test tank

c) polish test section

d) fill tank with 55 gallons of distilled water

e) turn on tank heaters

f) prepare ice bath for thermocouple reference junction

g) place cover on test tank

h) start circulating propellor motor

Approximately five hours were required for the water to reach saturation conditions. During this period and during tests makeup water was necessary to maintain the proper water level.

2. Test Section Heater Operation

The current for the test section heater was supplied from the welding transformer and was controlled from the main control panel. Before the transformer was available for operation, however, the safety switch which energized the coil in the magnetic switch box had to be turned on. Then the control knobs for the parallel switching circuit resistors were turned to indicate minimum resistance and the circuit switch was turned to indicate that the low resistance circuit was energized. At this point the transformer was turned on. The indicator light for the transformer was energized; and the current through the test section, as indicated by the ammeter, was zero or close to it. The current was slowly increased by increasing the resistance in the low resistance circuit. When the knob was rotated clockwise to its maximum position, the parallel circuit switch was switched to indicate that the high resistance circuit was energized. If the knob was in the properly indicated position, the current through the test section neither increased nor decreased. To increase the current, the knob was turned in a clockwise manner slowly to its maximum position. When this had been achieved, the parallel circuit switch was rotated to the "off" position and the parallel circuit was no longer in the line. The current through the test section was approximately 44 amperes. To increase the current further, the transformer was controlled carefully by the crank handle on the transformer shaft or grossly by the motor control switch on the control panel. The current never exceeded 160 amps and care was taken when the current exceeded 100 amps. Sudden increases or decreases in current were not tolerated. During the course of normal increases in current care was always taken to note the range setting on the ammeter and never exceed the limits of the meter.

3. Test Section Vibration Operation

Due to the nature of the vibration device and the controlling mechanism, the vibration absorber, the vibrator should be operated very carefully. Since the location of the weights for the vibration absorber was a function of frequency only, it should be set first. This and succeeding steps are given as follows:

a) decide on the frequency of operation

b) consult Figure 3-8 for the length of the cantilever arm corresponding to the frequency of operation

c) Set the combined weights on each cantilever arm so that the distance from the enge of the cantilever to the center of mass of the weights corresponds to the length given by Figure 3-8

d) decide on the amplitude of operation

e) set the vibration head which is graduated in the thousandths of an inch with the hexagonal hand wrench

f) the equipment is ready for operation

The operating frequency must be approached rapidly after the vibrator has been started in order to pass through the first resonance point.

4. Method of Recording Data

To take data which is both meaningful and accurate, it is necessary to develop a method of data taking. This is in addition to any precautions which must be taken to avoid errors in the reading of instruments. This method may involve nothing more than deciding in advance the order in which the variables will be recorded, or it may involve a special technique necessary to record the data. The methods used in this investigation are discussed in this section.

The order in which the variables were recorded are as follows:

a) frequency

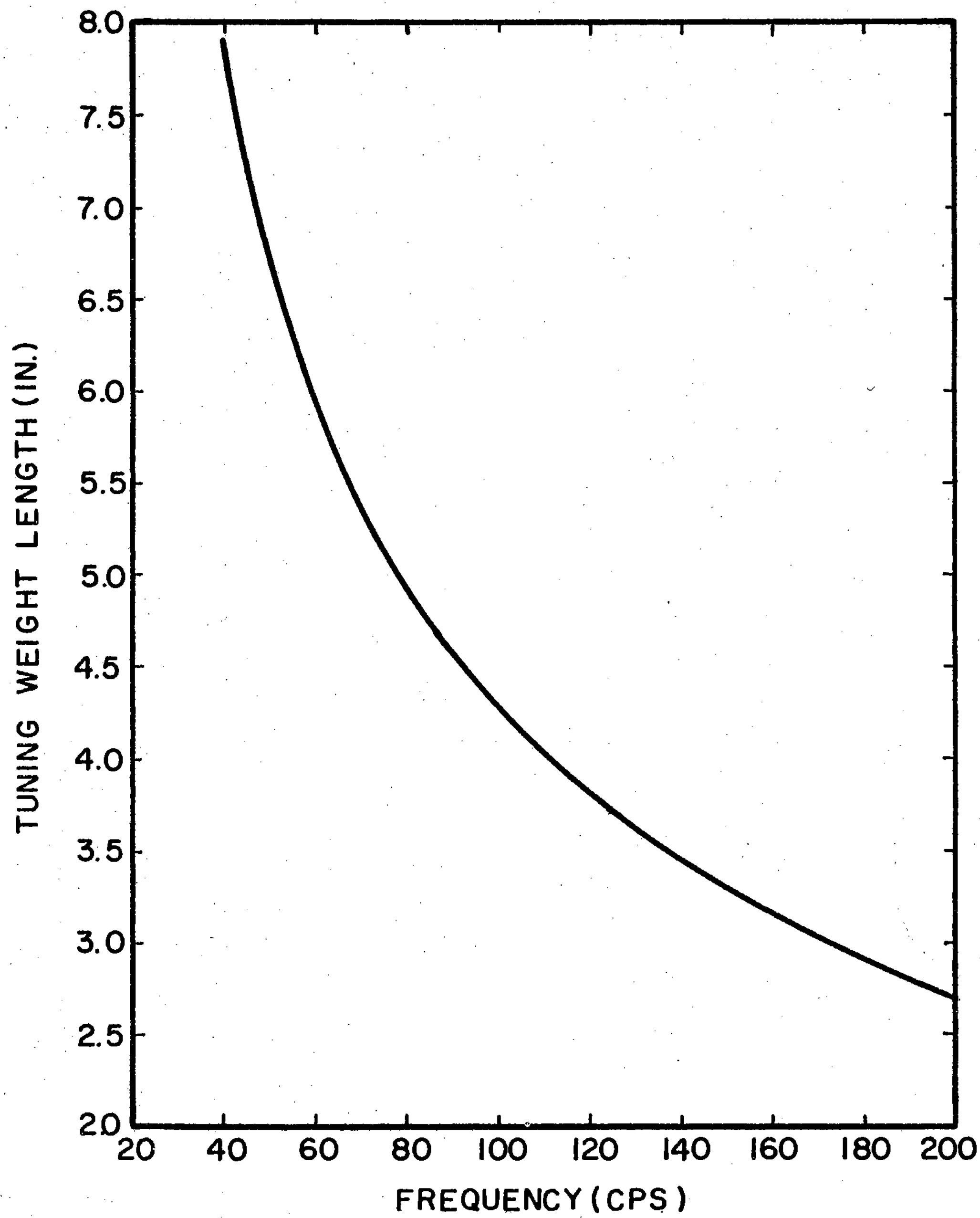

Figure 3-8. Length of Cantilever Arm as a Function of Frequency

b) amplitude

c) current

d) voltage

e) surface temperatures

f) water temperatures

g) physical observations or photographs

The frequency was recorded immediately upon reaching steady state operation of the vibration device. This was easily accomplished by one person. The measurement of the amplitude, however, required two people. This was due primarily to the nature of the differential transformer used to measure the amplitude. The input voltage to the transformer was noted since the output signal of this type of differential transformer is proportional to the input voltage. Then the outer core was varied in position by one person while the other person observed the Ballantine voltmeter for the minimum output signal. When the outer core was positioned so that the minimum output signal resulted, that value was recorded and later converted into a unit of distance by employing the calibrated sensitivity of the differential transformer-voltmeter system.

The remainder of the variables recorded presented no problem at all and required no special precautions to insure good values.

Experimental Uncertainty

Although every effort was made to eliminate both mechanical and human error in the experimental process, a number of uncertainties still exist. These uncertainties have been analyzed and are discussed in this section.

1. Vibration Apparatus

There are three basic vibratory factors which influence the results of the experimental investigation:

a) frequency of vibration

b) amplitude of vibration

c) nature of vibratory apparatus

The frequency of vibration was measured very accurately with the method described in the previous section. Except for slight variances in the speed of the varidrive motor, the frequency seldom changed from the prescribed value. The amplitude of vibration, however, was an entirely different matter. The method used to measure the amplitude has been previously discussed. Due to the nature of this method, some uncertainties certainly exist. Every effort was made to be exceedingly careful, however, and some degree of confidence is associated with the amplitude values. In addition to this type of error, there are other factors which influence the output of the differential transformer. Specifically, there was a noise level associated with the signal generated by the differential transformer. With the differential transformer placed in its null position, i.e., no signal being generated by the transformer, the Ballantine voltmeter indicated from

1.5 to 2.0 millivolts. The minimum signal indicated by the voltmeter during operation of the differential transformer was approximately 20.0 millivolts. This indicates a signal to noise ratio of from 10 to 13. The signal to noise ratio was even more favorable at the higher amplitudes. In order to achieve this low noise level, a severe problem with the instrument grounds had to be overcome. These problems were solved more by luck and chance rather than by any technological ability. In particular, running a separate ground wire from the instrument to a stake driven deep in the ground outside the laboratory had an adverse effect on the grounding problems when it should have solved the problem completely. Finally the instrument grounds were "floated," i.e., not connected to anything; and special care was taken to keep all signal wires away from each other and from all power wiring. As each of these steps was accomplished, the noise level was seen to decrease.

When the signal from the differential transformer was viewed on an oscilloscope, it was found not to be of a pure sinusoidal wave pattern. It appeared as though several frequencies were involved in the basic signal, each at a different amplitude. The signal from the Ballantine voltmeter did not show this since it averages the input signal.

In an attempt to analyze this situation, an accelerometer was placed on the yoke of the vibration device. The output of this accelerometer was fed into a wave analyzer which reduced the signal down to its frequency components and compared the acceleration amplitude at each of the higher frequencies to the acceleration amplitude at the primary frequency. Since the acceleration is a function of the square of the frequency, the amplitude of the signal at the higher frequencies does not have to be very large for the acceleration signal to be of the same order of magnitude as the acceleration signal at the primary frequency. In actuality, there were several higher frequencies where very small signals could be observed, but at approximately 1000 cycles per second there appeared to be a signal which was almost equal to the signal at the primary frequencies of 50, 80, and 120 cycles per second. The corresponding amplitude of vibration at this high frequency was very small, small enough to be neglected as far as its contribution to the signal generated by the differential transformer was concerned. This was mainly due to the nature of the differential transformer which measured amplitude and not acceleration.

This high frequency vibration was a direct result of the nature of the vibration device. The vibration device was mechanical in nature, and this type of device has several forms of error inherent in it. First of all it was almost impossible to isolate the device completely from its surroundings since a vibration pad was not available. Secondly, all of the play in the bearings and relative motion in the device had not been eliminated completely. This tended to eliminate the smooth motion which would have been so desirable in a device of this type. It is this relative motion which generated these high frequency vibrations.

2. Heat Transfer Apparatus

There are four basic areas in the heat transfer part of the investigation that may have contributed uncertainties to the experimental results:

a) power measurements

b) temperature measurements

c) basic construction of test section

d) tank geometry and fluid variables

The power measurements were perhaps the simplest and most accurate measurements to make. The current and voltage were measured separately and independently on two very accurate instruments. The power dissipated in the test section was simply the product of the two readings. A standard uncertainty analysis was performed on the maximum power level available with the present test section using the method described in Kline and McClintock (23). The uncertainty as calculated by this method was less than 0.75 per cent of the total power level. At lower power levels the error involved was even less. Nothing about the power measurements indicated that the accuracy level would change with the beginning of vibration of the test section.

The temperature difference between the surface of the cylinder and the water in the tank was one of the most important variables in the experiment. The thermocouples which were used to measure the water temperature were commercially constructed, calibrated, and rated as to their accuracy. This calibration was checked and found to be correct. The calibration process is discussed in the appendices. The thermocouples which were used to measure the surface temperature were carefully imbedded into the copper cylinder surface. Good contact was assured by careful application of procedures and practice. Several dummy cylinders were constructed and then systematically destroyed to test construction principles. The lead wire from the thermocouple junction was extracted from the interior of the cylinder in such a way that the conduction error due to the temperature gradient in the thermocouple wire was negligible.

The indicating instrument for the millivolt signal generated by the thermocouples was calibrated according to recommended procedures. This calibration procedure and the accuracy of the instrument is discussed in the appendices.

The construction of the test section is discussed in detail in the appendices. There are certain aspects of the construction, however, which will influence the results of the investigation. In general, guard heaters are incorporated into the design of test sections to reduce the amount of conduction error in the test section. This method has often been employed in research involving cylindrical heaters in all cases except those employing water as the fluid. In a recent article, Fand (24) commented on the difficulty of constructing a heater section of this type but indicated that in his experimental work the problems have been overcome. Cited as the past problems are:

a) structural difficulties

b) problems of temperature measurement

c) the need for high heat fluxes for heat transfer to water

For these identical reasons guard heaters were not employed in the present investigation. The problem of conduction error in the test section was investigated and is discussed in the appendices.

In the actual construction of the heater, care was taken to:

a) locate the heater in the center of the cylinder

b) provide a homogeneous medium to transfer the heat from the heater to the surface

c) reduce contact resistance in the heater to a minimum

In fact, one test section was constructed and then systematically cut apart to gain insight into the construction process. Invaluable information was gained through this procedure and several basic changes in the design and construction resulted from this study. In the final analysis, great confidence was placed in the construction and design of the test section.

The test tank was designed and constructed in such a way as to eliminate all of the foreseeable errors. The tank was large compared to the size of the test section, and the test section was placed exactly in the center to reduce wall effects. To isolate the test section surface from any extraneous fluid motion and to reduce unnecessary convective currents, baffles were used. These baffles worked very well upon observation of the experimental process.

The fluid used was pure distilled water and was replaced before each test. The tank was clean and distilled makeup water was slowly added in between experimental runs to insure a large and consistent mass of water in the test tank. To reduce the amount of water lost by evaporation, a top was made against which the vapor condensed. There was probably a slight increase in the pressure of the system. Any effect of this increase in pressure was neglected. In summary, every effort was made to reduce absolute error and, it is believed, eliminate relative error between the comparisons between those cases "with" and "without" vibration.

3. Photography Apparatus

The photography equipment was described in an earlier section of this chapter. The pictorial results of the investigation were very good with the exception of a few minor problems. Since the test section was enclosed by the tank on the bottom and the four sides and was completely covered by approximately 12 inches of water in every direction, lighting was a very real problem. The Fastax camera was operated very near the slowest speed available and the lens was set at f-2.0 which was at the largest lens opening. The depth of field was therefore reduced and focusing was very critical. The lights were placed just above the surface of the water aimed at the top of the cylinder. This produced a light gradient from the top to the bottom of the cylinder.

For high speed camera work, lighting became an increased problem due to the short period of time a frame was exposed. To counter this problem, the speed of the camera was reduced as low as possible and Tri-X reversal film, which has a high film rating, was used. The original films, when developed, produced pictures of fairly high quality although dark in texture and of high contrast.

From this point on, however, problems began to occur. When a copy of the original footage was made, the results were poor. The copy was entirely too dark for extensive use, although it was learned later that a higher quality copy could have been made at a slightly higher cost. The problem here was one of film technology. The original film used was reversal film which resulted in a positive original. To copy this, a negative exposure of the projected image must be made from which a positive print can be made. If negative film had been used in the first place, this problem could have been avoided.

Resulting from this same problem, another problem presented itself when attempts were made to enlarge individual frames so that they might be presented on paper. The procedure here was identical to the one just described. The individual frame was blown up in a special enlarger which allowed a 35 mm camera to be attached. When the frame was enlarged and focused, the 35 mm camera took a time exposure of the frame. This negative was developed and enlargements were made from this. These photographs are presented in the next chapter but no special claim as to the quality is made. In future work of this type, it is believed that this problem may be easily eliminated.

One other noticeable uncertainty in observing the 16 mm film was that the cylinder appeared to jump suddenly from time to time. This was explained as a phenomenon known as "prism jump." It was discovered later that this was a common occurrence with some high speed cameras.

CHAPTER IV

EXPERIMENTAL RESULTS

The experimental investigation consisted of two separate studies. The first study was a quantitative investigation in which the several basic parameters were varied and measurements made. The parameters were:

1) frequency of vibration
2) amplitude of vibration
3) heat flux level

As these quantities were varied through a range of values, measurements were made of the temperature of the surface of the vibrating cylinder and the temperature of the test fluid.

The second study was a qualitative investigation of the effect of surface vibration on the rate of growth, maximum diameter and motion of bubbles. Hydrodynamic effects were noted along with a number of other general observations that were of interest. These observations were preserved for further study through a 16 mm high-speed motion picture film of the process at two key heat flux values. These motion pictures are available in film strip form and several individual frames have been enlarged and are discussed in detail in this chapter.

This section of the discussion will concern itself primarily with the facts presented through the films. A general physical mechanism will be developed in the next chapter.

Quantitative Investigation

The three primary parameters in the investigation are frequency, amplitude, and heat flux. The three basic frequencies at which data were taken were 50, 80, and 120 cycles per second. The maximum amplitude for each frequency is given below.

Frequency (Cycles per second)	Maximum Amplitudes (inches)
50	0.058
80	0.038
120	0.023

The heat fluxes were varied through a range from zero to 50,000 BTU / hr ft^2.

The basic parameter in the investigation was taken to be the frequency of vibration. The frequency was held constant at each of the three values while the heat flux was varied in ten or twelve steps through the range mentioned previously. For each value of heat flux the amplitude was varied in five or six steps up to the maximum value. This wide range of data points afforded ample opportunity to observe the data and measure the effect of vibration on the heat transfer coefficient.

For the range of values of the various variables mentioned, vibration had no noticeable influence on the numerical value of the heat transfer coefficient. This effect or lack of effect was measured by monitoring the surface temperature of the cylinder. From the definition of the heat transfer coefficient given by

$$q = hA\,(T_w - T_{sat}) \tag{4-1}$$

it is apparent that for constant values of heat flux and water temperature, the surface temperature of the cylinder must decrease if the heat transfer coefficient is to increase. Since no change in the surface temperature was measured, it must be concluded that there was no numerical change in the heat transfer coefficient due to the vibration of the cylindrical heating surface. This was true in both the free convection and nucleate boiling regimes.

A summary of the numerical data is presented in Table I showing the effect (or lack of effect) of the frequency and amplitude of vibration for various heat fluxes in the range studied. The surface temperature of the cylinder is shown for both the vibrating and non-vibrating cases. This data indicates only random variations in surface temperature with no dependency on the vibration parameters.

The data taken for normal nucleate pool boiling over a wide range of heat fluxes for saturated water at atmospheric pressure are compared to similar data taken by previous investigators in Figure 4-1. The scatter of the data points is due to time aging of the surfaces as indicated

TABLE 4-1

SUMMARY OF DATA FOR BOILING HEAT TRANSFER FROM A VIBRATING SURFACE

Heat Flux (BTU/hr ft^2)	T_{sat} (^oF)	Frequency (cps)	Amplitude (inches)	$T_{surface}$ (^oF)
2300	210.7	--	--	211.4
		50	0.008	210.8
		50	0.012	211.1
		50	0.017	212.0
		50	0.022	210.8
2300	210.3	--	--	212.9
		80	0.008	212.9
		80	0.014	211.0
		80	0.018	214.0
		80	0.023	214.0
15000	210.7	--	--	223.8
		50	0.009	224.0
		50	0.012	224.0
		50	0.014	224.0
		50	0.021	224.0
15000	210.3	--	--	226.6
		80	0.010	226.6
		80	0.012	226.6
		80	0.018	226.6
		80	0.024	226.3
40300	210.7	--	--	235.1
		50	0.008	235.4
		50	0.012	235.2
		50	0.014	235.0
		50	0.024	235.3

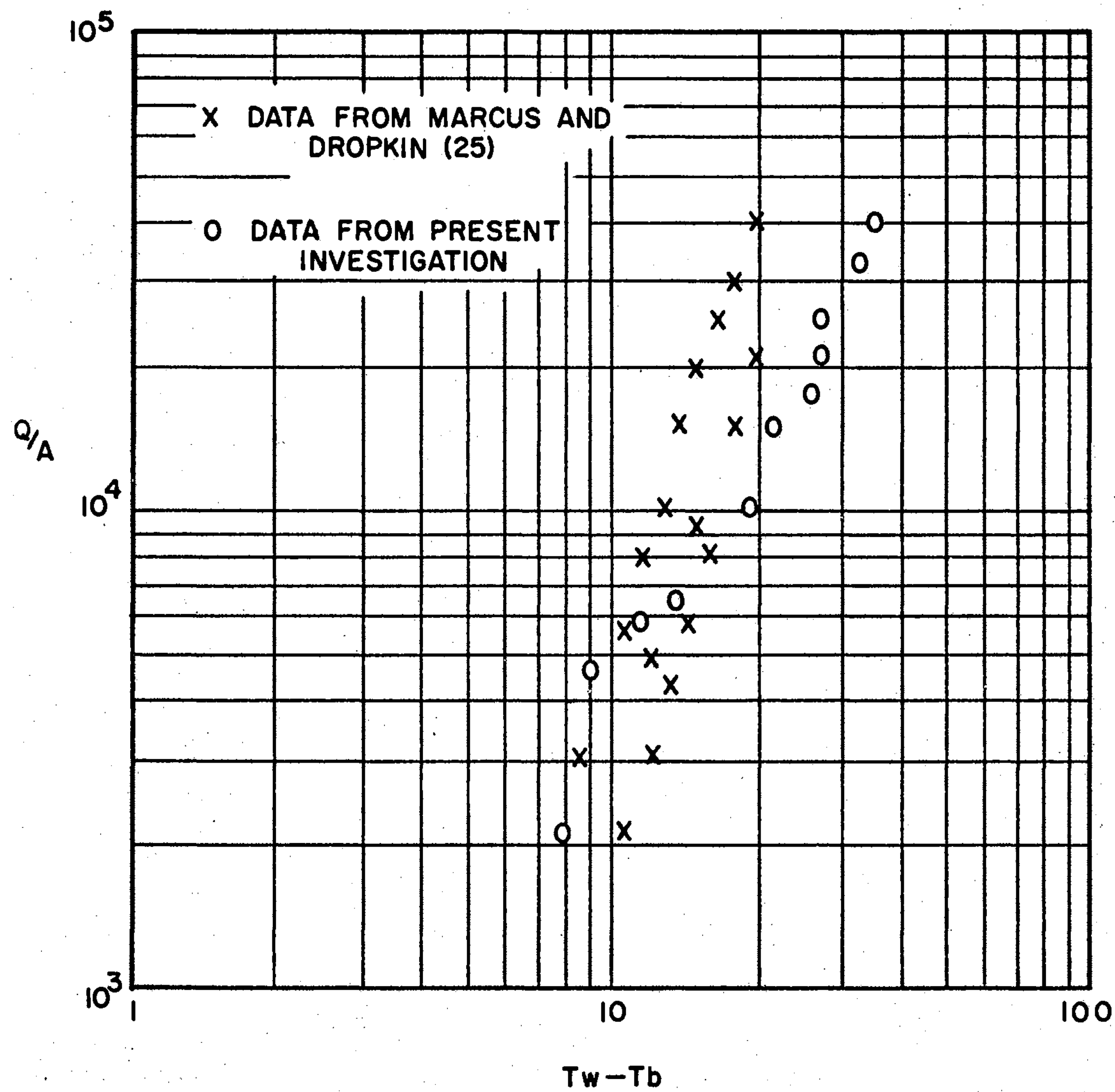

Figure 4-1. Comparison with Boiling Data from Marcus and Dropkin (25)

by the investigators, Marcus and Dropkin (25). This is one of the main reasons a plot of heat flux versus temperature difference is unacceptable for a meaningful correlation and more sophisticated methods have been developed.

Qualitative Investigation

A. Preliminary Observations

In addition to the numerical data, a number of physical observations were made exclusive of the high speed motion pictures. These observations will be discussed at this time.

1. Cavitation

Observations were made to determine if the vibration of the cylinder produced cavitation on the surface. These tests were made with an adiabatic cylinder immersed in water at several different temperatures. The cylinder was vibrated at several different frequencies and amplitudes. Even at the highest intensities of vibration and with the water in the tank near the saturation temperature, cavitation was unnoticeable to the unaided eye. Subsequent studies indicated that cavitation might be occurring, but at such a rapid rate that only high speed motion pictures could detect it. As part of the continuing investigation, this aspect of the problem is under study with the hope that this question can be resolved.

2. Ebullition Point

The vibration of the boiling surface was found to influence the initiation of nucleate boiling by decreasing the temperature of the surface at which the first nucleation was observed. The temperature at which the nucleation process normally began was located. The surface temperature of the cylinder was then decreased slightly and the cylinder was vibrated. If nucleation was still noted, the cylinder temperature was lowered again and again until finally a temperature was reached whereby no nucleation was present even with vibration. In this manner it was determined that surface vibration decreased the temperature at which nucleation first begins.

3. Tank Circulation

During the course of the investigation careful attention was given to the circulatory conditions of the water in the tank. Even during intense vibrations of the cylinder, no circulation currents were observed. This was thought to be due to the presence of the baffles in the tank which isolated the cylindrical test section from the yoke of the vibration device and the tank heaters on either side.

4. Oscillatory Turbulence

Prior to the heat transfer experiments, tests were performed to determine the degree of agitation produced by the vibrating cylinder. The water in the tank was kept at room temperature and the unheated cylinder was vibrated at several frequencies and amplitudes. Some agitation could be observed with the unaided eye and sensed by the touch of the fingers. Even though the measurement was very crude, the tips of the fingers of the hand are very sensitive and detected motion in the fluid near the cylinder. Near the top and bottom of the cylinder, little motion could be detected compared to the motion of the fluid near the sides of the cylinder. Several observers detected this motion and thought it to be some sort of oscillatory field. This same effect was noted later during the study of the bubble motion and will be discussed when the pictorial observations are presented.

B. General Observations

General observations of the hydrodynamic effects of the vibration of the boiling surface led to the construction of a glass viewing window so that an unobstructed view of the test section would be available. In order to preserve the many interesting phenomena that were seen, a high speed movie camera was used so that they could be studied at leisure.

Photographs were taken at heat fluxes of 15,200 and 22,300 BTU / hr ft^2. These were two key heat fluxes in the range in which data were previously taken. The lower heat flux demonstrated the early beginnings of nucleate boiling where a small number of bubbles were present. The higher heat flux demonstrated the regime where nucleate boiling had been firmly established. For each of these heat fluxes, data were recorded for all three frequencies and for amplitudes throughout the ranges mentioned previously.

After extensive study of the films from several viewpoints, a number of conclusions have been formed. As a basis for these conclusions, a common method of comparison was developed. For each flux under study here, an analysis was made of the boiling process "without surface vibration." Then, when certain effects were observed under the vibration conditions, these were compared to the "no vibration" case. In some instances, comparisons between two vibratory cases were necessary to discover the effect of frequency or amplitude. The results of these comparisons are discussed in this section.

1. Normal Nucleate Boiling

Normal nucleate boiling photographic studies were made for the two heat fluxes. Since the mechanism is different for these two cases, they are discussed separately.

a) Low Heat Flux

The lowest heat flux used in the photographic study was 15,200 BTU / hr ft^2. For this case, the surface nucleation was very spotty with a very low bubble density. This can be seen in Plate VII. The bubbles which formed on the top of the cylinder were very small and left the surface to rise directly into the fluid above the cylinder. The bubbles on the sides of the cylinder, however, formed and, as they left the surface, coalesced with the bubbles rising

PLATE VII
Low Heat Flux Conditions without Vibration
$q/A = 15{,}200$ BTU/hr ft^2

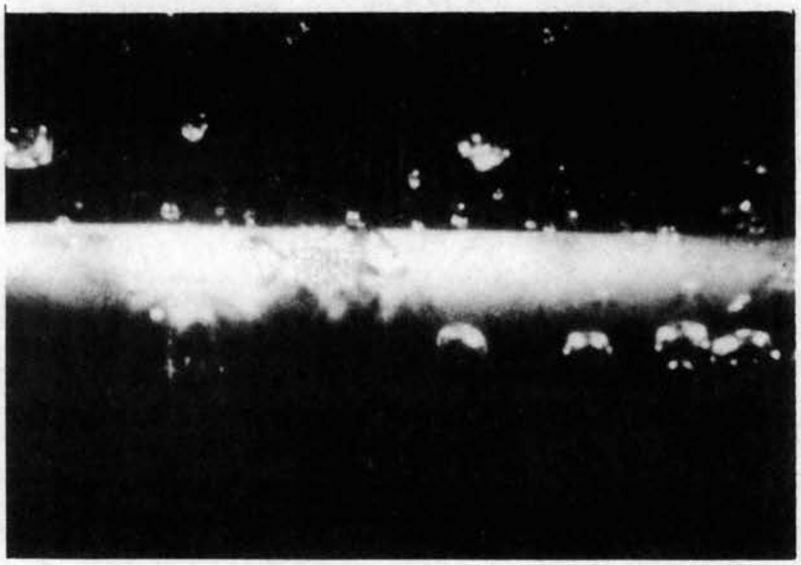

from the bottom of the cylinder. These bubbles grew to be very large as they absorbed vapor from all of the smaller bubbles on the surface.

b) High Heat Flux

The highest heat flux used in the photographic study was 22,300 BTU / hr ft^2. In this case the bubble density has increased tremendously with respect to the low heat flux case. Plate VIII shows this very clearly. In addition to this larger number of bubbles, the bubble action from the bottom of the cylinder was more pronounced. From a study of the films, it was concluded that the bubbles were, in general, larger and more violent than at the lower heat flux. The sequence of frames shown in Plates VIII and IX show more clearly the action of these large bubbles moving around the surface from below, growing larger, and leaving the surface. The area in the center of the pictures that was swept clean by the bubble remained clean for a relatively long period of time before new bubbles started to nucleate in this region.

2. General Effect of Vibration

The general effect of the surface vibration was to change the growth rate, frequency of formation, maximum diameter and general hydrodynamic action of the bubbles. The bubbles forming on the top of the cylinder appeared to be ejected from the surface with a "larger than normal" velocity. The bubbles which

PLATE VIII

High Heat Flux Conditions without Vibration

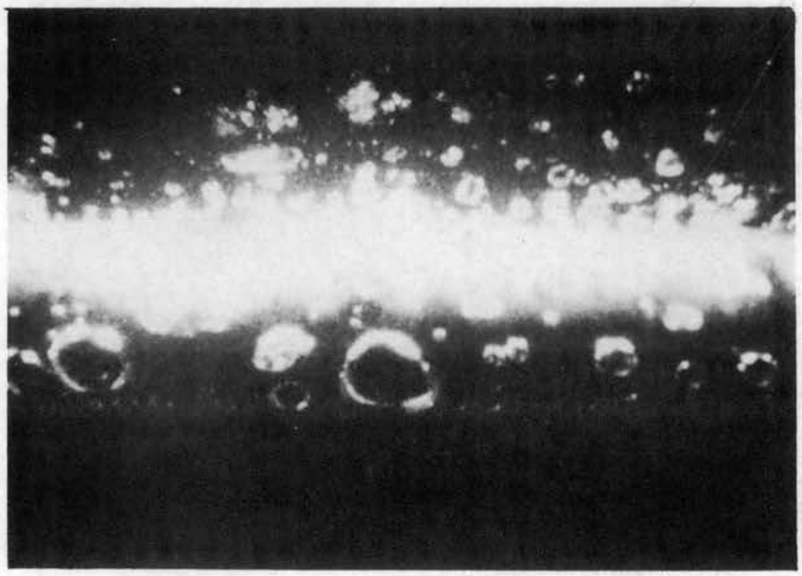

a) Large bubble forms on bottom of cylinder near midpoint

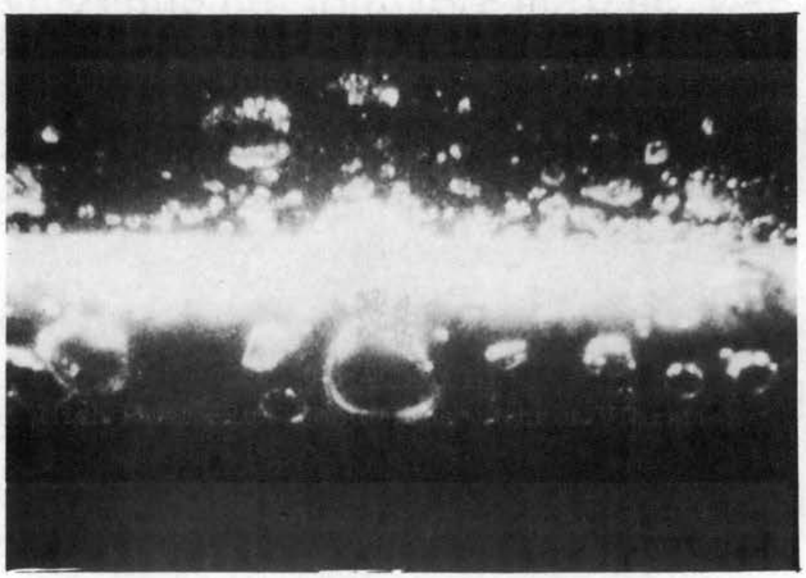

b) Bubble moves upward around the cylinder's side

PLATE IX

Higher Heat Flux Conditions Without Vibration

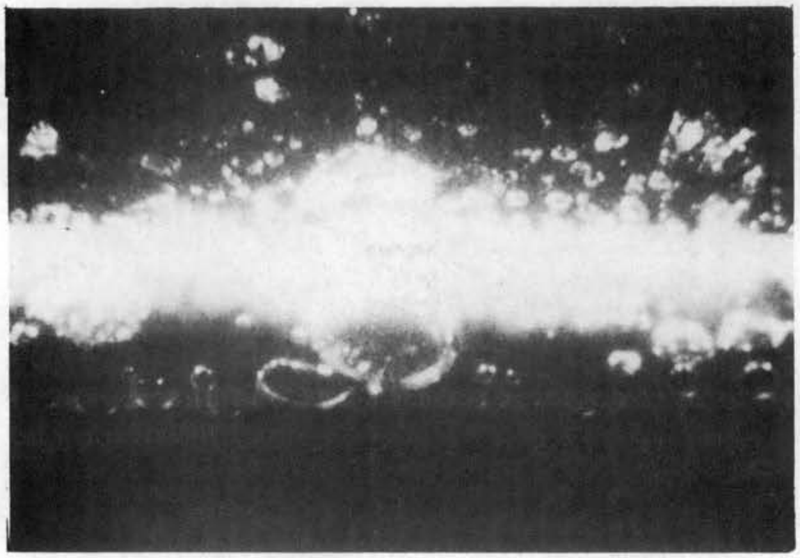

a) Bubble has grown to a large size by additional vapor from small bubbles

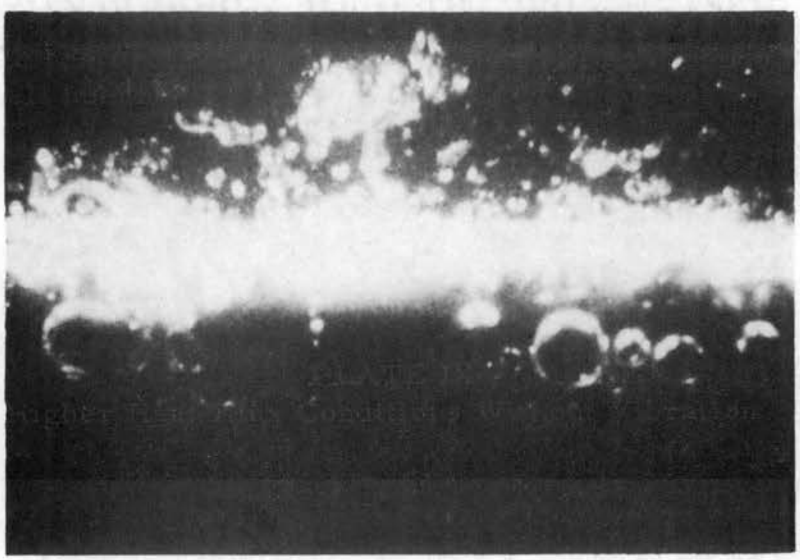

b) Bubble leaves surface and surface remains free of bubbles for a long period of time previously had grown so large as they rose around the sides of the cylinder were caught in an oscillating turbulence. The increased turbulence levels to which the large bubbles were then exposed circulated cooler fluid near the surface. This caused a collapse of the larger bubbles much in the same way that bubbles collapse in a subcooled fluid. Upon observation of the films, it was noted that in no case did a large bubble fail to decrease rapidly in size as it rose from the bottom of the cylinder to the side of the cylinder. In every case, where the intensity of the vibration was sufficiently high, the bubbles collapsed completely.

In general, the bubble density increased uniformly over the entire surface with a large number of smaller bubbles replacing a more limited number of larger bubbles. These conclusions were formed after many comparisons of the motion pictures of the boiling process with and without vibration at identical heat flux conditions.

To illustrate this study, Plate X presents these two conditions. All of these aspects can be seen in the still pictures except for the collapse of the larger bubbles caused by the oscillatory turbulence. This could be observed clearly in the motion pictures.

3. Effect of the Frequency of Vibration

In the range of frequencies studied in the present investigation very little, if any, effect of the frequency of vibration was

PLATE X

Comparison of Identical Heat Fluxes with and without Vibration

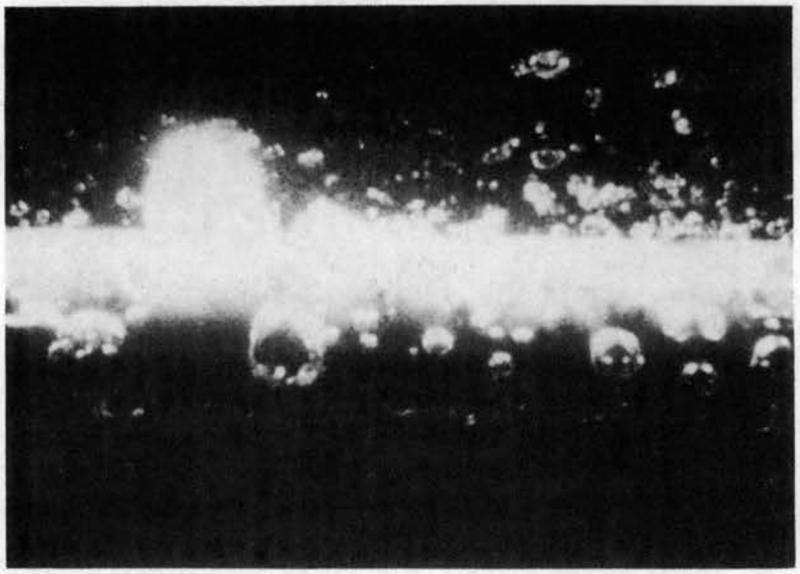

a) $q/A = 22,300$ BTU/hr ft^2, no vibration

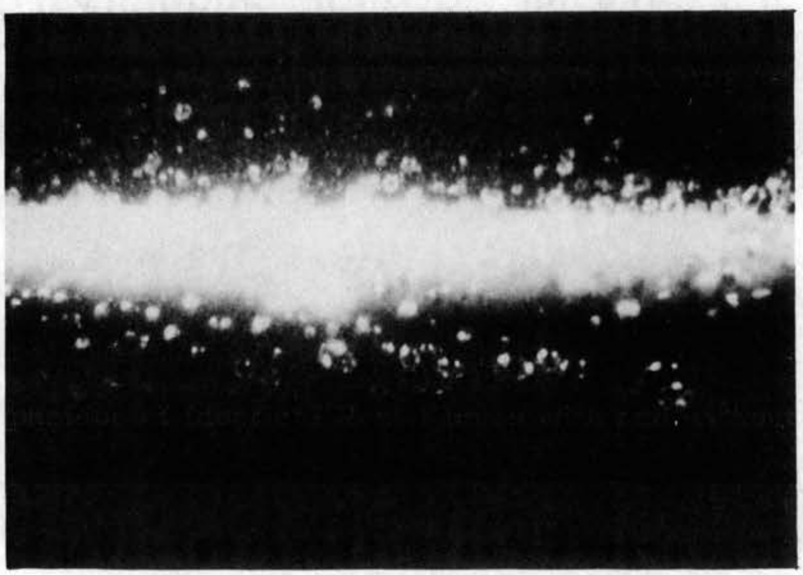

b) $q/A = 22,300$ BTU/hr ft^2; $f = 80$ cps; and $a = 0.037$ in.

noted. Several tests were made at identical heat fluxes and amplitudes and no difference in the hydrodynamic action of the bubbles or any other bubble parameters was noted due to a change in frequency. This is not meant to imply that higher frequencies than those available in the present investigations would not have a significant effect.

4. Effect of the Amplitude of Vibration

The amplitude of vibration has a pronounced effect on the hydrodynamic process of bubble growth. As the amplitude of vibration increased at constant frequency and constant heat flux, the size of the bubbles on the top of the cylinder increased slightly. This can be partially observed in Plate XI . At the lower amplitudes, some of the large bubbles that were discussed previously still formed and traversed around the sides of the cylinder. As the amplitude increased, these were seen to disappear altogether. At the highest amplitudes most of the bubbles seemed to form and collapse rapidly without appreciable vertical motion. In addition, some degree of regularity of bubble formation on the top of the cylinder was evident. All of the bubbles forming on the top of the cylinder seemed to form and leave the surface simultaneously in phase with the vibration of the cylinder.

5. Effect of the Intensity of Vibration

In previous studies of the effect of vibration on free convection, as discussed in an earlier chapter, the intensity of

PLATE XI
Effect of Increasing Amplitude of Vibration

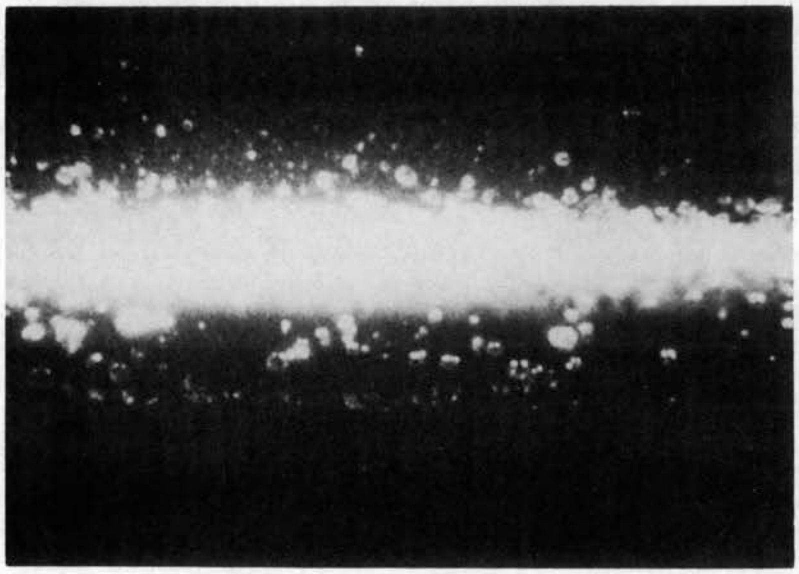

a) $q/A = 22,300$ BTU/hr ft^2; $f = 80$ cps; and $a = 0.014$ in.

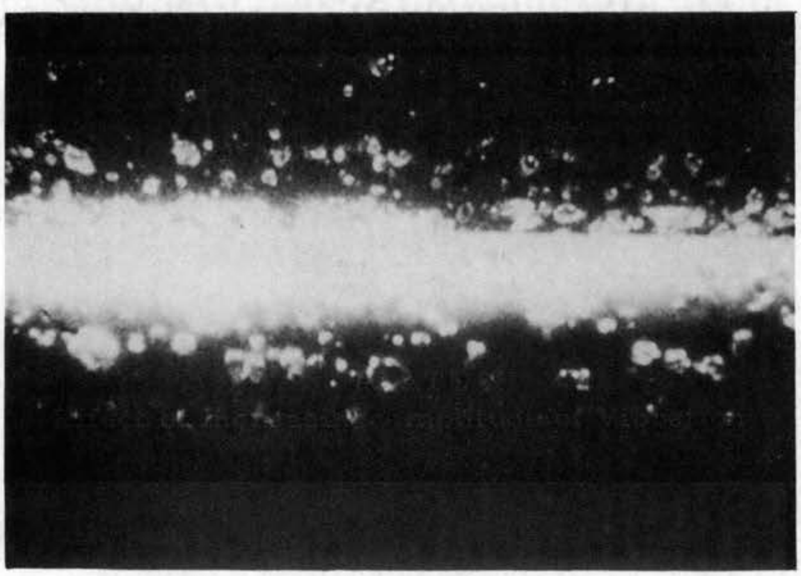

b) $q/A = 22,300$ BTU/hr ft^2; $f = 80$ cps; and $a = 0.037$ in.

vibration, defined as the product of the frequency and amplitude, was a significant parameter. It became significant, however, only after a threshold value was reached and the product continued to increase.

The level of intensity in the present study did not produce a quantitative effect on the heat transfer coefficient but there was some degree of influence on the hydrodynamic process. This influence was due to the amplitude effect discussed previously. There was no significant effect, however, which depended on a simultaneous increase in frequency and decrease in amplitude to give a constant intensity. In other words, the hydrodynamic characteristics present at one frequency and amplitude were not necessarily present at another frequency and amplitude representing the same intensity of vibration. Some characteristics were identical but the similarities were not strong enough to allow the formation of any definite conclusions. It is therefore assumed that for the intensities studied, the only effects encountered were due to changes in the amplitude of vibration.

6. Special Effect of Vibration at Low Heat Fluxes

At the lower heat flux of 15,200 BTU / hr ft^2, an unusual phenomenon was observed. Coinciding with the frequency of vibration of the cylinder, bubbles formed suddenly and simultaneously over the entire upper surface of the cylinder. The sequence shown in Plate XII demonstrates this.

PLATE XII
Cavitation Effect at Low Heat Flux

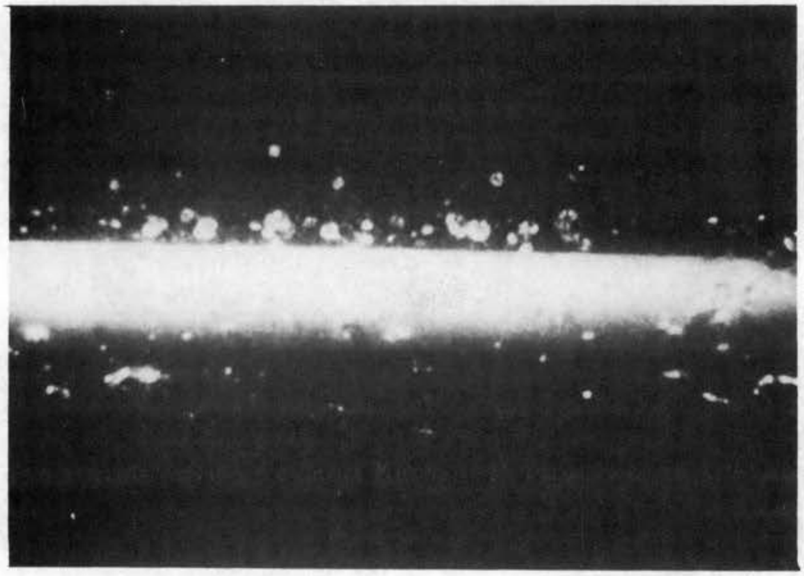

a) $q/A = 15,200$ BTU/hr ft^2; $f = 50$ cps; and $a = 0.021$ in.
Surface relatively clear of bubbles

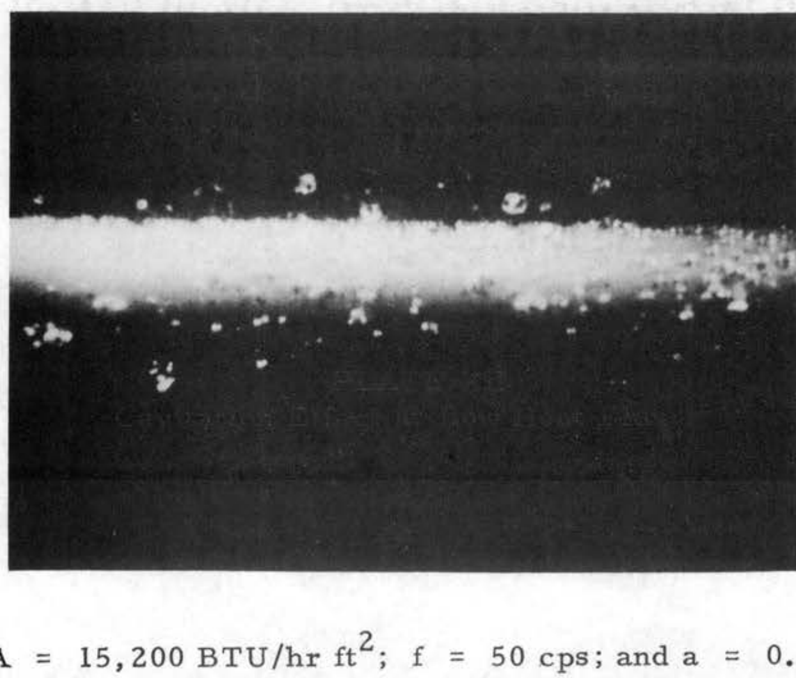

b) $q/A = 15,200$ BTU/hr ft^2; $f = 50$ cps; and $a = 0.021$ in.
Surface suddenly covered by small bubbles an instant later

This sudden formation of the small bubbles was caused by a decrease in pressure on the surface of the cylinder due to its motion through the water. This and the subsequent collapse of the bubbles will be discussed in the following chapter when a physical mechanism is proposed. This effect, while present at the higher heat fluxes also, was "obvious" only at the lower heat flux where the bubble density was low.

7. Effect of the Oscillatory Turbulence

The oscillatory turbulence that was noticed in the adiabatic tests was again found to be present during the boiling experiments. The bubbles which formed on the bottom portion of the cylinder were caught in this turbulence at the sides of the cylinder. The turbulence caused the bubbles to collapse and form a number of smaller bubbles by oscillating them up and down in the fluid surrounding the cylinder. The significance of this will also be discussed in the following chapter.

CHAPTER V

PHYSICAL MECHANISM

In any experimental investigation it is always desirable to analyze the physical mechanism involved. Since this experimental study was not microscopic in nature, it became necessary to make several assumptions and hypotheses as to the effect of vibration of the boiling surface on nucleate boiling.

There are a large number of factors which control the nucleate boiling process, some of which are thought to be severely affected by surface vibration. An attempt was made to analyze the effect of vibration on each of these factors separately. From these discussions a simple physical model was developed which encompassed all of these effects.

Factors That Influence Nucleate Boiling

Boiling heat transfer is a very complex process and depends on a number of factors. The rate of heat transfer per unit area of surface is primarily controlled by the temperature distribution in the thermal boundary layer. There are a number of other factors which, in one way or another, affect this thermal boundary layer. They are also closely interrelated in their effects on each other. These factors and their influences are shown graphically in Figure 5-1 taken in part from Merte and Clark (26). By observing the figure it can be seen that the external effects such as:

1) Forced convection
2) Subcooled fluid temperature
3) Fluid agitation
4) Surface vibration
5) High or low gravity fields

directly affect only the temperature level and distribution in the thermal boundary layer and the maximum size the bubble attains before departing the surface. Pressure imposed on the boiling process influences the fluid properties, which in turn affect the rate of bubble growth, the thermal boundary layer, the maximum bubble size, and the number of active sites which are available for bubble production. The number of active sites and the maximum bubble size are also affected by the condition of the heater surface. It appears that the major influence on the boiling process, however, is wielded by the thermal boundary layer which has a pronounced effect on the:

1) Bubble growth rate
2) Bubble frequency
3) Fluid properties
4) Maximum bubble size

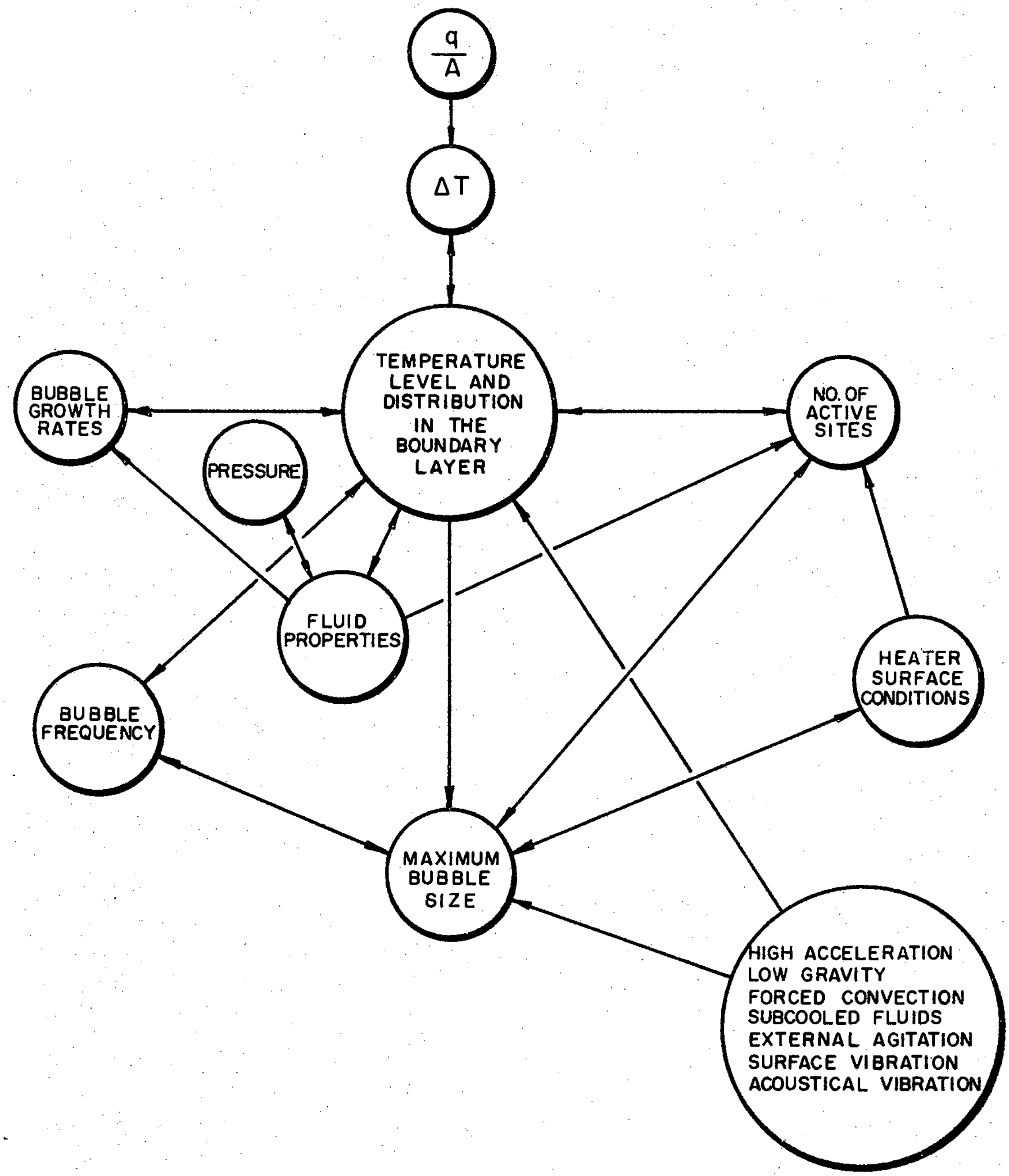

Figure 5-1. Interdependence and Complexity of the Various Boiling Elements, Merte and Clark (26)

5) Number of active sites

6) Temperature difference

This thermal boundary layer, however, is affected greatly by the vibration of the surface and other forms of agitation.

From this discussion it can be seen that the boiling process is a complicated one. The interaction of the various parameters has made it difficult for investigators to agree on a unified theory to explain the nucleate boiling mechanism. A number of different theories have been published in the literature and are discussed in the following section.

Normal Nucleate Boiling

1. Mechanisms

As an explanation for the high rates of heat exchanged in the nucleate boiling regime, Jakob (27), Rohsenow and Clark (28), Rohsenow (29), and Levy (30) suggested the following mechanism. Since in nucleate boiling large bubbles are produced, it is hypothesized that the increase in heat transfer is due solely to the agitation produced by the bubbles as they leave the surface. To formulate this hypothesis a physical model has been developed.

The model consists of a heated surface in contact with a saturated fluid which forms a layer of superheated liquid to support the temperature gradient between the surface and the fluid. This layer of superheated liquid is called the thermal boundary layer and plays a major role in the hypothesis. The energy passing from the heater surface is transferred to this thermal layer by conduction. This heat is then transferred to the bubbles growing within the thermal layer and to the fluid external to the layer. This basic concept is shown in Figure 5-2.

The total heat leaving the surface, q_1, is separated into two portions. In the low range of nucleate boiling a portion, q_3, is transmitted by conduction through the thermal layer to the saturated fluid external to the layer. This is commonly called natural convection. The remaining portion, q_2, is transferred by conduction through the surface of the bubble surface. The vaporization of the fluid near the bubble surface and the subsequent addition of the vapor to the mass of the bubble causes the bubble to grow in size and eventually leave the surface. These bubbles create a convective turbulence within the fluid. As the heat flux increases, the number of bubbles increases and the portion of the total heat flux dissipated by this bulk convection increases.

Later Forster and Grief (31) and Han and Griffith (32) proposed an additional feature for the mechanism. They suggested that as the bubble grows in size, it displaces the superheated thermal layer above it. This thermal layer is then exposed to the cooler fluid. As the bubble departs the surface it carries away the thermal layer from a wide region around the bubble called the area of influence. Then when the bubble leaves the surface and moves away, the cooler fluid

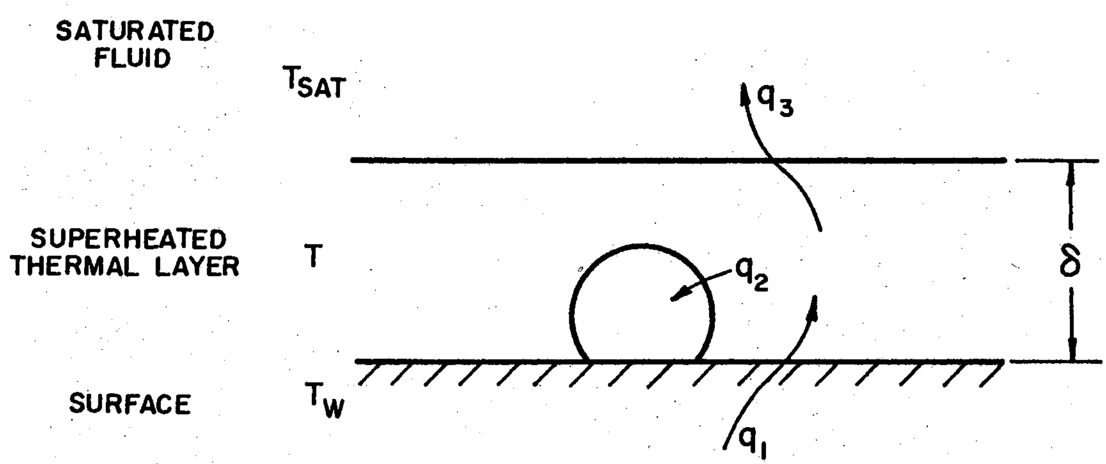

Figure 5-2. Heat Flux Distribution Model

rushes in behind it. This cooler fluid may even contribute to the velocity with which the bubble departs the surface and its final shape. The cooler fluid then must become superheated in order to support the growth of another bubble at the same site.

Another proposed mechanism which has been discussed at some length in the literature is that of heat addition through the base of the growing bubble. Most investigators state that this is a negligible portion of the total heat transfer. It is possible that this is not the case. Recently, Moore and Mesler (33) recorded a number of sharp drops in surface temperature during nucleate boiling using an unusual surface temperature measurement technique. They devised a microthermocouple that was constructed separately and then imbedded into the heat transfer surface. The surface was then polished smooth again. The thermocouple had an extremely fast response time and provided an instantaneous measurement of the actual temperature of the surface of the heater. After much study, they concluded that the microlayer vaporization theory might be valid after all and proposed a more detailed physical mechanism. Later, Rogers and Mesler (34) performed a controlled experiment with an artificial nucleation site at the location of the thermocouple. The remainder of the surface was highly polished and supported the growth of very few bubbles. The result of this investigation supported the work of Moore and Mesler (33) and the following mechanism was proposed.

At the base of each bubble a microthin layer of liquid wets the surface of the heater. As the bubble begins to grow, the interior of the bubble is exposed to this microlayer. This portion of the micro-layer is then exposed to conditions which are conducive to a change of phase and vaporizes. As the liquid vaporizes, the loss of energy from the surface causes a sudden decrease in the surface temperature. After the layer is completely vaporized, the bubble grows to its maximum diameter and departs the surface. The surface tempera-ture at the nucleation site rises rapidly as soon as the vaporization is completed.

To verify earlier estimates of Moore and Mesler (33), Hospeti and Mesler (35) measured the thickness of the microlayer using a unique experimental technique. The liquid was contaminated with deposits of radioactive solids which formed a coating on the surface after the microlayer vaporized. Knowing the concentration of the solids in the liquid and measuring the mass of the radioactive material coating the surface, they were able to calculate that the microlayer is on the order of magnitude of 80 microinches in thickness. This roughly agreed with the earlier estimates.

2. Bubble Growth

At certain privileged points on the heater surface called active sites, bubbles are continuously being formed. The number of active sites is a characteristic of the individual surface under consideration. Naturally the roughness of a surface will determine, to a major extent, the "number" of active sites available. The criterion used to determine what constitutes an "active" site is another matter. It is based on the cavity radius which is most favorable to initiate growth with the understanding that initiation of growth is a statistical problem with some cavities both smaller and larger contributing nuclei to the boiling process.

In order for these bubbles to grow in size, they must receive heat from the vaporization of the microlayer and by conduction through its moving boundary from the thermal boundary layer. This growth is divided into three basic periods:

1) waiting period
2) unbinding period
3) departure period

During the waiting period the thermal layer is formed and grows in thickness and superheat. The microlayer, which forms as soon as the liquid wets the surface of the heater, initiates the growth of a bubble at a favorable nucleation site. The bubble grows as it receives heat by conduction from the thermal layer and by vaporization of liquid in the microlayer directly under the base of the bubble. This period is known as the unbinding or growth period. As the bubble grows large enough to overcome the circumferential surface tension and inertia of the fluid, the rate of growth is then controlled by the rate of heat transfer through the bubble surface. This is called the departure period because, at the end of this period, the bubble has grown large enough to leave the surface due to increased buoyancy effects. As the bubble begins to leave the surface, the fluid surrounding the bubble rushes in behind it and forces it from the surface with an even higher velocity. This cooler fluid then forms the layer which eventually becomes superheated and contributes to the growth of the next bubble. These periods of bubble growth are shown in their relation to each other in Figure 5-3. In addition, the rate of growth of the bubble and the velocity and acceleration of the bubble surface are shown. It can be seen that the velocity and acceleration of the surface of the bubble are zero during the waiting period and the radius has a small constant value. In the unbinding period the bubble begins to increase in size slowly while the velocity increases very rapidly. During this period the acceleration increases and decreases very quickly also. The major growth of the bubble occurs in the departure period where the velocity decreases to zero while the acceleration increases to zero from a negative value.

The growth of a vapor bubble is controlled by a number of factors which are described by the equations of:

1) continuity
2) momentum
3) energy

The equation of continuity deals with the conservation of mass as the liquid in the superheated layer supplies heat and mass to the growing bubble. The equation of momentum governs the growth of the bubble

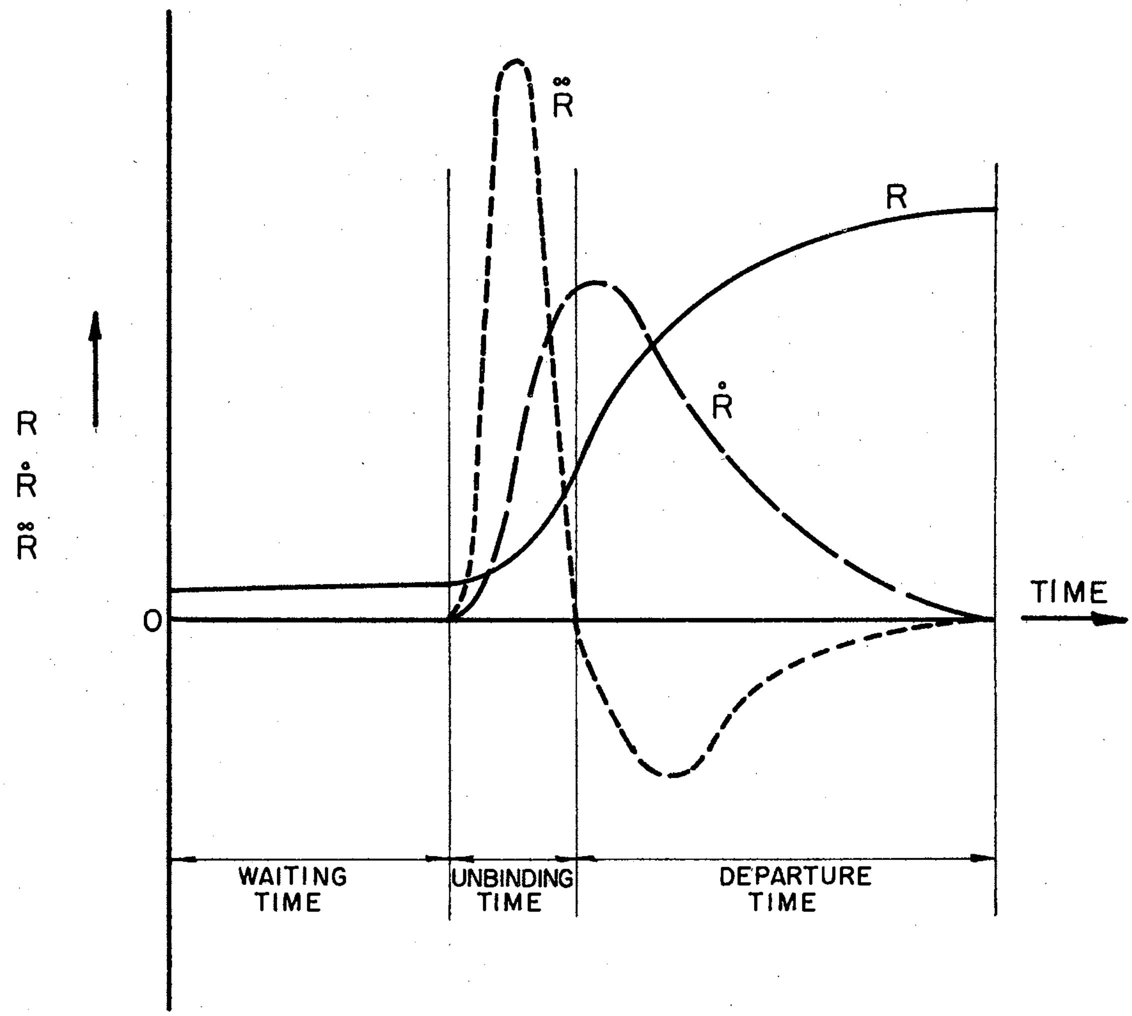

Figure 5-3. Bubble Growth as a Function of Time

during the unbinding period and takes into account a number of factors. This is given by Barlow and Langlois (36) and Scriven (37) in its complete form as

$$\frac{p_V - p_\infty}{\rho_L} = R\ddot{R} + \frac{3}{2}\dot{R}^2 + 4\frac{\mu_L}{\rho_L}\frac{\dot{R}}{R} + \frac{2\sigma_{LV}}{\rho_L R} \tag{5-1}$$

The term on the left of the equation represents the difference in pressure between the vapor inside the bubble, p_V, and the ambient pressure of the fluid, p_∞. The first two terms on the right of the equation are the terms which represent the fluid inertia as the bubble expands against the ambient fluid. The third term on the right is the viscous term representing the force due to the viscosity of the fluid in which the bubble grows and the final term represents the surface tension against which the bubble grows. As the bubble grows in size and enters into the departure period, the term representing the fluid inertia,

$$R\ddot{R} + \frac{3}{2}\dot{R}^2 \tag{5-2}$$

the viscous action

$$4\frac{\mu_L}{\rho_L}\frac{\dot{R}}{R} \tag{5-3}$$

and the surface tension

$$\frac{2\,\sigma_{LV}}{\rho_L\,R} \tag{5-4}$$

become negligible. It is immediately obvious that the growth of the bubble must now be controlled by another mechanism. The growth of the bubble quickly becomes limited by the rate at which the latent heat of vaporization can be supplied at the bubble surface. The energy equation represents this flow of heat to the bubble and is given by Scriven (37) as

$$\frac{\partial T}{\partial \tau} = k\left[\frac{\partial^2 T}{\partial r^2} + \frac{2}{r}\frac{\partial T}{\partial r}\right] - \frac{R^2\dot{R}}{r^2}\frac{\partial T}{\partial r} \tag{5-5}$$

The solutions of the preceding equations for the various stages of growth have been studied extensively by Plesset and Zwick in References (38) through (43) and by Forster and Zuber in References (44) through (47).

The frequency of bubble formation is determined by the time required to form the thermal layer, nucleate a bubble, and allow the bubble to grow to its maximum size and depart the surface. The frequency of bubble formation is therefore given by

$$f_B = \frac{1}{t_w + t_{ub} + t_d} \tag{5-6}$$

where

t_w = length of waiting period

t_{ub} = length of unbinding period

t_d = length of departure period

The waiting period is largely controlled by the thermal boundary layer and the length of time required to form it. The thermal layer must be formed before bubble growth may start. The unbinding period and the departure period are controlled by the relative magnitudes of the forces acting on the bubbles. Keshock and Siegel (48) have recently made a study of these forces and Figure 5-4 demonstrates the results of that study. The forces shown in this figure are the inertia force of the fluid on the expanding bubble.

$$F_I = \frac{11\pi}{192}\frac{\rho_L}{g_c}\left[D^3\ddot{D} + 3(D\dot{D})^2\right] \tag{5-7}$$

the buoyancy force tending to lift the bubble from the surface

$$F_B = \frac{g}{g_c}(\rho_L - \rho_v)\frac{\pi D^3}{6} + \frac{\pi}{2} D\,\sigma_{LV}\sin^2\beta \tag{5-8}$$

and the surface tension force acting to hold the bubble to the surface

$$F_S = D\,\sigma_{LV}\sin^2\beta \tag{5-9}$$

The derivation of these equations may be found in Keshock and Siegel (48) and several other references in the literature. The derivation is based on a spherical bubble model truncated at the base as shown in

Figure 5-5. The data presented in Figure 5-4 were taken from motion picture films of bubble growth and represent the forces calculated using bubble diameters and growth rates measured from the films. The inertia and surface tension forces are shown to be in control early in the growth while the magnitude of the buoyancy force is still small. Later in the growth the buoyancy force is seen to dominate and eventually causes the bubble to leave the surface as its magnitude continues to increase.

The maximum bubble diameter upon its departure from the surface is determined by a force balance on the bubble. This force balance equates the buoyancy force and the surface tension force: since, for large bubble diameters, it is usually assumed that the inertia force is negligibly small as was done by Ruckenstein (49) and Cole (50). This assumption seems to be substantiated by Figure 5-4. To achieve a usable solution, however, requires that a specification of the bubble geometry be made. Since there is no general agreement on the shape of bubbles, a universal equation is not in existence. For the geometry as specified by Figure 5-5 the maximum diameter achieved by a bubble growing on a surface may be given as

$$D_{max} = \sqrt{3}\ \sin \beta \left[\frac{g}{g_c} \left(\frac{\sigma_{LV}}{\rho_L - \rho_v} \right) \right]^{1/2} \tag{5-10}$$

This aspect of bubble growth and the general effect of surface tension were first investigated by Bashforth and Adams (51), Wark (53),

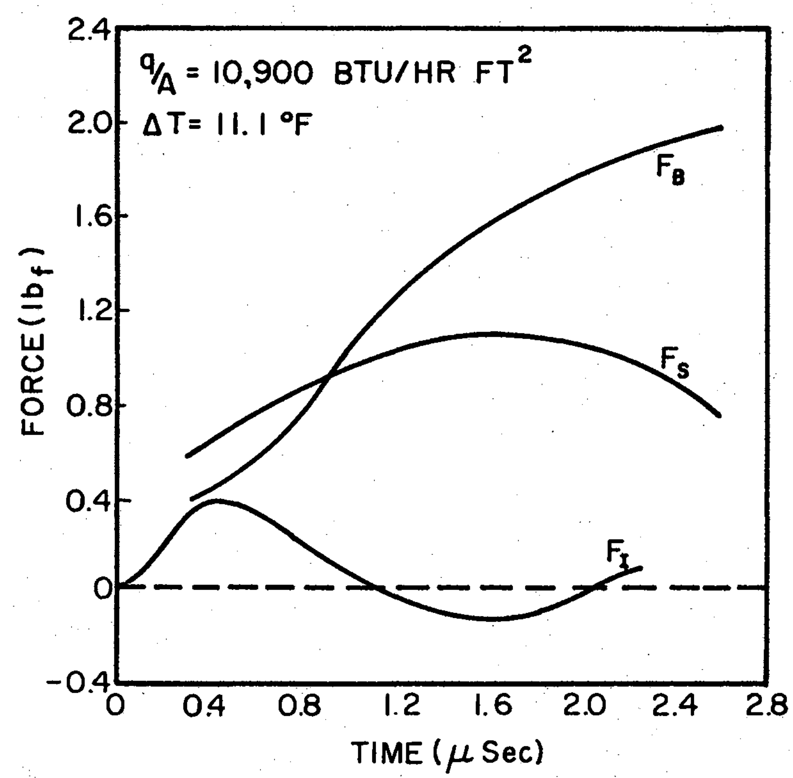

Figure 5-4. Inertia, Buoyancy, and Surface Tension Forces for Bubbles in Saturated Water at Atmospheric Pressure

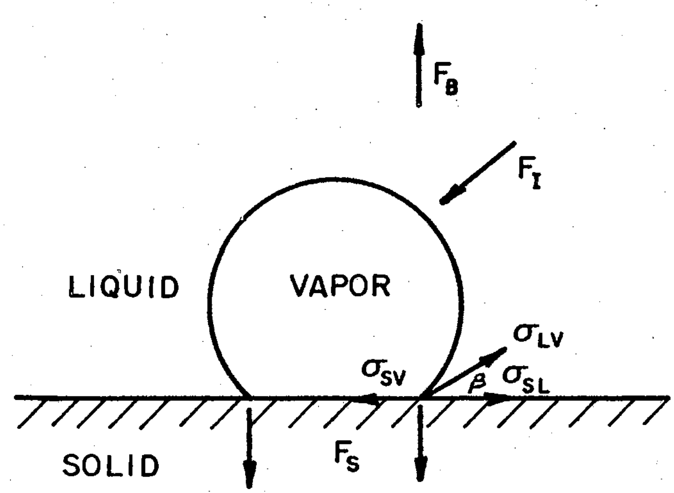

Figure 5-5. Bubble Force Model

and Fritz (53). From this equation it may be seen that the maximum diameter of a normal bubble depends on

1) contact angle

2) surface tension

3) liquid and vapor density

Other factors such as the convective currents of the surrounding fluid, the irregularity of bubble shape, the surface condition of the wall, the neighboring bubbles, and the bubble population density will strongly affect the departure diameter (32).

The diameter of influence surrounding a bubble was observed by Hsu and Graham (54) to be about twice the diameter of the bubble at departure. Since the mass of fluid carried in the wake of a bubble was found to decrease rapidly with decreasing bubble radius (55), the agitation effect caused by the detaching bubble will probably show the same trend. In other words the smaller the bubble the less the agitation.

Jakob (27) noted that for a certain range of variables the relation between the maximum bubble diameter and the bubble frequency were related as

$$f_B D_{max} = \text{constant} \tag{5-11}$$

Perkins and Westwater (56) noted that, for low heat fluxes, Jakob's equation was indeed correct, but that at the higher heat fluxes the product of the frequency and maximum diameter increased with increasing heat flux. Several years later, first Cole (50) and then McFadden and Grassman (51) correlated the experimental data to show that for low heat fluxes

$$f_B D_{max} = \text{constant} \tag{5-12}$$

and for high heat fluxes

$$f_B D_{max}^{1/2} = \text{constant} \tag{5-13}$$

Therefore it may then be concluded that the frequency of departure and the maximum diameter are related in such a way as to equalize the loss of agitation due to smaller bubbles. An attempt was made to justify this assumption through a theoretical analysis by Forster and Zuber (58).

Effect of Surface Vibration on Nucleate Boiling

A vibrating cylindrical surface was chosen as the physical model for this experimental investigation. This corresponded very nicely with models used in the previous investigations of surface vibration effects on convective phenomena which were discussed in detail in an earlier chapter. In this respect the choice of the model was a wise one but the model becomes inconvenient when used to attempt to explain complicated physical mechanisms. A more logical and useful model for this purpose would be one in which the various parameters that control the mechanism could be isolated for study. Such an experimental model is described in detail in the chapter dealing with recommended future research since it is a logical extension of this investigation.

The model in this investigation is a vibrating cylindrical surface which has been separated into three regions as shown in Figure 5-6. In region A, the sides of the cylinder, the pressure of the liquid is decreased due to the increased velocity as the liquid accelerates around the surface. This pressure varies as the cylinder starts, stops, and changes direction, but for the major part of the motion the pressure is below normal levels. In regions B and C, however, the pressure reacts much differently as the cylinder vibrates. For instance, as the cylinder moves upward, the pressure in region B increases above normal levels in proportion to the velocity of the cylinder as given by

$$p_1 = p + \frac{1}{2} \rho u^2 \tag{5-14}$$

where

p_1 = pressure at cylinder surface

p = normal pressure

ρ = density of fluid

u = velocity of cylinder

During this same period the pressure in region C will be somewhat less than normal due to the frictional losses as the fluid decelerates near the surface at the rear of the cylinder. It becomes obvious that,

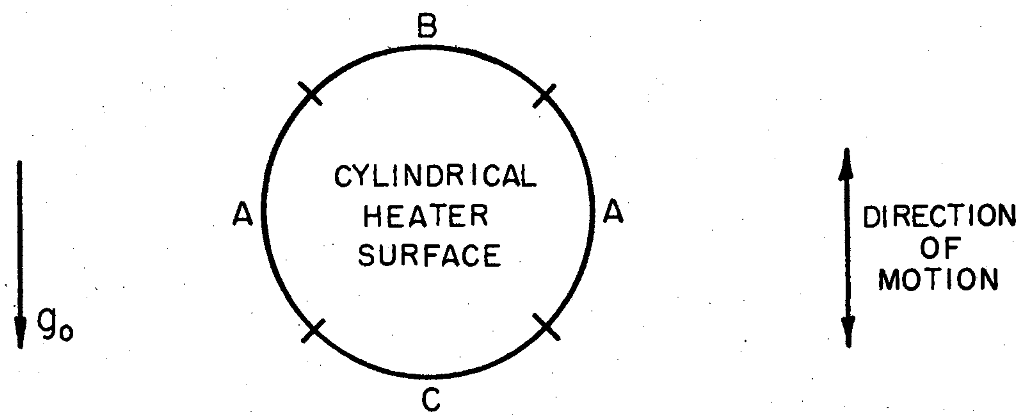

Figure 5-6. Orientation and Growth Regions of the Cylindrical Heater Surface

as the cylinder changes direction, there will be a decrease in the pressure in region B and an increase in region C. The pressure in each of these regions oscillates between a maximum and minimum pressure which are functions of the frequency and amplitude of vibration. This decrease in pressure along the sides of the cylinder and the constant fluctuation in pressure on the top and bottom of the cylinder have a serious effect on the boiling process.

1. Natural Convection

The free convection regime of pool boiling is the region of lowest heat fluxes prior to the start of nucleation. In this region the surface temperatures are only slightly larger than the saturation temperature of the fluid. Data were recorded in this region and indicated no effect of surface vibration on the free convection heat transfer rates. Upon analysis this is not found to be as unusual as might be anticipated.

In the previous investigations on the effect of surface vibration on free convection, large temperature differences were prevalent and the effect of vibration was unnoticeable until a critical intensity level was surpassed. Temperature differences of 100° F were not unusual and the critical intensities were on the order of magnitude of 1.0 ft/sec or greater.

The maximum temperature difference in the present investigation did not exceed 35° F and for the most part was below this level. The maximum intensity achieved during any of the vibratory tests was 0.27 ft / sec. It is not surprising, therefore, that no effect in the free convection range was found.

It should be safe to conclude that the addition of the nucleation process to complicate the mechanism does nothing to affect the results concerning the free convection regime and that the natural convection portion of the total heat transfer in the nucleate boiling regime is likewise unaffected by the surface vibration. In the event that larger temperature differences (such as those for subcooled nucleate boiling) or larger intensities of vibration are used, this natural convection portion of the heat flux may become more important to the overall mechanism.

2. Bulk Convection

The bulk convection portion of the total heat flux is the major contribution in the nucleate boiling regime. It is the heat which is carried from the surface to the surrounding fluid through the growth and departure of the vapor bubbles. Assuming that some combination of the proposed mechanisms for nucleate boiling is correct, the heat flux due to bulk convection is the sum of three different heat transfer rates as given by the following equation.

$$q_{BC} = q_{MV} + q_C + q_E \tag{5-15}$$

where

q_{BC} = total bulk convection energy

q_{MV} = energy added to the bubble due to microlayer vaporization

q_C = energy added to the bubble due to conduction through the surface of the bubble as the bubble grows in the superheated layer

q_E = energy associated with the liquid-vapor interchange mechanism

Each of these quantities depends on the growth rate, maximum diameter, and physical characteristics of the bubbles on the surface. For the present time a single bubble will serve as the model for discussion. Later the effect of surface vibration on the number of active sites and the frequency of bubble formation will be discussed to determine the effect on the total heat transfer.

According to earlier discussions, much of the surface of the vibrating cylinder is in a region of decreased pressure due to the motion of the cylinder. This decreased pressure will create a larger pressure differential between the vapor inside the surface of the bubble and the superheated liquid outside the surface. This increased pressure differential is much more favorable to bubble growth and encourages the bubbles to grow at an increased rate. The decreased pressures on the surface also affect the growth rate in an indirect manner. When the pressure decreases, there is an effective increase in the level of superheat to which the growing bubbles are exposed. Plesset and Zwick (41) and Dergarabedian (59) (60) have studied the effect of increasing superheat on bubble growth rates through the use of both analytical and experimental techniques. Their results are presented graphically in Figure 5-7 to show that the growth rate increases sharply with only slight increases in the number of degrees of superheat. It might therefore be concluded that in the regions that the pressure is decreased below normal levels for the major part of the motion and in the regions where it is periodically decreased (according to the frequency of vibration), the rate of growth of bubbles will be at least slightly increased.

On the top and bottom of the vibrating cylinder, the pressure oscillates between a pressure higher and a pressure lower than atmospheric with the changes taking place suddenly as the cylinder changes direction. This sudden decrease in pressure was seen to actually control the start of nucleation and influence the growth cycle to the extent that the bubbles initiate their growth, grow to their maximum size and leave the surface within one complete cycle of vibration. This effect is directly influenced by the frequency of vibration of the cylinder where the action of the bubbles on the remainder of the surface is only indirectly influenced by the frequency. The indirect influence takes several forms. The relative velocity between the fluid and the surface increases with increasing frequency and constant amplitude. In addition to this, an induced turbulence along the sides of the cylinder has been shown to exist. These two factors combine to limit the maximum size of the bubbles over all of the surface except the top and bottom where the bubble size is controlled directly by the frequency. In any event the size of the bubbles over the surface is decreased

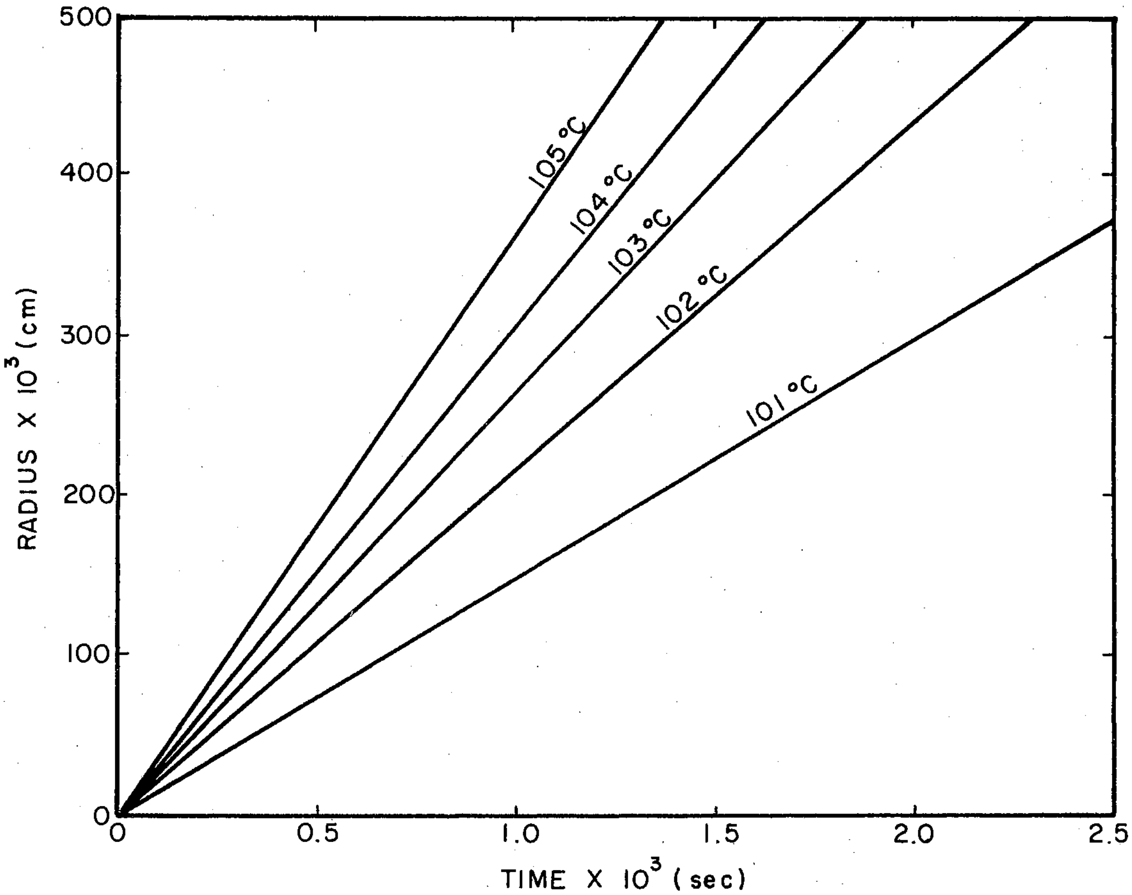

Figure 5-7. Actual Radius of Bubble for Various Values of Water Temperature as a Function of Time

below normal and will play an important role in the new physical mechanism.

Since the bubbles have been shown to grow to a maximum size which is smaller than normal, the various components of the proposed mechanism for nucleate boiling, a combination of the several discussed previously, are probably affected. That portion of the bulk convection due to microlayer vaporization, q_{MV}, will probably be decreased since the bubble will have a smaller base and a smaller contact area. The total mass of liquid vaporized will therefore be decreased. It is also possible that insufficient time will be available for the layer to vaporize since its thickness probably remains constant and the bubble departure is governed by the frequency of vibration. The portion due to conduction of heat across the interface between the surface of the bubble and the superheated liquid surrounding it and the subsequent addition of vapor to the bubble due to vaporization at the interface should also be decreased. This decrease would be due to the decreased surface area available for heat exchange resulting from the decrease in size of the bubbles. The smaller bubbles would also have a decreased area of influence and a greatly reduced agitation rate. The "pumping" effect of the bubbles to force the superheated layer surrounding them into the saturated fluid and allow cooler fluid to replace it near the surface will be reduced and with it the liquid-vapor exchange portion of the total bulk convection, q_E.

It has been postulated now that the energy from each of the three contributors to the total bulk convection would be decreased due to the decrease in size of the bubbles and the increased frequency with which they leave the surface. It is evident that if the number of bubbles forming on the surface remains constant with surface vibration the total heat transfer would be decreased. This, however, is not the case.

The number of active sites on the surface has been shown to increase as the surface vibrated. This was thought to be due to the decrease in pressure over the surface of the cylinder and to the slight increase in the superheat level caused by this decrease in pressure. The more favorable pressure differential is the major factor but investigators have shown that the number of active sites also increases with increasing superheat. It seems assured that if the bubbles formed at this increased number of sites grow to the same size, remain on the surface for the same length of time, contain the same amount of vapor, etc., the total heat transferred by the bulk convection mechanism would be increased in proportion to the number of sites. Actually, the size of the bubbles is much smaller on the vibrating surface than for a stationary surface. This has been verified visually and has been explained fully in the previous discussion.

It would appear, therefore, that the larger number of smaller bubbles combine to produce the same mass of vapor from the liquid surrounding the surface and the same degree of agitation in the thermal layer and exterior fluid regions. For this reason the mechanism might be termed one of "constant vapor production" or "constant bubble volume." It is considered most unusual for this to occur but this would serve as an explanation for the absence of increases in the total heat transfer rate with surface vibration. It is therefore concluded that the combination of an increase in the number of active sites, an increase in the frequency of bubble formation at each site, and a simultaneous decrease in the size of the bubbles serves to produce the same heat transfer rates due to the bulk convection mechanism.

CHAPTER VI

CONCLUSIONS

The experimental investigation was separated into two distinctively different studies. The quantitative investigation was concerned with the measurement of the heat transfer coefficient for a stationary surface and a vibrating surface under identical conditions, while the qualitative investigation was concerned with the visual changes in the hydrodynamics of bubble growth and departure.

A study of the literature available for normal nucleate boiling and of the numerous investigations of the effect of miscellaneous agitation on the boiling process formed the basis for the formulation of a physical mechanism to explain the results of the present study. This mechanism is discussed in detail and comparisons made between the theory and the results of the experimental investigation.

Quantitative Investigation

In this investigation a one-inch diameter cylinder with an internal electrical heater was immersed in a tank of water at atmospheric pressure and near the saturation temperature. The heat flux from the surface of the cylinder was varied from zero to 50,000

BTU/hr ft^2 and measurements made of the temperature of the surface of the cylinder and of the water. From this a normal nucleate boiling heat transfer coefficient was calculated. The cylinder was then vibrated at frequencies from 50 to 120 cycles per second and at amplitudes up to 0.058 inches. For this range of variables the vibration of the surface produced no noticeable influence on the numerical value of the heat transfer coefficient.

Qualitative Investigation

The qualitative investigation consisted of a high speed photographic study of the influence of surface vibrations on the boiling process. From this study, it was seen that the hydrodynamic action of the bubbles was greatly affected by the vibration of the surface. The general, most noticeable effect was to alter the overall pattern of bubble formation on the surface. Prior to vibration, the surface was randomly covered with large bubbles which grew slowly and left the surface with a large diameter. As soon as vibration began, the number of bubbles on the surface increased tremendously and the size of the bubbles decreased drastically.

In normal boiling the large bubbles that grew in size as they travelled from the bottom of the cylinder around the sides swept the surface clean. After the bubble passed, there was a definite period with no new bubbles forming on the surface when the thermal layer was rebuilding its level of superheat for the next series of bubbles.

For a vibrating surface, these large bubbles never really developed. The bubbles would start to increase in size, but as they approached the region at the side of the cylinder, the turbulence produced by the vibration exposed the bubbles to the cooler fluid outside the thermal layer and caused them to collapse due to the condensation of the vapor in the bubbles. In almost every case observed this collapse had taken place by the time the bubble had risen to the halfway point on the surface of the cylinder. This collapse of the large masses of vapor near the sides of the cylinder might be compared to the effect of a subcooled liquid on nucleate boiling.

Prior to the vibration of the surface the bubbles formed in a completely random manner over the surface and the number of active sites were a direct function of the heat flux. When the surface vibrated, the bubbles formed in a more orderly fashion over the surface and the number of active sites increased as the amplitude of vibration increased. The growth rate of the bubbles and the maximum bubble diameter were influenced to the extent that the bubbles covering the surface were much smaller than normal.

The vibration of the surface also controlled the frequency of formation of the bubbles on the top and bottom of the cylinder and influenced the frequency on the sides. The vibration parameter found to be the most important for the range of variables studied was the amplitude of vibration. At constant frequency an increase in the amplitude was seen to amplify the effect of vibration. At constant amplitude, however, an increase in frequency did not result in any visual change in the bubble dynamics. The intensity of vibration did not produce any significant changes except as they reflected a change in the amplitude of vibration.

Physical Mechanism

The physical mechanism for the effect of vibration on nucleate boiling is based on the concept that the total heat flux is comprised of two portions:

1) natural convection

2) bulk convection

The natural convection portion is analyzed by comparison with the previous work on the effects of vibration on free convection, while the bulk convection portion requires an involved physical model. This model includes the thermal layer conduction concept, the microlayer vaporization concept, and the liquid-vapor exchange mechanism.

Due to the low intensities of vibration used in this investigation the natural convection portion of the total heat flux remains unchanged as the surface vibrates. The bulk convection portion however must be analyzed one factor at a time for a single bubble and then the effect on the total number of bubbles must be taken into account.

An analysis of normal bubble growth characteristics and the various mechanisms which have been proposed in the literature for normal nucleate boiling was made. This knowledge was then combined with the hydrodynamic characteristics of the flow about a vibrating cylinder and, with a number of other assumptions, formed the basis for the following conclusions about the physical mechanism for boiling from a vibrating surface.

The energy lost by the heater surface by the microlayer vaporization mode for a single bubble should decrease since the size of the bubble is decreased and it has a smaller base area. The smaller base area would limit the potential mass of liquid under the bubble for vaporization; and if the bubble is forced to leave the surface rapidly enough, only a fraction of this potential may be utilized.

The decreased size of the bubble should also influence the amount of heat conduction through the growing surface since the available surface area is less. The amount of vapor added to the vapor inside the bubble should therefore be reduced and less vapor will be transported to the fluid outside the thermal layer.

The smaller bubbles have a decreased area of influence and this will result in a decreased level of agitation. The "pumping" effect of the bubble will be reduced thereby reducing the energy lost by the surface through the liquid-vapor exchange mode of heat transfer.

Except for the increase in the number of active sites and the increased frequency of formation of the bubbles, the effect of vibration would be to decrease the rate of heat transfer by bulk convection. With the knowledge that the experimental results indicate no change in the total heat flux from the surface and that the intensity of vibration was probably of insufficient magnitude to influence the natural convection from the surface, it must be concluded that the heat flux lost by the surface due to the bulk convection mode also remained constant. With the energy associated with a single bubble decreased according to every mechanism of nucleate boiling that has gained acceptance in the literature, the effect of surface vibration must be to increase the number of active sites and frequency of bubble formation to such an extent that the total heat transfer remains constant. This might be termed a "constant vapor production" process or a "constant bubble volume" process in accordance with the assumptions that have been made.

This explanation of the mechanism of interaction between surface vibrations and nucleate boiling leaves something to be desired due to the myriad of assumptions that have been made throughout the discussion. It is hoped, however, that enough insight into the nature of the problem has been gained to direct future research efforts. A number of questions have been raised and several new research problems have been uncovered during the course of this work. These are discussed in detail in the next chapter.

CHAPTER VII

RECOMMENDATION FOR FUTURE RESEARCH

Since the present investigation was the initial effort in this field, it is natural that a number of problems would develop and a number of new research areas would be discovered. In this chapter several improvements in the present research effort are suggested for the benefit of those who follow, and additional configurations and ranges of variables are proposed. Several new research areas are proposed that should definitely help to solidify the physical mechanism for the effect of surface vibration on nucleate boiling.

Improvements in the Present Research

There are several ways in which the present research could have been improved. Each of these, however, would have required additional funds for capital equipment. Each of these changes are discussed in the succeeding paragraphs.

The amplitude of vibration, in the final analysis, was found to be the most important vibratory variable in this investigation. This amplitude was measured with a differential transformer but several other devices exist which could have produced reliable data in a way which would have been easier and relatively trouble free. As an example of such a method, an optical device consisting of a telescopic lens system and a simple wedge attached to the yoke of the vibration device could have been used to measure the amplitude accurately and would have been entirely free of electrical problems.

Before any more high speed pictures are taken, a more uniform lighting should be provided for the test section. The bottom of the test section was covered in shadows and was a source of many problems when an analysis of the bubble growth on the bottom of the cylinder was attempted. If the contrast in the final pictures had been more uniform, the reproduction of the enlarged frames would also have been of higher quality.

Another source of some disappointment in the experimental equipment was the lack of a pure sinusoidal vibration. With a vibration device of the type used, a pure sinusoidal vibration could not be expected. It would therefore be desirable to change the form of vibration before additional measurements are made. This would preferably involve the use of an electrodynamic shaker table which was not available when this work was initiated.

Increased Range of Variables

The effect of surface vibration on a higher heat flux range approaching the burnout point should be investigated. The present investigation was limited to heat fluxes up to 50,000 BTU / hr ft^2. This was done so that the effect of vibration could be studied in a heat flux range where the number of bubbles on the surface was relatively small. At higher heat fluxes the action of individual bubbles could not be easily observed and might be obscured by the large mass of vapor produced at these higher heat fluxes. In addition, when more power than was used is required a number of design and construction problems preclude an easy solution. These are discussed in the Appendix on the design of the test section.

A complete series of tests could be made for subcooled liquid temperatures. For boiling in fluids that are not saturated, the mechanism is entirely different from that described in the earlier chapters. It would be very interesting to see how the subcooled mechanism is affected by the surface vibration. As mentioned previously, the number of degrees of subcooling could influence the effect of surface vibration on the thermal layer and the rate of heat transfer due to natural convective currents.

In previous investigations of the effect of surface vibration on convective processes, the ratio of the amplitude of vibration to the diameter of the cylinder was found to be a significant parameter (11), (12), (15), and (22). For cylinders whose diameters are on the order of magnitude of wire sizes, Keshock and Siegel (48) discovered that the effect of reduced gravity on nucleate boiling was influenced by the diameter. This was thought to be a function of the effect of circumferential surface tension on the wire as opposed to the case of the cylinder. It is entirely possible that an effect of this type might also be present for the vibrating system. If cylinders of several different diameters were used, this effect could be determined.

The most effective way that a range could be extended to yield more meaningful results would be through an increase in the intensity of vibration. If a change is made in the device producing the vibration, it may become possible to increase the intensity of the vibration beyond the levels achieved in this investigation. Then the influence of surface interaction on the natural convection mechanism may be large enough to affect the total heat transfer from the surface.

At the same time higher frequencies of vibration may also influence the boiling mechanism. The vibration frequencies used in the present investigation were of the same order of magnitude as the frequency of bubble formation. Han and Griffith (31) reported bubble frequencies from 40 to 80 bubbles per second in the range of heat fluxes used in this investigation. The frequency of surface vibration in this investigation ranged from 50 to 120 cycles per second. Any effect which the frequency of vibration might have on the formation of the bubbles on the surface would almost certainly show up if the frequency were increased by an order of magnitude of 10. It might also be that the frequency of vibration will indicate an influence on the boiling process after the intensity of vibration has been sufficiently increased.

Finally, the mechanism proposed could be further tested if the orientation and mode of vibration of the heater surface were changed. An obvious change that could be made and still conform to the types of orientations discussed earlier would be to vibrate the cylinder in a horizontal direction. At the same time, it has been suggested that the cylinder could be vibrated in a longitudinal direction (along its axis). This would produce a relative velocity that would result in a shearing force acting on the bubbles but the large pressure gradients that are present with vertical vibration of the cylinder would not exist.

New Research Problems

During the course of the present investigation several new research areas were seen to need additional study and are discussed in the following paragraphs.

1. Bubble Growth Study

In the past much has been learned of the mechanism of nucleate boiling through microscopic examination of the growth of bubbles. A similar study for bubble growth on a vibrating surface would be extremely helpful, since a relationship between the frequency and amplitude of vibration and the bubble growth rates could be developed. From the photographs the maximum diameter at breakoff could be determined. A series of higher intensities, including higher frequencies of vibration, could be employed to good advantage in this investigation to provide data for a wide range of boiling and vibration parameters.

In order to provide more meaningful data, a prism and lense system could be employed to take pictures of the bubble from two views at the same time. This would aid in determining the rate of change of volume of the bubble, which would be very valuable if the bubbles were not uniform in shape. An artificial nucleation site placed on a highly polished heating surface would allow the study of isolated bubbles. This heating surface would have a variable orientation mechanism so that the relationship between the growing bubble and the vibrating surface could simulate the surface of a vibrating cylinder. The surface would be oriented in such a way as to preserve the cylindrical pressure distribution and the relative velocity between the surface and the fluid at each point.

2. Thermal Layer Study

Since the superheated thermal layer near the surface is so important in the boiling mechanism, it would be most desirable to know the effect of surface vibration on the temperature distribution in this region. The thermal layer has been studied extensively for normal surface conditions. Romie (61) studied the thermal layer thickness and the turbulence caused by the bubbles using a shadowgraph technique. Hirano and Nishikaya (62), in a later study, used the shadowgraph method to measure the thickness of the thermal layer. Then Treshchov (63) used a microthermocouple to measure the temperature profile in the thermal layer for forced convection boiling. Finally, the most extensive measurements of this thermal layer temperature gradient were made by Marcus and Dropkin (25). They found a direct correlation between the thickness of the thermal layer, δ, and the convective heat transfer coefficient, h, which is given by

$$\delta = \frac{0.619}{h^{1.0}} \tag{7-1}$$

for $h < 700$ BTU / hr ft^2 $^\circ$F and

$$\delta = \frac{0.0244}{h^{0.5}} \tag{7-2}$$

for $h > 700$ BTU / hr ft^2 $^\circ$F. These relationships are good for heat fluxes from 1000 to 40000 BTU / hr ft^2. In addition, very careful measurements were made of the temperature profile which revealed that the profile is linear in the region near the surface and that this linear region can be extrapolated to determine the thermal layer thickness. Similar information as to the thickness of the thermal layer and the temperature profile for the fluid adjacent to a vibrating surface is desirable. It is recognized that this is a most difficult problem in measurement but the information would be extremely valuable in the formulation of an adequate physical mechanism for the case of the vibrating surface.

3. Pressure Profile Study

Due to the importance of the pressure at the surface of the cylinder it would be highly advantageous for any future work to know the pressure distribution on the surface. This could be done experimentally with an appropriate pressure transducer placed in the surface of the cylinder. The cylinder could be rotated a total of 180 degrees to get the pressure as a function of the angular position of the pressure transducer. With the same range of vibratory variables as in the previous studies, the pressure profile can be given as a function of the frequency and amplitude of vibration.

SELECTED BIBLIOGRAPHY

1. Ibele, Warren, Modern Developments in Heat Transfer, Academic Press, New York and London, pp. 85-158, 1963.

2. Irvine, T. F., Jr. and J. P. Hartnett, Advances in Heat Transfer, Vol. I, Academic Press, New York and London, pp. 185-267, 1964.

3. Clark, J. A., Theory and Fundamental Research in Heat Transfer, Pergamon Press, New Yor, 1963.

4. Kutalatadze, S. S., Fundamentals of Heat Transfer, Academic Press, New York, 1963.

5. Martinelli, R. C. and L. M. K. Boelter, "The Effect of Vibration on Heat Transfer by Free Convection from a Horizontal Cylinder," Proceedings of the Fifth International Congress on Applied Mechanics, pp. 518-584, 1938.

6. Lemlich, L., "Effect of Vibration on Natural Convection Heat Transfer," Symposium on Pulsatory and Vibrational Pheno-Mena, Industrial and Engineering Chemistry, Vol. 47, No. 6, pp. 1175-1180, June, 1955.

7. Shine, A. J., "Effect of Transverse Vibrations on Heat Transfer Rates from Heated Vertical Plates in Free Convection," A.S.M.E. Paper No. 59-HT-27, 1959.

8. Teleki, C., R. M. Fand, and J. Kaye, "The Influence of Vertical Vibrations on the Rate of Heat Transfer from a Horizontal Cylinder in Air," WADC Tech. Note 59-357, October, 1960.

9. Dougall, R. S., T. Chiang, and R. M. Fand, "A Study of the Differential Equations of Coupled Vibrations and Free Convection from a Heated Horizontal Cylinder," ARL-148, Part I, 1961.

10. Fand, R. M., and J. Kaye, "The Influence of Sound on Free Convection from a Horizontal Cylinder," Trans. A.S.M.E., Series C, J. of Heat Transfer, Vol. 83, No. 2, pp. 133-148, May, 1961.

11. Fand, R. M., and J. Kaye, "The Influence of Vertical Vibrations on Heat Transfer by Free Convection from a Horizontal Cylinder," 1961 International Heat Transfer Conference, Part II, pp. 490-498, 1961.

12. Fand, R. M., and E. M. Peebles, "A Comparison of the Influence of Mechanical and Acoustical Vibrations on Free Convection from a Horizontal Cylinder," Trans. A.S.M.E., Series C, J. of Heat Transfer, Vol. 84, No. 3, p. 268, August, 1962.

13. Fand, R. M., and E. M. Peebles, "A Comparison of the Influence of Mechanical and Acoustical Vibrations on Free Convection from a Horizontal Cylinder," ARL - 148, Part II, 1961.

14. Russ, R. M., "Effect of Vibration on Heat Transfer from Cylinders in Free Convection," Govt. Research Report AD-292335, August, 1962.

15. Deaver, F. K., W. R. Penny, and T. B. Jefferson, "Heat Transfer from an Oscillating Wire to Water," Trans. A.S.M.E., Series C, J. of Heat Transfer, Vol. 84, No. 3, pp. 251-256, August, 1962.

16. Blankenship, V. D., and J. A. Clark, "Effects of Oscillation on Free Convection from a Vertical Finite Plate," Trans. A.S.M.E., Series C, J. of Heat Transfer, Vol. 86, No. 2, pp. 149-158, May, 1964.

17. Blankenship, V. C., and J. A. Clark, "Experimental Effects of Transverse Oscillations on Free Convection from a Vertical Finite Plate," Trans. A.S.M.E., Series C, J. of Heat Transfer, Vol. 86, No. 2, pp. 159-165, May, 1964.

18. Scanlan, J. A., "Effects of Normal Surface Vibration on Laminar Forced Convection Heat Transfer," Industrial and Engineering Chemistry, Vol. 50, No. 10, pp. 1565-1568, October, 1958.

19. Sreenivasan, K., and A. Ramachandran, "Effect of Vibration on Heat Transfer from a Horizontal Cylinder to a Normal Air Stream," Inter. J. of Heat and Mass Transfer, Vol. 3, pp. 60-67, 1961.

20. Kovalenko, V. F., "An Experimental Investigation of the Vibration Effect on Heat Transfer in the Process of Boiling," Teploenergetika, Vol. 5, No. 2, pp. 76-77, 1958.

21. Lemlich, R., and M. R. Levy, "The Effect of Vibration on Natural Convection Mass Transfer," A.I.Ch.E. Journal, Vol. 7, No. 2, pp. 240-242, June, 1961.

22. Jameson, C. J., "Mass (or Heat) Transfer from an Oscillating Cylinder," Chem. and Engr. Science, Vol. 19, pp. 793-800, 1964.

23. Kline, S. J., and F. A. McClintock, "Describing Uncertainties in Single Sample Experiments," Mechanical Engineering, Vol. 75, pp. 3-8, January, 1953.

24. Fand, R. M., "The Influence of Acoustic Vibrations on Heat Transfer by Natural Convection from a Horizontal Cylinder to Water," Trans. A.S.M.E., Series C, J. of Heat Transfer, Vol. 87, No. 2, pp. 309-310, May, 1965.

25. Marcus, B. C., and D. Dropkin, "Measured Temperature Profiles within the Superheated Boundary Layer above a Horizontal Surface in Saturated Nucleate Pool Boiling," A.S.M.E. Paper No. 64-WA/HT-4, 1964.

26. Merte, H., and J. A. Clark, "Pool Boiling in an Accelerating System," Trans. A.S.M.E., Series C, J. of Heat Transfer, Vol. 83, pp. 233-242, August, 1961.

27. Jakob, Max, <u>Heat Transfer</u>, John Wiley and Sons, New York, Vol. I, pp. 614-652, 1949.

28. Rohsenow, W. M., and J. A. Clark, "A Study of the Mechanism of Boiling Heat Transfer," Trans. A.S.M.E., Series C, J. of Heat Transfer, Vol. 73, pp. 609-620, July, 1951.

29. Rohsenow, W. M., "A Method of Correlating Heat Transfer Data for Surface Boiling of Liquids," Trans. A.S.M.E., Series C, J. of Heat Transfer, Vol. 74, pp. 969-976, August, 1952.

30. Levy, S., "Generalized Correlation of Boiling Heat Transfer," Trans. A.S.M.E., Series C, J. of Heat Transfer, Vol. 81, No. 1, pp. 37-42, February, 1959.

31. Forster, K. E., and R. Grief, "Heat Transfer to a Boiling Liquid-- Mechanism and Correlations," Trans. A.S.M.E., Series C, J. of Heat Transfer, Vol. 81, No. 1, pp. 43-53, February, 1959.

32. Han, C. Y., and P. Griffith, "The Mechanism of Heat Transfer in Nucleate Pool Boiling," M.I.T. Research Report No. 7673-19, March, 1962.

33. Moore, F. C., and R. B. Mesler, "The Measurement of Rapid Surface Temperature Fluctuations During Nucleate Boiling of Water," A.I.Ch.E. Journal, Vol. 7, No. 4, pp. 620-624, December, 1961.

34. Rogers, T. F., and R. B. Mesler, "An Experimental Study of Surface Cooling by Bubbles During Nucleate Boiling of Water," A.I.Ch.E. Journal, Vol. 10, No. 5, pp. 656-660, September, 1964.

35. Hospeti, N. B., and R. B. Mesler, "Deposits Formed Beneath Bubbles During Nucleate Boiling of Radioactive Calcium Sulfate Solutions," A.I.Ch.E. Journal, Vol. 11, No. 4, pp. 662-665, July, 1965.

36. Barlow, E. J., and W. E. Langlois, "Diffusion of Gas from a Liquid into an Expanding Bubble," International Business Machine Journal, Vol. 6, No. 3, pp. 329-337, 1962.

37. Scriven, L. E., "On the Dynamics of Phase Growth," Chemical Engineering Science, Vol. 10, pp. 1-13, 1959.

38. Zwick, S. A., "Behavior of Small Permanent Gas Bubbles in a Liquid," J. of Math. Phys., Vol. 37, pp. 246-268, 1959.

39. Zwick, S. A., and M. S. Plesset, "Note on the Dynamics of Small Vapor Bubbles in Liquids," J. of Math. and Phys., Vol. 33, No. 4, pp. 308-330, 1955.

40. Plesset, M. S., "Bubble Dynamics," Govt. Research Report AD-298566, February, 1963.

41. Plesset, M.S., and S. A. Zwick, "The Growth of Vapor Bub-Bles in Superheated Liquids," J. of Applied Phys., Vol. 25, No. 4, pp. 493-500, 1954.

42. Plesset, M. S., and S. A. Zwick, "A Non Steady Heat Diffusion Problem with Spherical Symmetry," J. of Applied Phys., Vol. 23, No. 1, pp. 95-98, January, 1952.

43. Plesset, M. S., "On the Stability of Fluid Flows with Spherical Symmetry," J. of Applied Phys., Vol. 25, No. 1, pp. 96-98, January, 1954.

44. Forster, H. K., and N. Zuker, "Growth of a Vapor Bubble in a Superheated Liquid," J. of Applied Phys., Vol. 25, No. 4, pp. 474-478, April, 1954.

45. Forster, H. K., "On the Conduction of Heat into a Growing Vapor Bubble," J. of Applied Phys., Vol. 25, No. 8, pp. 1067-1068, August, 1954.

46. Forster, H. K., "Diffusion in a Moving Medium with Time Dependent Boundaries," A.I.Ch.E. Journal, Vol. 3, No. 4, pp. 535-538, December, 1957.

47. Forster, H.K., "Growth of a Vapor Filled Cavity Near a Heating Surface and Some Related Problems," Phys. of Fluids, Vol. 4, No. 4, pp. 448-455, April, 1961.

48. Keshork, E. G., and R. Siegel, "Forces Acting on Bubbles in Nucleate Boiling under Normal and Reduced Gravity Conditions," NASA TN D-2299, August, 1964.

49. Ruckenstein, E., "A Physical Model for Nucleate Boiling Heat Transfer," Inter. J. of Heat and Mass Transfer, Vol. 7, No. 2, pp. 191-198, February, 1964.

50. Cole, R., "A Photographic Study of Pool Boiling in the Region of the Critical Heat Flux," A.I.Ch.E. Journal, Vol. 6, No. 4, pp. 533-538, December, 1960.

51. Bashforth, F. R., and J. Adams, "Capillary Action," Cambridge, 1883.

52. Fritz, W., Physikalische Zeitschrift, Vol. 36, p. 379, 1935.

53. Wark, I. W., "The Physical Chemistry of Flotation--The Significance of Contact Angle in Flotation," J. of Physical Chemistry, Vol. 37, pp. 623-644, 1933.

54. Hsu, Y. Y., and R. W. Graham, "An Analytical and Experimental Study of Thermal Boundary Layer and Ebulition Cycle in Nucleate Boiling," NASA TND-594, 1961.

55. Hendrix, C. D., "Translation of Continuous Liquid Phase by Rising Single Drops of Dispersed Liquid Phase," M.S. Thesis, Univ. of Tennessee, June, 1960.

56. Perkins, A. S., and J. W. Westwater, "Measurement of Bubbles Formed in Boiling Methanol," A.I.Ch.E. Journal, Vol. 2, No. 4, pp. 471-476, December, 1956.

57. McFadden, P. W., and P. Grassman, "The Relation Between Bubble Frequency and Diameter during Nucleate Pool Boiling," Inter. J. of Heat and Mass Transfer, Vol 5, pp. 169-173, 1962.

58. Forster, H. K., and N. Zuber, "Dynamics of Vapor Bubbles and Boiling Heat Transfer," A.I.Ch.E. Journal, Vol. 1, No. 4, pp. 531-535, 1955.

59. Dergarabedian, P., "The Rate of Growth of Vapor Bubbles in Superheated Water," J. of Applied Mech., Vol. 20, No. 4, pp. 537-545, 1953.

60. Dergarabedian, P., "Observations on Bubble Growth in Various Superheat Liquids," J. of Fluid Mech., Vol. 9, No. 1, pp. 39-49, September, 1960.

61. Romie, F. E., "Fundamental Studies in Boiling Heat Transfer," Studies in Boiling Heat Transfer, Section III, Univ. of California, AEC COO-24, March, 1951.

62. Hirano, F., and K. Nishikaya, "The Phenomena of Boiling--Part 3, ". Machinery Research (Japan), Vol. 8, No. 5, p. 521, 1956.

63. Treshchov, G. G., "An Experimental Investigation of Heat Exchange Mechanism with Surface Boiling Water," Teploenergetika, Vol. 4, No. 5, p. 44, May, 1957.

64. Chang, Y. P., "An Empirical Modification of Nucleation Theory and its Application to Boiling Heat Transfer," Govt. Research Report ANL-6304, February, 1961.

65. Kreith, F., Principles of Heat Transfer, International Textbook Co., Scranton, pp. 89-109, 1958.

APPENDIX A

LIST OF REFERENCES

on

THE EFFECT OF GRAVITY FIELDS ON BOILING HEAT TRANSFER

APPENDIX A

LIST OF REFERENCES

on

THE EFFECT OF GRAVITY FIELDS ON BOILING HEAT TRANSFER

Low Gravity Fields

1. Steinle, H. F., "An Experimental Study of the Transition from Nucleate to Film Boiling under Zero-Gravity Conditions," Proc. 1960 Heat Transfer and Fluid Mechanics Institute, Stanford (June, 1960), pp. 208-219.

2. Siegel, R. and Vsiskin, C., "A Photographic Study of Boiling in the Absence of Gravity," Trans. A.S.M.E., Series C, J. of Heat Transfer, Vol. 81 (August, 1959), pp. 230-236.

3. Vsiskin, C. and Siegel, R., "An Experimental Study of Boiling and Zero Gravity Fields," A.S.M.E. Paper No. 60-HT-10, Trans. A.S.M.E., Series C, J. of Heat Transfer, Vol. 83, No. 3, 1961, pp. 243-253.

4. Merte, H. Jr., and Clark, J. A., "Boiling Heat Transfer Data for Liquid Nitrogen in Reduced and Zero-Gravity Fields," Advances in Cryogenic Engineering, edited by K. D. Timmerhaus, Vol. 7, 1962, pp. 546-550.

5. Clarke, J. A., and Merte, H. Jr., "Nucleate, Transition, and Film Boiling Heat Transfer at Zero Gravity," Advances in Astronautical Sciences, Vol. 14, American Astronautical Society, 1963, pp. 177-196.

6. Merte, H. Jr., and Clarke, J. A., "Boiling Heat Transfer with Cryogenic Fluids at Standard, Fractional, and Near Zero Gravity," Trans. A.S.M.E., Series C., J. of Heat Transfer, Vol. 86, No. 3 (August, 1964), pp. 351-359.

7. Siegel, R., and Keshock, E. G., "Effects of Reduced Gravity on Nucleate Boiling Bubble Dynamics in Saturated Water," A.I.Ch.E. Journal, Vol. 10, No. 4 (July, 1964), pp. 509-523.

8. Keshock, E. G., and Siegel, R., "Forces Acting on Bubbles in Nucleate Boiling under Normal and Reduced Gravity Conditions," NASA TN D-2299 (August, 1964).

9. Siegel, R., and Keshock, E. G., "Nucleate and Film Boiling in Reduced Gravity from Horizontal and Vertical Wires," NASA TR R-216 (February, 1965).

10. Zara, E. A., "Boiling Heat Transfer in Zero Gravity," RTD Technical Briefs, Headquarters, Research and Technical Div., Bolling AFB, Vol. 2, No. 1 (January, 1964), pp. 8-15.

11. Clodfelter, R. G., "Low Gravity Pool Boiling Heat Transfer," APL - TDR - 64 - 19, Air Force Systems Command, Wright - Patterson AFB (March, 1964).

12. Sherley, Joan E., "Nucleate Boiling Heat Transfer Data for Liquid Hydrogen at Standard and Zero Gravity," Advances in Cryogenic Engineering, edited by K. D. Timmerhaus, Vol. 8, 1963, pp. 495-500.

13. Adelberg, M., "Gravitational Effect upon Nucleate Boiling Heat Transfer," Advances in Astronautical Sciences, Vol. 14, American Astronautical Society, 1963, pp. 196-223.

High Gravity Fields

1. Merte, H. Jr., and Clark, J. A., "Pool Boiling in an Accelerated System," Trans. A.S.M.E., Series C, J. of Heat Transfer, Vol. 83 (August, 1961), pp. 233-242.

2. Merte, H. Jr., and Clark, J. A., "A Study of Pool Boiling in an Accelerating System," Michigan University Research Institute Technical Report (November, 1959).

3. Costello, C. P., and Adams, J. M., "Burnout Heat Fluxes in Pool Boiling at High Accelerations," 1961 International Heat Transfer Conference, 1961, pp. 255-261.

4. Chang, Y. P., and Snyder, N. W., "Heat Transfer in Saturated Boiling," Chem. Engr. Prog. Symp. Series, Vol. 56, No. 30, (November, 1960), pp. 25-38.

5. Costello, C. P., and Tuthill, W. E., "Effects of Acceleration on Nucleate Pool Boiling," Chem. Engr. Prog. Symp. Series, Vol. 57, No. 32, 1961, pp. 189-196.

6. Costello, C. P., and Adams, J. M., "The Interrelation of Geometry, Orientation, and Acceleration in the Peak Heat Flux Problem," A.I.Ch.E. Journal, Vol. 9, No. 5 (September, 1963), pp. 663-671.

7. Pomerantz, M. L., "Film Boiling on a Horizontal Tube in Increased Gravity Fields," A.S.M.E. Paper No. 63-HT-17, 1963.

8. Graham, R. W., and Hendricks, R. C., "A Study of the Effect of Multi-G Accelerations on Nucleate Boiling Ebullition," NASA TN D-1196, 1963.

9. Graham, R. W., Hendricks, R. C., and Ehlers, R. C., "Analytical and Experimental Study of Pool Heating of Liquid Hydrogen over a Range of Accelerations" NASA TN D=1883, 1964.

10. Beckman, W. A., and Merte, H. Jr., "A Photographic Study of Boiling in an Accelerating System," A.S.M.E. Paper No. 64-WA/HT-29, 1964.

11. Morozkin, V. I., Amenitskii, A. N., and Alad'eu, I. I., "Experimental Study of the Effect of Acceleration on the Boiling Crisis in Liquids at the Saturation Temperature," Soviet Physics - High Temperature, Vo. 1, No. 1 (July-August, 1963), pp. 88-92.

12. Ivey, J. J., "Acceleration and the Critical Heat Flux in Pool Boiling Heat Transfer," Proceedings of the Institute of Mechanical Engineering, Vol. 177, No. 1, 1963, pp. 15-42.

13. Adams, J. M., "A Study of the Critical Heat Flux in an Accelerating Pool Boiling System," Heat Transfer Laboratory Research Report, University of Washington (September, 1962).

APPENDIX B

LIST OF REFERENCES

on

THE EFFECT OF MISCELLANEOUS FLUID AGITATION

on

NUCLEATE BOILING

APPENDIX B

LIST OF REFERENCES

on

THE EFFECT OF MISCELLANEOUS FLUID AGITATION ON NUCLEATE BOILING

Vapor Agitation

1. Robinson, D. B., and Katz, D. L., "Effect of Vapor Agitation on Boiling Coefficients," Chem. Engr. Prog. Symp. Series, Vol. 27, No. 6 (June, 1951), pp. 317-324.

Mechanical Agitation

1. Pramuk, F. S., and Westwater, J. R., "Effect of Agitation on the Critical Temperature Difference for a Boiling Liquid," Chem. Engr. Prog. Symp. Series, Vol. 52, No. 18, 1956, pp. 79-83.

Ultrasonic Agitation

1. Isakoff, S. E., "Effect of an Ultrasonic Field on Boiling Heat Transfer," 1956 Heat Transfer and Fluid Mechanics Institute, Stanford University (June, 1956), pp. 15-29.

2. Romie, F. E., "Experimental Investigation of the Effects of Ultrasonic Vibrations on Burnout Heat Flux with Boiling," ATL - A - 113 (October - December, 1960).

3. Romie, F. E., "Experimental Investigation of the Effects of Ultrasonic Vibrations on Burnout Heat Flux with Boiling," ATL - A - 123 (July, 1961).

4. Ornatskii, A. P., and Shcheriakow, V. K., "Intensification of Heat Transfer in the Critical Area with the Aid of Ultrasonics," Original source unavailable, translated summary is available in Reference (3).

5. Markels, M., Durfee, R. L., and Richardson, R., "Annual Progress Report of Methods to Increase Burnout Heat Transfer," U.S. A.E.C., New York Operations Office 9500 (September, 1960).

6. Li, K. W., "An Investigation of Acoustical Effects on the Low Heat Flux Region of Nucleate Pool Boiling," Ph.D. Dissertation, Oklahoma State University (May, 1965).

Pressure Agitation

1. Howell, J. R., and Bell, K. J., "An Experimental Investigation of the Effect of Pressure Transients on Pool Boiling Burnout," Chem. Engr. Prog. Symp. Series, Vol. 59, No. 41, 1963, pp. 88-

2. DiCicco, D. A., and Schoenhals, R. J., "Heat Transfer in Film Boiling with Pulsating Pressure," Trans. A.S.M.E., Series C, J. of Heat Transfer, Vol. 86, No. 3 (August, 1964), pp. 457-461.

3. Bergles, A. E., "The Influence of Flow Vibrations on Forced Convection Heat Transfer," Trans. A.S.M.E., Series C, J. of Heat Transfer, Vol. 86, No. 4 (November, 1964), pp. 559-560.

Electrostatic Agitation

1. Markels, Michael Jr., and Durfee, R. L., "The Effect of Applied Voltage on Boiling Heat Transfer," A.I.Ch.E. Journal, Vol. 10, No. 1 (January, 1964), pp. 106-109.

Vortex Agitation

1. Gambill, W. R., and Green, N. D., "A Study of Burnout Heat Fluxes Associated with Forced Convection, Subcooled and Bulk Nucleate Boiling," Chem. Engr. Prog. Symp. Series, Vol. 54, No. 10 (October, 1958), pp. 68-76.

2. Oliver, L. R., and Blum, H. A., "Heat Transfer in a Decaying Vortex System," Mechanical Engineering Research Report, Southern Methodist University, 1965.

APPENDIX C

HEAT TRANSFER TEST SECTION

APPENDIX C

HEAT TRANSFER TEST SECTION

In the literature on heat transfer involving cylindrical test sections, several different methods are used to supply the heat fluxes desired. The method generally used depends on the size of the test section and the operating conditions involved. When the test section is in the form of a small diameter wire, the only method available employs electrical power imposed upon a high electrical resistance material. When the test section is in the form of a cylindrical element of larger diameter, it is possible to use both electrical power and steam to supply the heat flux. The electrical power may be applied directly to the cylinder itself or to resistance material imbedded inside the cylinder. If steam is used, it naturally is allowed to flow through the inside of the cylinder.

Severe design limitations involving the vibration of the test section virtually eliminated the use of steam as a source of test section heating. Of the two electrical heating methods available, the use of an internal electrical heater was chosen. Since the heater surface was to be made of copper and the electrical resistivity of copper is small, sufficient electrical resistance is calculated by

$$R_T = \frac{\rho L}{A} \tag{C-1}$$

could only be obtained if the cross sectional area, A, was very small and the length of the element, L, was very large. Due to spacial limitations this was not possible and the use of the cylinder material itself had to be eliminated. This dictated that an internal electrical heater be used. The design calculations for this type of heater follow in the next section.

Heater Design Calculations

It was the purpose of the present investigation to study the effect of vibration on the lower heat fluxes encountered in nucleate pool boiling. After a study of the nucleate boiling heat flux range, it was decided to build a test section heater that would allow heat fluxes up to 150,000 BTU / hr ft^2. The relation of this range of heat fluxes to the complete boiling curve is shown in Figure C-1, taken from Chang (64).

The total surface area of a cylinder is given by

$$A = \pi D L \tag{C-2}$$

For a 1.0 inch diameter cylinder, this area was 0.153 ft^2 since the heater element was 7 inches in length.

The power required by the test section was given by

$$P = \left(\frac{q}{A}\right)(A) \tag{C-3}$$

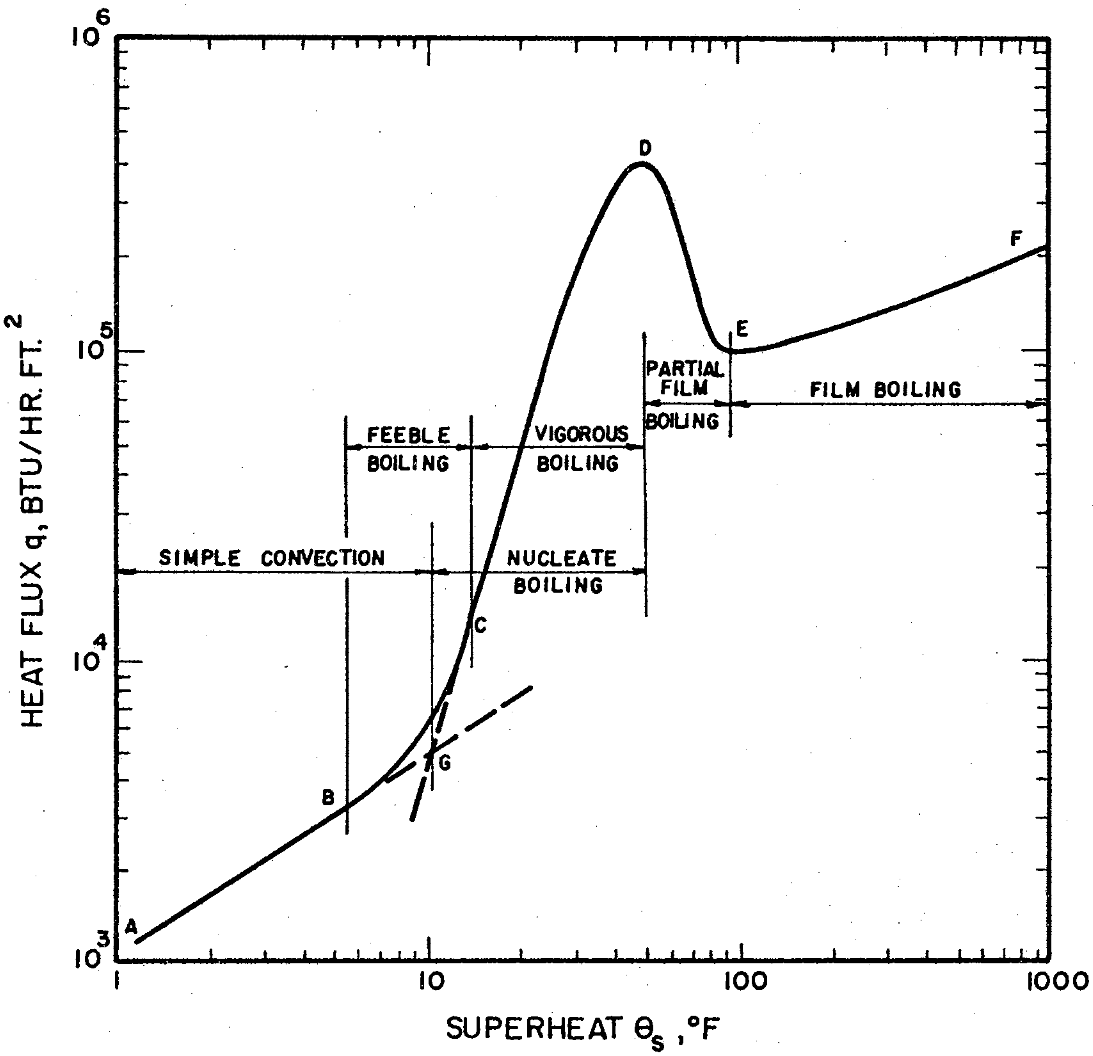

Figure C-1. Typical Boiling Curve

as 6700 watts. Since the Lincoln arc welder used as the power supply had an automatic voltage control which limited the voltage output to a maximum of 40 volts, the maximum current required was given by

$$i = \frac{P}{e} \qquad \text{(C-4)}$$

to be 167 amps and the resistance required in the test section was given by

$$R_T = \frac{P}{i^2} \qquad \text{(C-5)}$$

to be 0.24 ohms.

As a summary of the electrical requirements of the test section, they are listed as:

a) Power = 6700 watts

b) Voltage = 40 volts

c) Current = 167 amps

d) Resistance = 0.24 ohms

To provide an electrical heater with the appropriate resistance, Nichrome wire was chosen. The wire was wound around a ceramic core in three parallel legs of equal length. Each leg had approximately 0.75 ohms of resistance which resulted in an equivalent resistance for the entire heater of 0.25 ohms. After construction was completed, the resistance of the test section was measured using a Kelvin bridge. The actual value was exactly 0.245 ohms, slightly below the designed value. Since the coefficient of resistance of Nichrome wire increases slightly with temperature, it was more desirable to have the resistance at room temperature slightly undervalue than overvalue.

Test Section Temperature Distribution

Due to the method used in the construction of the electrical heater, guard heaters were not incorporated into the design. This guarded test section technique is often employed in studies of heat transfer from cylinders to gases, but it has not, at this time, been used to study the rate of heat transfer from a cylinder to water. Structural difficulties, problems of temperature measurement, and the need for high power levels in the test section have prevented the inclusion of guard heaters into the test section.

Since a uniform surface temperature could not be controlled experimentally, a study of the temperature distribution within the cylinder was made. The two dimensional heat conduction equation in cylindrical coordinates with internal heat generation is given by

$$\frac{\partial^2 T}{\partial r^2} + \frac{1}{r}\frac{\partial T}{\partial r} + \frac{\partial^2 T}{\partial z^2} + \frac{\dot{q}}{k} = 0 \qquad \text{(C-6)}$$

The solution to this equation was made most difficult since the test section was a composite body of several materials with different thermal conductivities. In addition, the generation of heat was not uniformly distributed but located in an annular ring within the body. The only solution which is feasible was numerical in nature and is presented at this time.

In order to begin a numerical solution, a mathematical model of the heat transfer test section was developed. This model is described by Figure C-2. The dimensions of the model corresponded to the actual dimensions of the test section as given by Figure 3-2. The model was represented by 27 nodes. Nodes 1 through 18 represented regions within the surface of the test section, and nodes 19 through 27 represented the fluid to which the heat was transferred.

There were a number of assumptions necessary in this numerical solution. These were as follows:

1) conduction in the radial and axial directions only
2) angular symmetry
3) half symmetry in the axial direction
4) internal heat generation at nodes 7, 8, 9, and 10
5) saturation temperature at nodes 19 through 27
6) constant thermal properties of all materials
7) nucleate boiling conditions at nodes 1, 2, 3, and 4
8) turbulent free convection at nodes 5, 6, 12, and 18

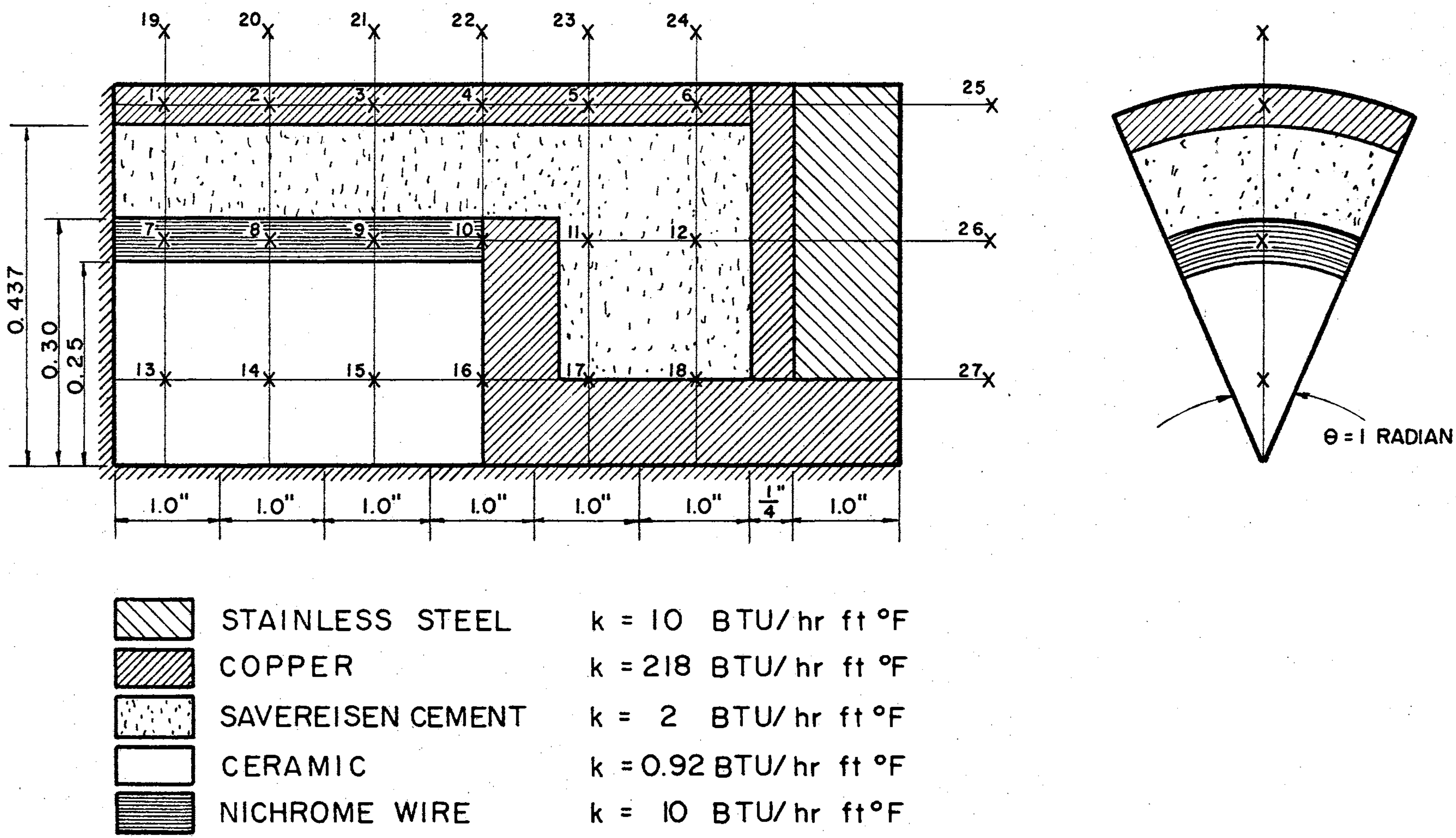

Figure C-2. Test Section Numerical Model

9) all other general assumptions and approximations which accompany a numerical solution of this type.

Using these assumptions and the method of writing residual equations for the relaxation solution as outlined by Kreith (65) there were eighteen equations and eighteen unknowns for which a solution was obtained. There was one equation for each of the eighteen nodes for which a temperature value was desired.

Assumptions 1 - 5 are standard to the numerical relaxation method of solution and were considered valid. Assumption 6 was completely valid except for the actual determination of the property values. All were easily obtained from tables except for the Sauereisen cement. The value of the thermal conductivity of the cement was heavily dependent on the actual composition and density of the final form. An assumption was made for this cement and could have affected the results to a slight degree. In order to determine the effect of assumptions 7 and 8 correctly, a computer program was utilized for the solution of the eighteen equations and eighteen unknowns. With this, it was possible to change the assumed values for the nucleate boiling and turbulent free convection heat transfer coefficients.

Figure C-3 is a graphical representation of the surface temperatures given by the values of nodes 1 through 6. This curve represents the results for a nucleate boiling coefficient of 5000 BTU/hr ft^2 °F. The various curves represent the difference in surface

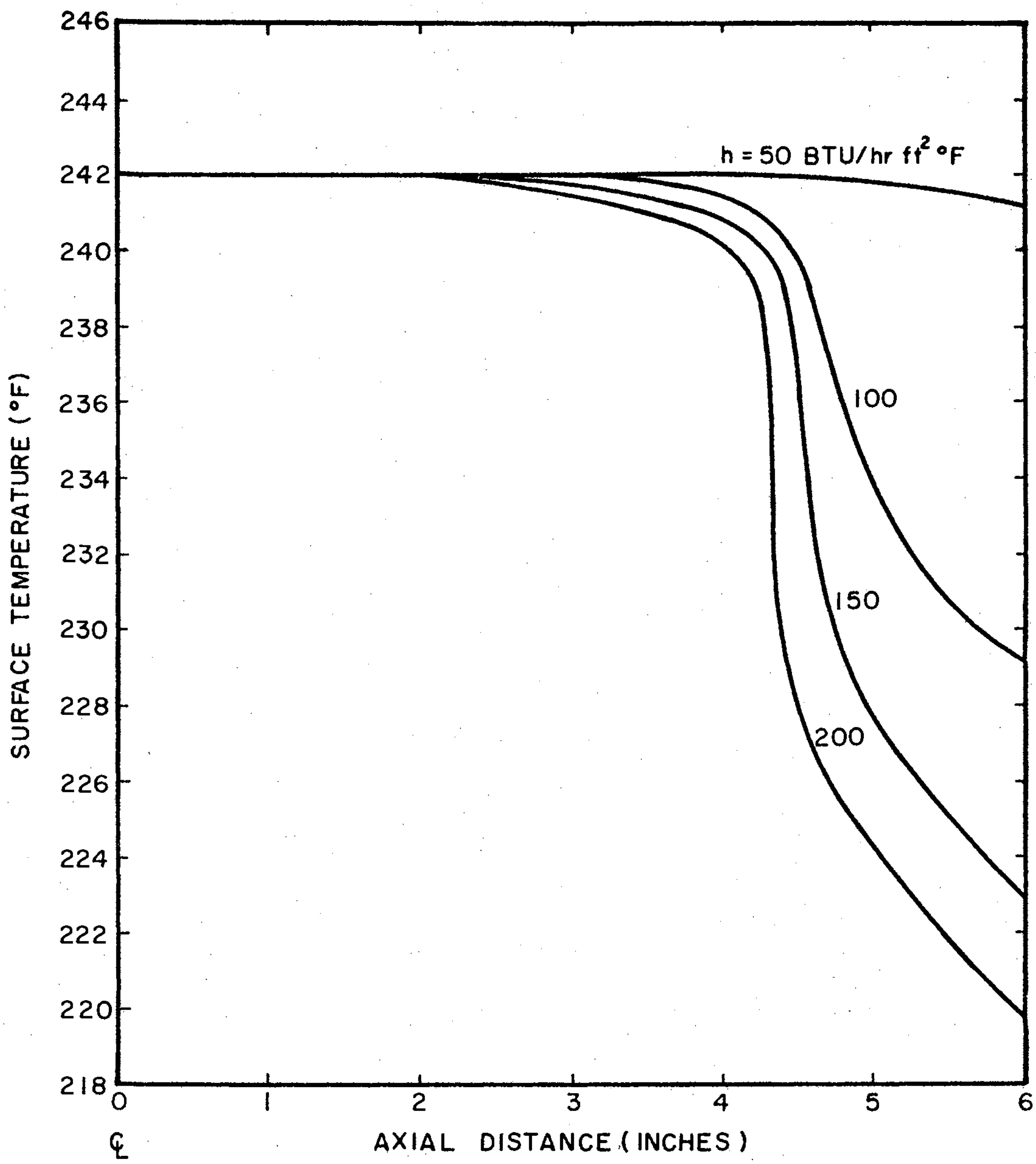

Figure C-3. Surface Temperature of Cylindrical Model temperature as the turbulent free convection coefficient was increased through the values 50, 100, 150, and 200 BTU / hr ft^2 ^oF.

The nucleate boiling coefficient used for the above calculation represented a heat flux of 150,000 BTU / hr ft^2 and a temperature difference of $30^o F$. Under these conditions, the surface temperature was a constant $242^o F$ for almost four inches in the center of the section. It was, therefore, assumed that the surface temperature remained constant over at least two to three inches in the center of the actual test section regardless of the accuracy of assumptions 7 and 8.

Surface Temperature Correction

From measurements of the inside temperature of the copper cylinder with the thermocouples, it was desired to calculate the surface temperature for correlation purposes. The equation for the rate of heat transfer in cylindrical coordinates is, assuming one dimensional heat flow,

$$q = \frac{2\pi L k (T_o - T_i)}{\ln \frac{r_o}{r_i}} \qquad \text{(C-7)}$$

From power measurements the heat generated in the center portion of the cylinder corresponding to the length, L, was calculated. The dimensions r_o and r_i were determined from physical measurements. Therefore, if the temperature of the inside surface, T_i, is given by experimental measurements, the outside surface temperature, T_o, may be calculated by

$$T_o = T_i + \frac{q}{2\pi k L} \ln \frac{r_o}{r_i} \tag{C-8}$$

This correction was applied to all surface temperature data and was the same regardless of the state of vibration of the surface.

Heater Element Construction

As stated in the previous section, the heater element was constructed of Nichrome wire wound on a 0.5 inch diameter ceramic rod seven inches in length. This was done in such a way that the three legs of equal length were evenly spaced and were not in contact at any point. To accomplish this a special jig was constructed using a small lathe. A steel rod 3/8 inch in diameter, placed in the chuck of the lathe at one end and in a live center at the other, was used as the form for coiling the wire. Three small holes were drilled in a small block of wood which was placed in the tool post of the lathe and three Nichrome wires were inserted in these holes. The wires extended to the chuck of the lathe where they were fixed between the jaws of the chuck and the steel rod. Special care was required so that the angle of the wire, the proximity of the tool post to the chuck, and angle of the tool post were correct for even wire application. The thread cutting mechanism of the lathe was engaged at the slowest available rate of four threads per inch. Many trials were necessary to get a coil which was acceptable.

A copper plug was made for each end of the heater section so that the aircraft cable leads could be soldered to the three Nichrome wires. The plug was made so that it was exactly the same diameter as the ceramic piece but 3/4 inches in length with a small hole drilled in one end for the aircraft cable. The cable was silver soldered into the hole and the Nichrome wire silver soldered to the surface of copper. As this was done, care was taken so that the three legs of the heater wire did not come into contact.

After the silver soldering was completed, the Sauereisen Cement was painted on with a paint brush in several separate applications. Between each application, the element was dried in an electronically controlled oven.

At this point in the construction, a mold was made for one end of the heater element. It was constructed of Teflon so that it would release easily after setting and made in such a way that a large base of Sauereisen Cement resulted on one end of the element. This allowed the element to be centered in the copper cylinder. The outside diameter of the base corresponded to the inside diameter of the copper cylinder. After the mold was in place and the Sauereisen Cement inserted, the mixture was allowed to harden in the oven. When the cement dried, the mold was taken from the element and four small grooves were ground along the sides of this base at 90 degree intervals.

The purpose of these grooves will be explained in the discussion of the final cementing process.

Preparation of the Copper Cylinder

The copper cylinder, with its mounting flanges on each end, was carefully marked off and small holes were drilled at 90 degree intervals for the four thermocouples which would eventually measure the surface temperature. The thermocouples were carefully placed in the holes in the cylinder and peened tightly into place. A ball peen hammer and special peening tool were used in a rotating manner around and around the hole until the thermocouples were firmly in place.

At this point, the entire cylinder was placed in a large lathe. The flanges were squared up and the cylinder surface turned down smooth and polished smooth with a fine grain polishing paper. Care was taken at this point since silver solder is softer than copper and pits would have resulted if extensive hard sanding had been applied.

Final Cementing Process

To achieve the final process of cementing the heater element inside the copper cylinder, a special rig was designed and built. The complete process is described in this section.

First, the heater element was placed in the center of the copper cylinder. The end of the element with the large grooved base was placed at one end and the thermocouple wires and the power lead were brought out the other end through a special flange.

This flange on the other end exactly matched the flange silver soldered to the copper cylinder so that they could be bolted together to seal. The flange was solid with the exception of one hole exactly in the center for the power lead, four very small holes at the perimeter for the four thermocouples, and one 1/4 inch hole slightly off center in which a copper tube was silver soldered. A plastic hose attached to a jar with an air aspirator was connected to this copper tube.

After the flange was in place, and all wires firm and taut, sealing wax was applied to the area around the wire at each opening. The entire apparatus was then suspended in a vertical attitude by a ring stand and ring stand clamps. The jar with the air aspirator was filled with a Sauereisen cement mixture and suspended from another ring stand.

The pumping action of the air aspirator forced the cement down the plastic hose and up into the bottom of the cylinder through the opening in the special sealing flange. As continued pressure was applied, the cement filled the annular cavity between the heater element and the cylinder wall forcing the air out through the grooves in the previously constructed base of the heater element. In a short time, all of the air was displaced and cement flowed out the top of the cylinder. The flow of the cement was then cut off, the entire apparatus cleaned up, and the completed cylinder placed in the oven for drying.

This drying process was accomplished in a series of steps. After increasing the temperature of the oven over a period of several hours, the cylinder was turned over and the special flange removed. From this point on the interior was allowed to dry with both ends open to the atmosphere. After approximately 48 hours of high temperature exposure, the test section was taken from the oven. It was then completely hard and dry and was ready for use as a test section in the experimental apparatus.

APPENDIX D

THERMOCOUPLE CALIBRATION

APPENDIX D

THERMOCOUPLE CALIBRATION

Method of Calibration

The thermocouples used to measure the surface temperature were made from wire taken from the center of a spool of standard B & S gauge # 24 Minneapolis Honeywell Regulator Co. thermocouple wire. Minneapolis Honeywell Megapak thermocouples were used to measure the temperature of the water. The thermocouples were calibrated using a hypsometer as the reference standard for the boiling point of water and a reservoir of light oil immersed in an ice bath as the reference standard for the ice point of water. The boiling point was fixed by a measurement of the barometric pressure and the ice point was taken to be 32^{o} F. For each thermocouple a series of successive independent measurements were taken using a Leeds and Northrup 8686 millivolt potentiometer with a period of time elapsing between each measurement. Before the initial reading of each thermocouple a long period of time was allowed so that thermal equilibrium might be obtained.

The thermocouples made from the 24 gauge wire were found to conform with the National Bureau of Standards Circular 561. The

Megapak thermocouples were found to be accurate to within $\pm$ 3/4 per cent, the accuracy range specified by the manufacturer.

APPENDIX E

MILLIVOLT RECORDER CALIBRATION

APPENDIX E

MILLIVOLT RECORDER CALIBRATION

Method of Calibration

As a recording instrument for the thermocouples used in this investigation, a Leeds and Northrup Speedomax H Azar recorder was chosen. To calibrate this instrument completely, two separate calibrations are necessary. The instrument must first be calibrated internally so that the range of measurements can be set. The selected range was from 1.0 to 6.0 millivolts. This required that the zero be suppressed. This part of the calibration procedure is standard with an instrument of this type and is not discussed here. The manufacturer specifies that after this calibration the instrument is accurate to within $\pm$ 0.3 per cent of scale span which is, for this case, 5.0 millivolts.

In order to check this calibration, the recommended procedure was followed. The emf output terminals of a Leeds and Northrup 8686 reference potentiometer were connected to the usual input leads of the recorder with copper wire. The potentiometer was then standardized and the emf set to the value at which it was desired to check the Speedomax H calibration. This was done at several values through the range from 1.0 to 6.0 millivolts. Figure E-1 represents the results of that calibration and indicates the millivolt value which should be added to the indicated reading to give the accuracy specified by the manufacturer.

The correction obtained from Figure E-1 was applied to the indicated reading to give a true reading. Reference to National Bureau of Standards Circular 561 gave the conversion from the millivolt reading to the related temperature.

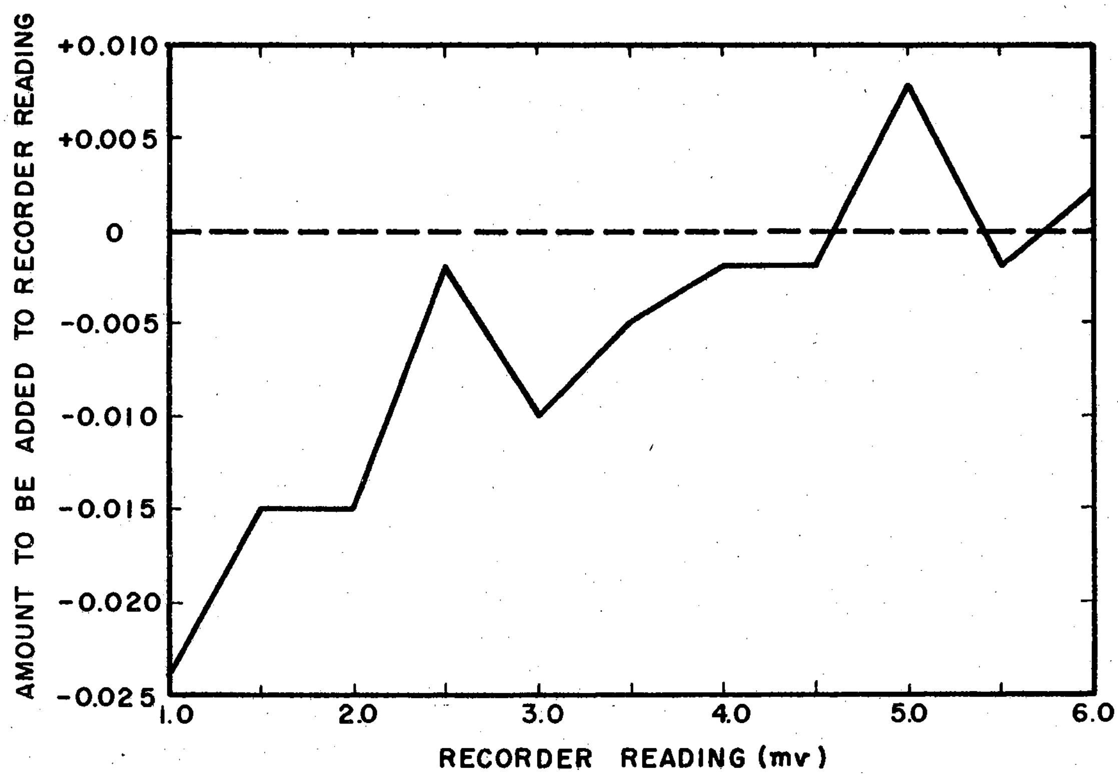

Figure E-1. Millivolt Recorder Calibration Curve

APPENDIX F

ACCELEROMETER CALIBRATION

APPENDIX F

ACCELEROMETER CALIBRATION

Method of Calibration

A Kistler Model 812 quartz accelerometer was used to measure the acceleration of the test section. The accelerometer had been recently calibrated using the recommended calibration fixture. This method involved the use of calibrating weights which apply known forces to the quartz crystal. It was found to be in good operating condition and within prescribed accuracy limits.

A specially designed Kistler Model 568 electrometer charge amplifier connected the charge signal to a voltage signal which was measured with standard instrumentation. The charge amplifier was factory calibrated to have standardized output sensitivities of 0.1, 1.0, 10, and 100 millivolts per unit of acceleration when the calibration factor of the instrument was set to the charge sensitivity of the accelerometer. The calibration factor adjustment was a ten turn, continuously variable, precision potentiometer and the standardized output sensitivities were selected by a four position range switch. Drift-free dynamic operation with the quartz transducer was possible with an adjustment for zero correction provided. A push button ground switch quickly removed any residual signal from the measuring system and restored the output to zero, and the amplifier contained a regulated power supply.

An oscilloscope was used to view the wave pattern of the signal generated by the accelerometer. The oscilloscope was calibrated following the instructions for calibration in the instrument manual. This was usually an extensive process but the timing coincided with the annual calibration cycle of the electronic equipment in the laboratory.

A Ballantine rms voltmeter was used to measure the voltage signal generated by the accelerometer. The Ballantine voltmeter had an internal calibration system which was periodically employed by use of a special circuit and the external meter screw for adjustment of the scale. This calibration was employed and the instrument was found to be within the limits of accuracy prescribed by the manufacturer.

In order to determine the charge sensitivity of the accelerometer and set the calibration factor of the charge amplifier, a dynamic calibration was employed using the MB Electronics Model C11-D Vibration Pickup Calibrator and Vibration Exciter and Model T-112531 Control. The signal generator was calibrated to be accurate within $\pm$ 1 per cent absolute from 5 to 2000 cycles per second. To measure the displacement and acceleration of the accelerometer as it was mounted on the vibration exciter, an MB Vibration Meter was employed. This measuring instrument had the following specified accuracies:

1.	Displacement	5 to 10 cps	$\pm$ 5 per cent
		10 to 1000 cps	$\pm$ 2 per cent

2. Acceleration 5 to 1000 cps ± 2 per cent

1000 to 2000 cps ± 5 per cent

The frequency of vibration was measured by a Berkeley Model 554 Eput Meter through a pickup on the control panel.

The vibration exciter was carried through the range of accelerations to be encountered in this investigation, and it was discovered that the charge amplifier should be set on its highest output sensitivity in order to achieve good accuracy in the measurements of the rms meter. The calibration factor dial was then varied until a reading was obtained on the rms voltmeter of 7.5 volts corresponding to an acceleration of 15 g's. This gave a calibration factor of 2.0 g's/volt. An investigation was made to determine if this was indeed the true calibration factor. It was found that this factor gave accurate values of acceleration throughout the range to be encountered in this investigation. In addition, tests were made with regard to the frequency response of the system. Throughout the range of frequencies used in this investigation, the system did not vary in its signal response to even a noticeable degree.

The calibration equipment for the calibration of the accelerometer is shown in Plate XIII. Plate XIIIa shows an overall view of the shaker table control panel, and other equipment. Plate XIIIb shows a close view of the shaker with the accelerometer in position and the charge amplifier close by.

PLATE XIII
Accelerometer Calibration Equipment

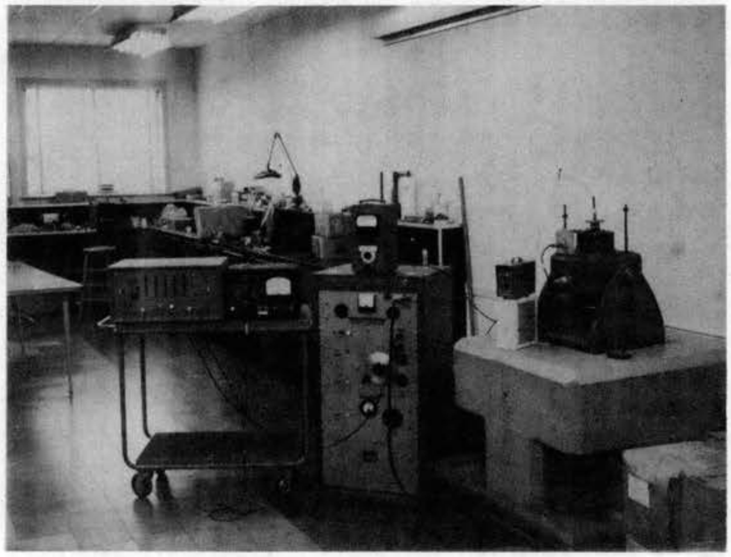

a) Accelerometer calibration equipment

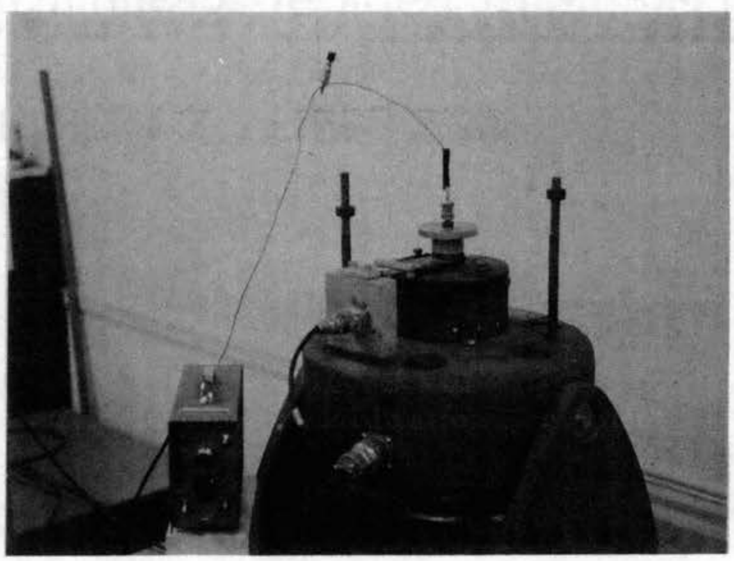

b) Calibration shaker and accelerometer

APPENDIX G

DIFFERENTIAL TRANSFORMER CALIBRATION

APPENDIX G

DIFFERENTIAL TRANSFORMER CALIBRATION

Method of Calibration

A Schaevitz Model E 300D linear variable differential transformer was used to measure the amplitude of vibration of the test section. A differential transformer is an electromechanical transducer which produces a signal proportional to the displacement of a movable core and is therefore most accurate in this application. This change of voltage is linear with linear core displacement within a specified range of displacement.

The primary or center coil is energized with alternating current and voltages are induced in the two outer secondary coils 180° out of phase. To obtain a differential output from the differential transformer, the primary leads are connected to a 6 volt, 60 cps, regulated power supply and the secondaries are connected in series opposition. With the transformer wired in this manner, the transformer may be adjusted so that, for any displacement, the output is equal to some minimum value. Displacement from this position results in increased voltages output and erroneous readings.

In order to determine the sensitivity of the differential transformer a calibration procedure identical to that of the accelerometer as described in Appendix F was employed. The MB Electronics Model C11-D Vibration Pickup Calibrator and Vibration Exciter and Model T-112531 Control were used to perform a dynamic calibration of the differential transformer. The shaker was placed in vibration and the position of the outer stationary coil was adjusted until a minimum signal was indicated. This signified that the outer coil was in the null position. The vibration exciter was then carried through the range of amplitudes to be encountered in this investigation. Throughout this range of amplitudes the sensitivity of the differential transformer was found to be 4 volts/inch. In addition, tests were made to determine the frequency response of the differential transformer. Throughout the range of frequencies used in the present investigation no variation in output voltage was noted at a constant value of amplitude.

APPENDIX H

LIST OF SYMBOLS

APPENDIX H

LIST OF SYMBOLS

Arabic Symbols

a	Zero to peak amplitude of vibration, inches.
A	Surface area of the heater, ft^2.
	Cross sectional area of the heater wire, in^2.
D	Diameter of the cylindrical test section, inches.
	Diameter of the bubble, inches.
$\dot{D}$	Derivative of the bubble diameter with time, ft/sec.
$\ddot{D}$	Second derivative of the diameter with time, ft/sec.
D_{max}	Maximum diameter of the bubble at breakoff, inches.
e	Test section heater voltage, volts.
f	Frequency of vibration, cycles per second.
f_B	Frequency of bubble formation, bubbles per second.
F_B	Buoyancy force acting on bubble, lb_f.
F_I	Inertia force acting on bubble, lb_f.
F_S	Surface tension force on bubble, lb_f.
g	Acceleration of gravity, ft/sec^2.
g_c	Proportionality constant, 32.2 lbm $ft/sec^2 lb_f$.
Gr	Grashof number

h	Heat transfer coefficient, BTU/hr ft^2 ^oF.
h_v	Coefficient with surface vibration, BTU/hr ft^2 ^oF.
h_s	Coefficient with sound field, BTU/hr ft^2 ^oF.
i	Test section heater current, amperes.
k	Thermal conductivity, BTU/hr ft ^oF.
L	Length of the cylindrical heater, ft.
	Length of the heater wire, ft.
p	Pressure, psi.
p_v	Vapor pressure, psi.
p_∞	Free stream pressure, psi.
p_l	Local surface pressure, psi.
P	Test section power, watts.
Pr	Prandtl number.
q	Heat transfer rate, BTU/hr.
$\dot{q}$	Heat generation rate per unit volume, BTU/hr ft^3.
q/A	Heat flux from cylindrical surface, BTU/hr ft^2.
q_c	Heat conducted into bubble from thermal layer, BTU/hr.
q_E	Heat transfer through vapor exchange, BTU/hr.
q_{BC}	Heat transfer by bulk convection, BTU/hr.
q_{mv}	Heat transfer by microlayer vaporization, BTU/hr.
R	Bubble radius, inches.
$\dot{R}$	Derivative of the bubble radius with time, ft/sec.
$\ddot{R}$	Second derivative of the bubble radius with time, ft/sec^2.

R_T Total resistance of the heater wire, ohms.

R_{e_v} Vibratory Reynolds number.

t_d Bubble departure time, seconds.

t_w Waiting time, seconds.

t_{ub} Unbinding time, seconds.

T_i Inside surface temperature of cylinder, ^oF.

T_o Outside surface temperature of cylinder, ^oF.

T_w Wall Temperature of cylinder, ^oF.

T_{sat} Saturation temperature of water, ^oF.

ΔT Temperature difference, ^oF.

v Velocity of the vibrating cylinder, ft/sec.

$\bar{v}$ Average velocity of vibration, ft/sec.

Greek Symbols

β Thermal coefficient of expansion, $1/^oF$.

β Bubble contact angle, degrees.

δ Thermal layer thickness, inches.

μ_L Viscosity of liquid, $lb_f\ sec/ft^2$.

ρ Density, lb_m/ft^3.

ρ_L Density of liquid, lb_m/ft^3.

ρ_v Density of vapor, lb_m/ft^3.

σ_{LV} Surface tension, lb_f/ft.

τ Time, seconds.

VITA

DONALD CRAIG PRICE

Candidate for the degree of

Doctor of Philosophy

Thesis: THE EFFECT OF SURFACE VIBRATIONS ON NUCLEATE POOL BOILING AT LOW HEAT FLUXES

Major Field: Mechanical Engineering

Biographical:

Personal Data: Born in Dallas, Texas, August 28, 1938, the son of Herman Jack and Mona Elizabeth Price.

Education: Attended John H. Reagan grade school in Dallas, Texas. Graduated with honor from W. H. Adamson High School in Dallas, Texas, in January, 1956. Received the Bachelor of Science in Mechanical Engineering Degree from Southern Methodist University in Dallas, Texas, in May, 1961. Received the Master of Science in Mechanical Engineering Degree from Southern Methodist University in Dallas, Texas, in January, 1963. Completed the requirements for the Doctor of Philosophy Degree at Oklahoma State University in Stillwater, Oklahoma, in July, 1966.

Professional Experience: Approximately two years cumulative experience in cooperative employment in industry while an undergraduate at Southern Methodist University in the years from 1957 through 1961. Teaching experience at both Southern Methodist University and Oklahoma State University during the years from 1961 through 1963. Member of Sigma Tau, Pi Tau Sigma, ASME, ASEE.